Starling Murmuration Optimizer: A Novel Bio-inspired Algorithm for Global and Engineering Optimization

Hoda Zamani[1, 2], Mohammad H. Nadimi-Shahraki*[1, 2], Amir H. Gandomi[3]

[1]Faculty of Computer Engineering, Najafabad Branch, Islamic Azad University, Najafabad, Iran

[2]Big Data Research Center, Najafabad Branch, Islamic Azad University, Najafabad, Iran

[3]Faculty of Engineering & Information Technology, University of Technology Sydney, Ultimo, Australia

* Correspondence: nadimi@iaun.ac.ir & nadimi@ieee.org, Tel: +98-3142292632.

Abstract. This paper presents a novel bio-inspired algorithm inspired by starlings' behaviors during their stunning murmuration named starling murmuration optimizer (SMO) to solve complex optimization problems. The SMO introduces a dynamic multi-flock construction and three new search strategies, separating, diving, and whirling. The separating search strategy aims to enhance the population diversity and local optima avoidance using a new separating operator based on the quantum harmonic oscillator. The diving search strategy aims to explore the search space sufficiently by a new quantum random dive operator, whereas the whirling search strategy exploits the vicinity of promising regions using a new operator called cohesion force. The SMO strikes a balance between exploration and exploitation by selecting either a diving strategy or a whirling strategy based on the flocks' quality. The SMO was tested using various benchmark functions with dimensions 30, 50, 100. The experimental results prove that the SMO is more competitive than other state-of-the-art algorithms regarding solution quality and convergence rate. Since the most appropriate application of metaheuristic algorithms is in optimizing engineering problems, after proving the SMO's sufficiency for global optimization, it is also applied to solve several mechanical engineering problems in which results demonstrate that it can provide more accurate solutions. A statistical analysis shows that SMO is superior to the other contenders.

Keywords: Optimization algorithm, Metaheuristic algorithm, Bio-inspired algorithm, Swarm intelligence algorithm, Quantum computing, Applied mechanics and engineering problems.

1. Introduction

Over the last decade, many metaheuristic algorithms have been proposed to solve real-world optimization especially for mechanical engineering problems [1-6] as the most application of these algorithms [7, 8]. The metaheuristic algorithms can be classified into different levels of classification based on the perspective and the source of inspiration [9]. When the focus and perspective are about the trajectory of the search path, they can be classified into two classes: trajectory-based and population-based [9-11]. Trajectory-based algorithms are more exploitation-oriented and start with just a single solution. The population-based algorithms benefit from the multiple agents' cooperation by sharing their experience to bypass the local optima and converge to the promising areas accurately. On the other perspective, the metaheuristic algorithms can be classified based on their sources of inspiration into four major classes [9]: swarm intelligence (SI) based, bio-inspired (but not SI-based), physics/chemistry-based, and others. SI-based algorithms are a subset of bio-inspired algorithms, and bio-inspired (but not SI-based) algorithms are a subset of nature-inspired algorithms (SI-based $\subset$ bio-inspired $\subset$ nature-inspired) [9].

SI-based algorithms are fundamentally inspired by real-life behaviors of diverse species in nature as the most significant problem solver. These algorithms use multiple agents to share information flow through the population, so that self-organization, co-evolution, and parallelization lead the search process effectively. Based on the behaviors of diverse species used by SI-based algorithms, they can be divided into four groups: insects, terrestrial animals, birds, and aquatic animals. The algorithms of the first group mimic self-organization and collective foraging behaviors. The well-known algorithms of this group are ant colony optimization [12, 13], the artificial bee colony (ABC) algorithm [14], best-so-far ABC algorithm [15], moth-flame optimization (MFO) [16], grasshopper optimization algorithm (GOA) [17], pity beetle algorithm (PBA) [18], butterfly optimization algorithm (BOA) [19], and mayfly algorithm (MA) [20]. A significant stream of algorithms has emerged by inspiring terrestrial animals' behaviors such as searching for prey, information sharing, herd leadership, prey encircling, and attacking. These algorithms are utilized using the social communication mechanism, which transfers information about promising reigns in the search space between members of the population. The lion pride optimizer (LPO) [21], grey wolf optimizer (GWO) [22], elephant herding optimization (EHO) [23], spotted hyena optimizer (SHO) [24], squirrel search algorithm (SSA) [25], gorilla troops optimizer (GTO) [26] and fox optimization algorithm (RFO) [27] are some terrestrial animal-inspired algorithms.

The third group of SI-based algorithms mimics birds' behaviors, such as nesting, feeding, mating, immigrating, protecting against predators, and interacting with others. The particle swarm optimization (PSO) [28] algorithm is the most well-known paradigm in this group, which has been developed for many applications [29]. Some of the algorithms developed using birds' behaviors are comprehensive learning particle swarm optimizer (CLPSO) [30], bird swarm algorithm (BSA) [31], harris hawks optimizer (HHO) [32], conscious neighborhood-based crow search algorithm (CCSA) [33], golden eagle optimizer (GEO) [34], African vultures optimization algorithm (AVOA) [35], quantum-based avian navigation optimizer algorithm (QANA) [36], and artificial hummingbird algorithm (AHA) [37]. The search patterns of instinctive behaviors in an aquatic animal, such as collective movement without the leader, searching for food, immigrating, mating, prey encircling, dealing with dangers, and interacting, provide the most inspiration in the fourth group of SI-based. This group has introduced some well-known algorithms such as artificial fish swarm algorithm (AFSA) [38], krill herd (KH) [39], whale optimization algorithm (WOA) [40], salp swarm algorithm (SSA) [41], yellow saddle goatfish algorithm (YSGA) [42], sailfish optimizer (SFO) [43] and jellyfish search (JS) [44].

Bio-inspired (but not SI-based) algorithms do not use directly the swarming behavior [14-17]. The most well-known bio-inspired (but not SI-based) algorithms are genetic algorithms (GA) [18], differential evolution (DE) [19], evolutionary strategy (ES) [20], gene expression programming [21], and biogeography-based optimizer (BBO) [22]. Physics/chemistry-based algorithms are proposed based on the mathematical model inspired by physical and chemical laws. The most popular algorithms in this class include the big bang–big crunch [24], optics inspired optimization (OIO) [25], henry gas solubility optimization (HGSO) [26], quantum HGSO (QHGSO) [27], arithmetic optimization algorithm (AOA) [28], and atom search optimization (ASO) [29]. In the fourth class, metaheuristic algorithms are developed based on a wide range of diverse sources away from nature such as social, and emotional [9]. The imperialist competitive algorithm (ICA) [45], social emotional optimization algorithm (SEOA) [46], anarchic society optimization (ASO) [47], league championship algorithm (LCA) [48], mine blast algorithm (MBA) [49], volleyball premier league algorithm (VPL) [50], political optimizer (PO) [51], and heap-based optimizer (HBO) [52] are prominent and recent developments of the fourth class. Fig. 1 shows the classification of the metaheuristic algorithms concentrated on the SI-based class.

The SI-based algorithms have been applied to solve a variant of continuous optimization problems [14, 32]. They can be adapted for discrete issues [4], feature selection problems [53-58], and intelligent planning [6, 59]. However, many of them are not powerful enough to solve a wide range of complex optimization problems because they lack a meaningful search strategy, making several weak points. Significantly, these algorithms suffer from low exploitation and exploration, inadequate balancing, losing diversity, and lack of scalability and robustness [60, 61]. Exploration and exploitation are the most important features for attaining success in solving optimization problems [62]. The poor exploration can be enhanced by spreading the search agents within different regions to discover a diverse of promising areas.

The balance between exploration and exploitation abilities is a trade-off problem for SI-based algorithms. Usually, the search philosophy of the algorithm is an efficient aspect that strikes this balance. Many search strategies have been proposed to achieve the balance between exploitation and exploration with the increasing complexity of optimization problems. More recently, the conscious neighborhood-based crow search algorithm (CCSA) [33] was established to consciously select the local and global search strategies to strike a balance for complex optimization problems. The canonical GWO algorithm suffers from a lack of effective search strategies and imbalance between exploration and exploitation abilities, which results in loss of the population diversity and tending to local optima. Hence, many GWO variants [63-65] were proposed to cope with the GWO's weaknesses.

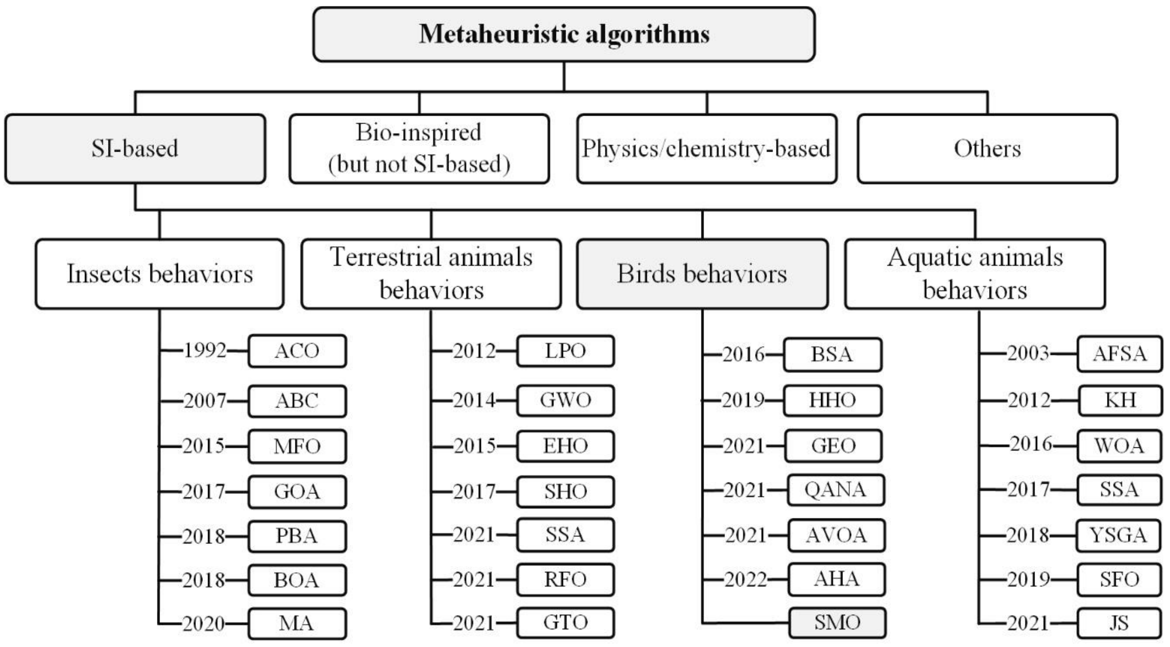

Fig. 1. A classification of metaheuristic algorithms.

To develop the right optimizer algorithms, different complexities of problems [8] such as high dimensionality, non-linear constraints, discrete and mixed type search spaces, and non-differentiability objective function should be considered [66]. Although many metaheuristic algorithms have been proposed, according to the no free lunch theorem the universally best optimizer does not exist that can cover every kind of problem and be superior to all optimizers [67]. Thus, different types of metaheuristic algorithms are needed to approximate the best solutions for different optimization problems, which is one of the underlying motivations for researchers to improve the current metaheuristic algorithms or introduce novel approaches. On the other hand, metaheuristic algorithms estimate the global optimum of a problem and they do not guarantee to find its exact solution. Therefore, new metaheuristic algorithms are introduced to make better estimations especially in solving complex problems.

In this study, a new population-based swarm intelligence algorithm, namely starling murmuration optimizer (SMO) inspired by the murmuration phenomenon is proposed in which huge flocks of starlings turn, twist, dive, and swirl across the sky in beautiful shapes. Some flocks of starlings intermittently split and then recombine in a highly synchronized manner to protect themselves in this stunning phenomenon, as further explained in Section 2. The proposed SMO models the starling murmuration using a new dynamic multi-flock construction. It introduces separating, diving, and whirling search strategies to enhance the search strategy for solving complex problems. First, a portion of the starlings is randomly selected and moved to another region using the separating search strategy. Then, the diving search strategy explores the search space by a new quantum random dive (QRD) operator, whereas the whirling search strategy uses a new cohesion operator to exploit the vicinity of promising regions. The diving and whirling search strategies are selected by computing each flock's quality, which causes it to strike a balance between exploration and exploitation during the optimization process.

The SMO algorithm was comprehensively evaluated by a multifarious combination of benchmark test functions, including CEC 2013 [68], CEC 2014 [69], and CEC 2017 [70] with different dimensions 30, 50, and 100 as the complex problems. Since the most appropriate application of metaheuristic algorithms is in optimizing engineering problems [7], the SMO is applied to solve several mechanical engineering problems after proving its sufficiency for solving global optimization. The most of engineering problems are taken from benchmark test-suite CEC 2020 [71] including tension/compression spring design, pressure vessel design (PVD), three-bar truss design, welded beam design (WBD), gas transmission compressor design (GTCD), Himmelblau’s function, hydro-static thrust bearing design, optimal design of industrial refrigeration system, and multiple disk clutch brake design. The SMO and comparative algorithms also compete on the crashworthiness design to investigate the vehicle side-impact [72]. The SMO algorithm was also statistically analyzed by the Wilcoxon signed-rank sum [73] and mean absolute error (MAE) tests. All experimental, real-world problems and statistical results were compared to some state-of-the-art algorithms, which further proved the superiority of SMO.

2. Inspiration

A murmuration of starlings is one of nature's most magnificent displays in which a mass of several flocks containing various starlings congregate and dive in the sky above their roost for about half an hour [74]. During this time, as Fig. 2 shows, the starlings continuously whirl and form intricately coordinated patterns of flight without colliding. Habitually, a murmuration behavior is sparked towards dusk by a predator's presence, like a peregrine falcon or hawk. The flocks of starlings are intermittently split and recombined in a highly synchronized manner in the murmuration. The starlings also regularly change their direction of motion to dodge predators, such as falcons and sparrow hawks. Nonetheless, the slightest uncertainty in this directional change may decrease cohesion between the flocks and push many starlings astray, where the predator is ready to prey [75].

To achieve such a synchronized murmuration, the certain whirling, direction changing, splitting, and recombining are propagated across the flocks from one starling to another by optimized decision making. Each starling tends to align its direction of motion with its neighbors without colliding and flying as close as possible. Accordingly, the neighbors of a starling in the flocks are frequently changed, which produces the dynamic neighborhood and different topologies in the murmuration. These optimized behaviors inspired us to propose the starling murmuration optimizer (SMO), a novel, bio-inspired algorithm. The following sections describe the model and algorithm in greater detail.

Fig. 2. A synchronized murmuration behavior of starlings [76]

3. Starling murmuration modeling

Using the above-described behaviors and inspiration, the starling murmuration M is modeled using a dynamic multi-flock construction, in which each starling does not belong to the same flock during iterations. Moreover, three new search strategies – diving, whirling, and separating – are defined, whereby the starlings can explore the search space broadly and exploit promising zones more efficiently. By respecting the nature of murmuration, the separating search strategy uses a new operator named quantum harmonic oscillator (QHO) to enhance the diversity of the starlings' population and to discourage the premature convergence problem. The starlings navigate in the broader space using the diving search strategy based on a new operator, named quantum random dive (QRD), while the whirling search strategy aims to exploit the vicinity of a promising area using a new operator called cohesion force (CF). Table 1 shows the parameters' description used in the following sections.

Table 1 The nomenclature used in the SMO algorithm.

Parameter	Description
S	A finite set of N distinct starlings.
$X_i(t)$	The current position of starling s_i in iteration t.
$F(X_i(t))$	Fitness of starling s_i in iteration t.
X_G (t)	The global position in iteration t.
X_N (t)	A random neighbor of starling s_i in iteration t.
R	Representative set of starlings.
Sf (t)	Fitness-ascending-ordered representation of starlings in iteration t.
f_i	The i-th flock.
$Q_q(t)$	Quality of the flock f_q in iteration t.
$\mu_Q(t)$	The average quality of flocks in iteration t.
$\|\psi(t+1, X_i)\rangle$	The next position of the starling s_i.
$\|\psi(R_D)\rangle$	A representative member in the diving search strategy.
$\|\psi^{Up}(X_i)\rangle$	Upward quantum dive of starling s_i.
$\|\psi^{Down}(X_i)\rangle$	Downward quantum dive of starling s_i.
X_{RW} (t)	A representative member in whirling search strategy.
C_i (t)	Cohesion operator in the iteration t.
$\xi(t)$	Cohesion coefficient in the iteration t.
P_{sep}	Separated population in the separating search strategy.
$\mathcal{Q}_1(y)$	Separation operator.

Suppose S= {s_1, s_2…s_N} is a finite set of N distinct starlings distributed by a uniform random distribution in a D-dimensional search space. Each starling s_i in the current iteration t is denoted by a 2-tuple s_i (t) = (X_i (t), F_i (t)), where X_i (t) = [x_{i1}, x_{i2} ... x_{iD}] and F_i (t) are the position and fitness value of starling s_i respectively. Starlings form the murmuration M using dynamic multi-flock defined in Definition 2. In the murmuration M, a portion of the starling is separated by Eq. (1) to enhance the population diversity using a separating search strategy.

Then, each constructed flock flies using diving or whirling search strategies based on Definition 3.

3.1 Separating search strategy (Diversity)

In a murmuration, some starlings are usually separated from their flocks, which is our motivation to model a separation search strategy to provide diversity. A portion of the starlings is randomly selected from the starling population S to construct a separated population or P_{sep}. For each iteration t, the number of P_{sep} is computed by Eq. (1), and some dimensions of starlings are randomly selected and changed using the separating search strategy defined by Eq. (2). Where X_G (t) is the global position obtained so far; and $X_{r'}$ (t) is selected from a proportion of the best starlings and separated population, and X_r (t) is randomly selected from a population. The separating search strategy also uses a new operator $Q_1(y)$ called separation defined by Definition 1.

$$P_{sep} = \frac{log(t+D)}{log(MaxIt) \times 2} \tag{1}$$

$$X_i(t+1) = X_G(t) + Q_1(y) \times \left(X_{r'}(t) - X_r(t)\right) \tag{2}$$

Definition 1 (Separation operator). The separation operator is applied to maintain the population diversity based on the quantum harmonic oscillator shown in Eq. (3) with n=1. In the quantum harmonic oscillator, $\alpha = \left(\frac{m \times k}{\hbar}\right)^{\frac{1}{4}}$, where m is the particle's mass, k is the strength, and the parameter h is Planck's constant [77]. The function H_n is the Hermite polynomial, which shows the multiple possible eigenstates existing in the system with integer index n, and y is a random number from the standard normal distribution.

$$Q_1(y) = \left(\frac{\alpha}{2^n \times n! \times \pi^{\frac{1}{2}}}\right)^{\frac{1}{2}} \mathrm{H_n}(\alpha \times \mathrm{y}) \times e^{-0.5 \times \alpha^2 \times \mathrm{y}^2}, \qquad \alpha = \left(\frac{m \times k}{\hbar}\right)^{\frac{1}{4}} \tag{3}$$

Definition 2 (Dynamic multi-flock construction). Let Sf (t) = {sf_1, sf_2… sf_i… $sf_{\acute{N}}$} be a fitness-ascending-ordered representation of the set S in the iteration t based on Eq. (4), where sf_i is the fitness value of starling s_i and $\acute{N}$ = N - P_{sep}. The representative set R is built using Eq. (5), including k first elements of the set Sf, which are the k best starlings or solutions in the iteration t. A dynamic multi-flock is defined using a particular partitioning in which the set Sf is partitioned into k non-empty flocks f_1…f_k. By this partitioning, each element of representative set R= {R_1… R_k} is assigned as the first element of flocks f_1 … f_k respectively. Then, as Fig.

3 shows, other elements of Sf are split using Eq. (6) into k equal portions $P_1 \ldots P_k$, and starlings of portion P_i are considered as members of flock f_i.

$$Sf\ (t) = \{sf_i\ (t) \in S \mid sf_i\ (t) \le sf_{i+1}\ (t)\ for\ \ i = 1, \ldots Ń\} \tag{4}$$

$$R\ (t) = \{sf_i\ (t) \in Sf(t)\ for\ \ i = 1, \ldots k\} \tag{5}$$

$$P = S - R\ and\ P = \bigcup_{i}^{k} P_i\ \ and\ |P_i| = |P_j|\ for\ i \neq j\ \in (1, \ldots k) \tag{6}$$

Therefore, each flock f_q consists of n starlings (n= Ń/k), including a representative (R_q) selected from the representative set R and a portion (P_q), including (Ń/k)-1 members. Since the fitness values of starlings are changed in the next iteration, the set Sf (t+1) is ordered differently from Sf (t). Then, the representative and members of each flock in the multi-flock $f_1 \ldots f_k$ are dynamically changed, which provides information sharing between flocks during iterations.

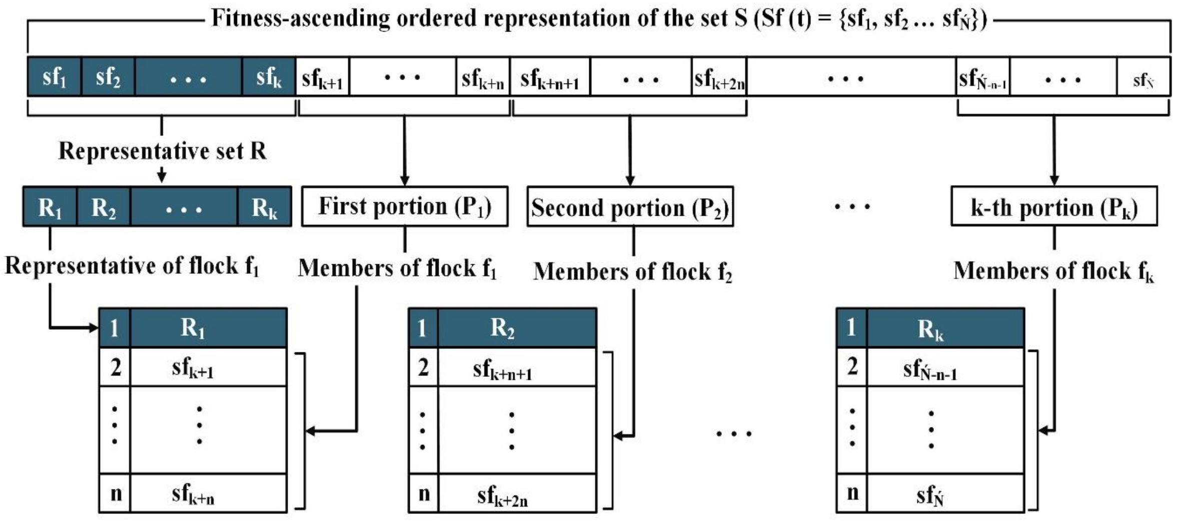

Fig. 3. Dynamic multi-flock construction.

In this modeling, the search space is sensed by the quality of flock f_q, which is denoted Q_q and determined by Definition 3.

Definition 3 (Flock quality). The flock quality f_q includes n distinct starlings in iteration t denoted by Q_q (t) and is determined by Eq. (7).

$$Q_q(t) = \frac{\sum_{i=1}^{k} \frac{1}{n} \sum_{j=1}^{n} sf_{ij}(t)}{\frac{1}{n} \sum_{i=1}^{n} sf_{qi}(t)} \tag{7}$$

where sf_{ij} (t) is the fitness value of the i-th starling in the subpopulation of the flock f_j; k is the number of flocks in a murmuration M, and n is the number of starlings in each flock.

As shown in Eq. (8), if the quality of the flock f_q (Q_q (t)) is less than or equal to the average of the quality of all flocks (μ_Q (t)), it means that flock f_q has a high chance for locating in an unpromising zone. Therefore, all n starlings of the flock f_q are moved using the diving search strategy to explore the search space. Otherwise, it means that flock f_q is located in a suitable zone, and its starlings explore around this zone using the whirling search strategy. The diving and whirling search strategies are subsequently described in detail.

$$X_i(t+1) = \begin{cases} Using\ diving\ search\ strategy & if\ \ Q_q(t) \le \mu_Q(t) \\ Using\ whirling\ search\ strategy & if\ \ Q_q(t) > \mu_Q(t) \end{cases} \tag{8}$$

3.2 Diving search strategy (Exploration)

The diving search strategy is designed to explore the search space effectively. Given that flock f_q, including starlings $\{s_1 \ldots s_n\}$ is located in an unpromising region. Then, this region is bypassed by the diving search strategy that is including the upward and downward quantum dives and a quantum random dive (QRD) operator for selecting the quantum dives. The QRD is defined by Definition 4. Before embarking on this definition, the next paragraph describes some essential principles of quantum computing.

Quantum bit or qubit: A qubit is an essential information unit in quantum computing theory. It is a quantization of a two-state system, which is represented by a linear superposition of its two orthonormal basis states or basis vectors denoted by $|0>= \begin{bmatrix}0\\1\end{bmatrix}$ and $|1>= \begin{bmatrix}1\\0\end{bmatrix}$. A qubit state $|\psi\rangle$ is a superposition of these orthonormal states and described by Eq. (9), where α and β are the probability amplitudes in the corresponding states. The probability of qubit outcome $|0>$ with value '0' is $|\alpha|^2$, and the probability of qubit outcome $|1>$ with value '1' is $|\beta|^2$.

$$|\psi> = cos\frac{\alpha}{2}\ |0> + sin\frac{\alpha}{2}\ e^{i\beta}\ |1> \tag{9}$$

A quantum random walker: Suppose the particle i is a walker in the Hilbert space H built by the inner product of two quantum systems, H_c and H_p. In this space, H_c is the coin Hilbert space of two basis states {|0>, |1>}, and H_P is the Hilbert space spanned by the positions of the particle i. These systems can be described by repeating a unitary evolution operator U=S.C, where S is a conditional shift operator, and C is a rotation matrix of qubit defined by Eq. (10) [78] that represents a rotation by angles θ and φ.

$$C = \begin{bmatrix} e^{i\varphi} cos\,\theta & e^{i\varphi} sin\,\theta \\ -e^{-i\varphi} sin\,\theta & e^{-i\varphi} cos\,\theta \end{bmatrix} \tag{10}$$

Therefore, the new state of the i-th walker denoted by $|\psi(t+1, X_i)>$ can be computed by Eq. (11).

$$\psi(t+1, X_i) >= U \times |\psi(t, X_i) >= S \times C \times |\psi(t, X_i) > \quad (11)$$

If the flock f_q has been located in an unpromising region because of its quality, $Q_q(t) \leq \mu_Q(t)$. Then, $|\psi(t+1, X_i)\rangle$ as the next position of each starling s_i in this flock is determined using the diving search strategy defined in either Eq. (12) or Eq. (13).

$$|\psi(t+1, X_i)\rangle = \mathit{Downward\ quantum\ dive} = |\psi(R_D)\rangle - |\psi^{Down}(X_i)\rangle \times (|\psi(X_i) - |\psi(X_r)\rangle) \quad (12)$$

$$|\psi(t+1, X_i)\rangle = \mathit{Upward\ quantum\ dive} = |\psi(R_D) + |\psi^{Up}(X_i)\rangle \times (|\psi(X_i)\rangle - |\psi(X_j)\rangle + |\psi(\delta_1)\rangle) \quad (13)$$

In Eqs. (12 and 13), $|\psi(R_D)\rangle$ is the representative member of the flock, $|\psi(X_i)$ is the current position of starling s_i, and $|\psi^{Up}(X_i)\rangle$ and $|\psi^{Down}(X_i)\rangle$ are two quantum probabilities defined in Definition 4. In Eq. (12), $|\psi(X_r)\rangle$ is the position of a random starling in the flock. In Eq. (13), $|\psi(X_j)\rangle$ is randomly selected from the union set of the current population and the best starlings set, and $|\psi(\delta_1)\rangle$ is a random position selected from the current population and the best starlings set obtained so far. The dive search strategy selects either upward or downward quantum dive using a quantum random dive operator defined in Definition 4.

Definition 4 (Quantum random dive operator): A quantum random dive operator (QRD) is defined by Eq. (14). $|\psi^{Up}(X_i)\rangle$ and $|\psi^{Down}(X_i)\rangle$ are two quantum probabilities that are determined based on the unitary evolution operator U= S.C for selecting either upward or downward quantum dive.

$$QRD = \begin{cases} \mathit{Upward\ quantum\ dive} & \mathit{if}\ |\psi^{Up}(X_i) > |\psi^{Down}(X_i)| \\ \mathit{Downward\ quantum\ dive} & \mathit{if}\ |\psi^{Up}(X_i)| \leq |\psi^{Down}(X_i)| \end{cases}$$

$$|\psi^{Up}(X_i)\rangle = e^{i\varphi} \cos\theta \times |\psi(\delta_2)\rangle - e^{-i\varphi} \sin\theta \times |\psi(\delta_2)\rangle \quad (14)$$

$$|\psi^{Down}(X_i)\rangle = e^{i\varphi} \sin\theta \times |\psi(\delta_2)\rangle + e^{-i\varphi} \cos\theta \times |\psi(\delta_2)\rangle$$

In Eq. (14), $|\psi(\delta_2)\rangle$ is an inverse-Gaussian distribution (iGd) which is computed by Eq. (15) to generate the random numbers with values of λ and μ. Also, y is a random number from the standard normal distribution.

$$|\psi(\delta_2)\rangle = \sqrt{\frac{\lambda}{2 \times \pi \times y^3}} \times e\left[-\frac{\lambda(y-\mu)^2}{2 \times \mu^2 \times y}\right] \quad (15)$$

Fig. 4 shows the flock f_q consists of n starlings using the diving search strategy that selects either the upward or downward quantum dive using the QRD operator.

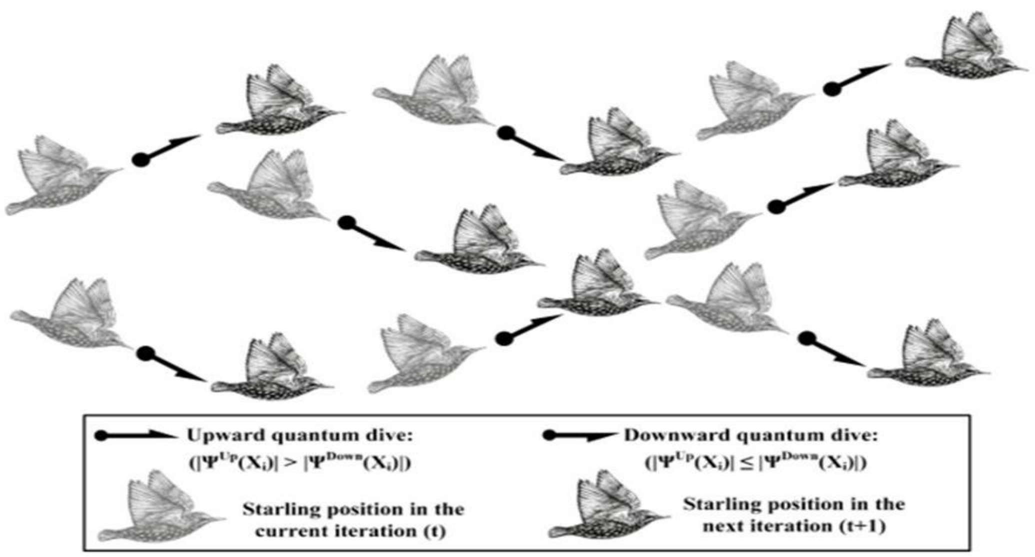
Upward quantum dive:
(|Ψ^Up(X_i)| > |Ψ^Down(X_i)|)
Downward quantum dive:
(|Ψ^Up(X_i)| ≤ |Ψ^Down(X_i)|)
Starling position in the current iteration (t)
Starling position in the next iteration (t+1)

Fig. 4. The diving search strategy for flock f_q using upward and downward quantum dive.

3.3 Whirling search strategy (Exploitation)

When flock f_q has a good quality (Q_q (t) > μ_Q (t)) in iteration t, then based on Eq. (8), the next position of each starling s_i in flock f_q is determined using the whirling search strategy. Inspired by the nature of murmuration [79], we define the whirling search strategy in Eq. (16) to locally exploit search zones. In Eq. (16), X_i (t) is the current position of starling s_i, and X_{RW} (t) is randomly selected from the representative members of those flocks, which are considered for the whirling search strategy. Also, X_N (t) is a random neighbor in the neighborhood of starling s_i with a radius equal to the average of the maximum and minimum Euclidean distances s_i with other starlings of its flock. Moreover, to prevent the exploitation from losing its diversity, the whirling search strategy applies a new cohesion operator, C_i (t) defined in Eq. (17), in which the cohesion coefficient $\xi(t)$ is a random number in the range of (0, 1].

$$X_i(t+1) = X_i(t) + C_i(t) \times (X_{RW}(t) - X_N(t)) \tag{16}$$

$$C_i(t) = cos(\xi(t)) \tag{17}$$

4. SMO algorithm

This section proposes a novel, bio-inspired algorithm named starling murmuration optimizer (SMO) based on the murmuration modeling introduced in the previous section. Fig. 5 shows the flowchart of the proposed SMO algorithm in which first, N starlings are randomly distributed in the D-dimensional search space using Eq. (18) where x_{id}, x_d^U, and x_d^L are d-th dimension of starling s_i, upper and lower bounds of the search space, respectively.

$$x_{id} = x_d^L + rand(0,1) \times (x_d^U - x_d^L), \qquad d = 1, 2, ..., D; \qquad i = 1, 2, ..., N \tag{18}$$

Then, a portion of the starlings is separated using Eq. (1) to explore the problem space using the separating search strategy defined by Eq. (2). The rest of the starlings are considered to construct the multi-flock dynamically using Algorithm 2 shown in Fig. 7, where first, the representative set Sf is built including ascending-ordered fitness values of the set S. Then, as shown in Fig. 3, the multi-flock is constructed using Definition 2. Next, the quality of flocks is computed by Eq. (7) to either select the diving or the whirling search strategy. Finally, at the end of each iteration, the best solution of each starling and the global best solution are updated. The pseudocode of the proposed SMO algorithm is presented in Fig. 6.

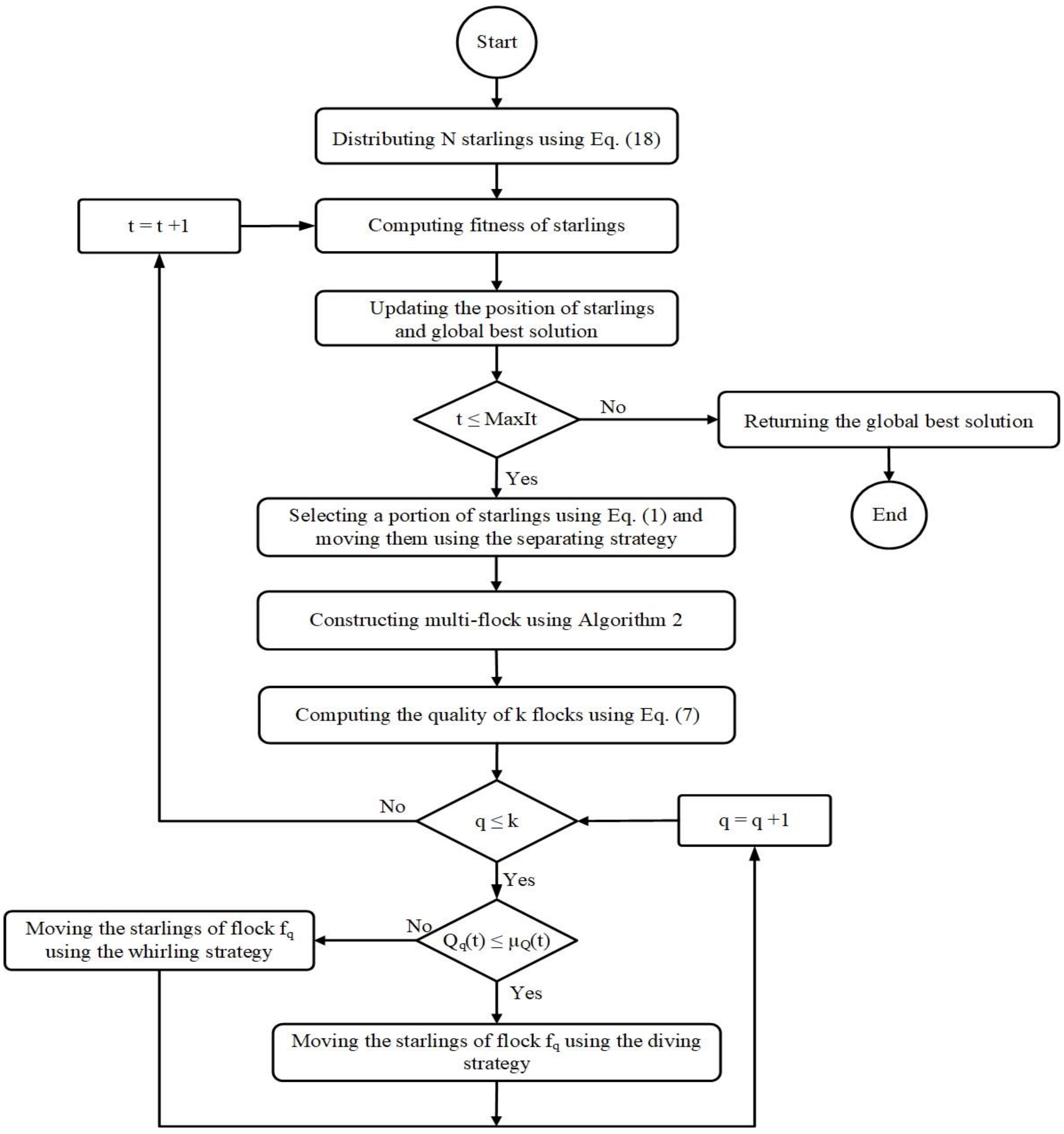

Start
Distributing N starlings using Eq. (18)
t = t +1
Computing fitness of starlings
Updating the position of starlings and global best solution
t ≤ MaxIt
No
Returning the global best solution
End
Yes
Selecting a portion of starlings using Eq. (1) and moving them using the separating strategy
Constructing multi-flock using Algorithm 2
Computing the quality of k flocks using Eq. (7)
No
q ≤ k
q = q +1
Yes
Moving the starlings of flock f_q using the whirling strategy
No
Q_q(t) ≤ μ_Q(t)
Yes
Moving the starlings of flock f_q using the diving strategy

Fig. 5. The flowchart of the starling murmuration optimizer (SMO)

```
Algorithm 1. Starling Murmuration Optimizer (SMO)
Input: N (Number of starlings), k (Number of flocks), and MaxIt (Maximum iterations).
Output: The global best solution.
 1:  Begin
 2:  Randomly distribution N starlings in the search space.
 3:  Set t =1.
 4:  While   t ≤ MaxIt
 5:      Select a portion of starlings by Eq. (1) and move them using the separating strategy.
 6:      Multi-flock construction by Algorithm 2.
 7:      Compute the quality of k flocks by Eq. (7).
 8:      For  q = 1→ k
 9:          If   $Q_q(t) \le \mu_Q(t)$ */ Comparing the flock quality $f_q$ to select movement strategy
10:              Move the starlings of flock $f_q$ using the diving strategy.
11:          Else
12:              Move the starlings of flock $f_q$ using the whirling strategy.
13:          End if
14:      End for
15:      Update the position of starlings and global best solution.
16:      t = t + 1.
17:  End while
18:  Return the position of the best starling as a global best solution.
19:  End
```

Fig. 6. Pseudocode of starling murmuration optimizer (SMO)

```
Algorithm 2. Multi-flock construction
Input: S (The set of N starlings), and k (Number of flocks).
Output:  Multi-flocks $f_1 \dots f_k$.
1:   Procedure multi-flock construction
2:       Sf = fitness-ascending-ordered representation of the set S.
3:       R= the k first elements of Sf, including $R_1 \dots R_k$.
4:       P= the k portions $P_1 \dots P_k$ built from Sf –R={$Sf_{k+1}$, $Sf_{k+2}$, …, $Sf_{Ń}$}.
5:       For i = 1→ k
6:           $f_i$= {$R_i$, $P_i$}     */ Constructing flock $f_i$ using Definition 2.
7:       End For
8:       Return multi-flocks $f_1 \dots f_k$.
9:   End Procedure
```

Fig. 7. Pseudocode of multi-flock construction

4.1 The computational complexity of the SMO algorithm

Fig. 6 shows that the computational complexity of the proposed SMO algorithm is determined mainly by the following four phases: (1) initialization, (2) separating search strategy (3) multi-flock construction, and (4) diving or whirling search strategy. In the initialization phase, the SMO algorithm creates N solutions with D dimension using Eq. (19) with computational complexity O (ND). Then, in the worst case, for all starlings, the separating phase is used with the computational complexity O (ND). Next, in the third phase using Algorithm 1, k flocks are constructed by partitioning Ń starlings based on their ascending-ordered fitness values with O (NlogN + k). Finally, in the fourth phase, the quality of each flock is computed by Eq. (7) with computational complexity O (nD), and each flock is moved either by the diving or whirling search strategy by O (nD). The fourth phase is used for all k flocks; thus, the computational complexity of this phase is O (2knD). These phases are repeated by the maximum iterations T, then the overall computational complexity of SMO is O (ND + T ((NlogN+k) + 2knD + ND). Since kn = N, the computational complexity of SMO is equal to O (TNlogN+2TND), and when D is much larger than logN, it is equal to O (TND).

5. Experimental evaluation of SMO algorithm

The SMO algorithm was evaluated by numerical experiments using a multifarious combination of benchmark test functions. These experiments were set up differently to analyze the behaviors of SMO from both qualitative and quantitative aspects. All experiments were run on a personal computer with the following features: Intel(R) Core (TM) i7-3770 CPU, 3.4 GHz, and 8 GB RAM, Windows 7, 64-bit operating system. All algorithms were implemented by using version R2018b of MATLAB programming.

In the following subsections, the properties of test functions are first described in detail. Then, a set of experiments was conducted to analyze the qualitative behavior of the SMO algorithm. Finally, its quantitative behavior was compared with other competitive algorithms via different tests.

5.1 Multifarious combination of the benchmark test functions

Since 2005 a series of different benchmark test functions with various properties have been introduced as a part of the IEEE congress on evolutionary computation (CEC Competitions). The CEC 2013 [68], CEC 2014 [69], CEC 2017 [70], and CEC 2018 benchmark test functions were designed for evaluating single objective optimization algorithms whereas other CEC benchmark functions such as CEC 2009, 2019, and 2020 were designed for assessing multi-objective evolutionary algorithms, 100-digit challenges special session, and constrained engineering optimization. The CEC 2018 with 29 test functions is also the same as CEC 2017, excluding the second test function "shifted and rotated sum of different power". Thus, benchmark functions CEC 2013, 2014, and 2017 are the best nominate for evaluating the single objective optimization algorithms such as the proposed SMO.

From the literature, algorithms have shown both outstanding and poor performances on different test functions, therefore to have a comprehensive evaluation, we selected a multifarious combination of complex test functions from CEC 2013, 2014, and 2017. As shown in Tables A.1-A.4 of Appendix A, we selected the most complex test functions with properties such as a non-separable, smooth but narrow ridge, complex landscapes, many basins of attraction, multi-modal, symmetric/asymmetrical. For all functions, the search space's bounds were scaled between $[-100, 100]^D$, where D is the dimension of the problems. This combination is classified into four groups: unimodal, multi-modal, hybrid, and composition as follows.

Unimodal group functions: This combination consists of functions F_1–F_8, each including one global optimum that is usually smooth but narrow ridge, and the difficulty for solving these functions generally increases with the dimensionality. Therefore, they are suitable for testing the exploitation ability and convergence speed of the SMO algorithm.

Multi-modal group functions: The second combination is a collection of the functions F_9–F_{18} designed by many local optima, and the global best solution is hidden in many hills and narrow valleys. These test functions, there are highly potential for evaluating the ability of exploration, skipping the local optima, and avoiding premature convergence on the valley floor.

Hybrid group functions: As shown in Table A.3, this combination consists of the test functions F_{19}–F_{28} to evaluate the performance of the algorithm for solving real-world problems with many subcomponents and different properties. Moreover, these functions are used to assess the abilities of the balance between exploration and exploitation.

Composition group functions: The fourth combination includes functions F_{29}-F_{38}, which are very challenging because it is difficult to determine their global optimum. These functions are also suitable to evaluate the abilities of the balance between exploration and exploitation.

5.2 Qualitative analysis

This subsection describes the analysis of the convergence behavior of SMO and its ability to balance exploration and exploitation by some of the benchmark test functions. This experiment set was performed by 200 starlings distributed equally in 10 flocks on a 2-dimensional search space.

5.2.1 Convergence analysis

In convergence analysis of SMO, four metrics are used including search history, trajectory, average fitness values of all starlings, and the convergence rate. The search history of all starlings for the sampled points for iterations shows the ability of SMO for exploring the search space and exploiting the vicinity of the global optimum. The trajectory of the representative starling s_1 is tracked in the first dimension to show how SMO has abrupt movements in the initial iterations and gradually converges to a point in the final iterations. In the second column of Fig. 8, where the search history is covered along the contour lines, the sampled points are colored in black, and the global optimum solution is marked with a red star. The results reveal that the SMO algorithm exploits in the vicinity of the global optimum very accurately in the unimodal test functions, and it bypasses the local optima to reach the promising regions by exploring the multi-modal test functions. Therefore, in all of the test functions, the SMO algorithm can search globally and eventually converge to a point in the search space.

The trajectory curves illustrated in the third column indicate that the representative starling s_1 starts its evolution with large fluctuations at the initial iterations. Its changes gradually decrease over the course of iterations, which guarantees the convergence to a point in the search space. The average fitness values and the best solutions over the course of iterations are gradually decreased by tracking the curves shown in the fourth and fifth columns, which means the movement strategy is evolving their candidate solutions. The decreasing of average fitness values indicates that the SMO algorithm can dynamically focus on more promising areas and converge to a point. Meanwhile, the decrease shown in the fifth column proves the SMO can improve the quality of the starlings' position over the course of the iterations. It initially explores the search space to bypass the local optima, and then a growing attraction contributes to exploiting the promising local regions. Thus, it can reveal an accelerated convergence trend toward the global optimum.

5.2.2 Exploration and exploitation behavior analysis

It is expected that using the dynamic multi-flock and diving search strategy in the SMO algorithm increases the diversity and opportunity of finding the global optimum position by exploring undiscovered regions, while the starlings of a flock, through the whirling search strategy, efficiently exploit around a promising area. This experiment analyzed the exploration and exploitation ability of the SMO algorithm to solve different problems.

The impact of the exploration and exploitation is computed by the dimension-wise diversity measurement approach [80] and illustrated in Fig. 9. According to this approach, increasing the distance value within dimensions indicates that the flock of starlings is scattered and explores the search space. In contrast, the flock of starlings is placed close to each other for converging to a condensed area when the mean value is reduced. The dimension-wise diversity of SMO in the current iteration t (Diversity (t)) is computed by Eq. (20). Where the parameter $Diversity_d$ is the diversity of dimension d computed by Eq. (21); x_{id} is the position of dimension d of starling s_i, and the median (x_d) is the median value of dimension d for all N starlings. The percent of the exploration and exploitation abilities are computed by Eqs. (22) and (23), where $Diversity_{max}$ is the maximum diversity found by Eq. (20) in all iterations. Fig. 9 shows the obtained results of exploration and exploitation abilities of SMO in each iteration for different functions.

$$Diversity(t) = \frac{1}{D}\sum_{d=1}^{D} Diversity_d \tag{20}$$

$$Diversity_d = \frac{1}{N}\sum_{i=1}^{N} median(x_d) - x_{id} \tag{21}$$

$$Exploration\ (\%) = \frac{Diversity(t)}{Diversity_{max}} \times 100 \tag{22}$$

$$Exploitation(\%) = \frac{|Diversity(t) - Diversity_{max}|}{Diversity_{max}} \times 100 \tag{23}$$

This experiment's results were conducted by some unimodal, multi-modal, hybrid, and composition functions with different dimensions of 30, 50, and 100 with the maximum number of iterations 500. The curves are plotted in Fig. 9 prove that the SMO algorithm has an outstanding exploitation ability to solve F_6 from unimodal group functions with D 30, 50, and 100. In the initial iterations, SMO mostly explores the search space by the diving search strategy because a few flocks can find a promising area. Then, it gradually exploits some flocks located in the promising area, and finally, many flocks are highly exploited by the whirling search strategy in the final iterations. This behavior proves the exploitation ability of the proposed algorithm.

There are many local optima in multi-modal functions that exponentially increase when the dimension is increased, which is essential for evaluating the exploration behavior. For instance, the results on function F_{17} show that the percentage of exploration of the SMO algorithm is more than its exploitation, except in the final iterations; thus, it has superb exploration. This is due to the diving search strategy that moves the starlings from inferior regions, while the separating search strategy also increases the diversity and corrects the starlings trapped in the local optima. The results show a high exploration in the initial iterations for the candidate hybrid and composition functions F_{20}, F_{22}, F_{24}, and F_{37} and then a balance between exploration and exploitation, and finally, more exploitation in the final iterations. This behavior proves that the SMO algorithm can strike a balance between exploration and exploitation. Such an ability is achieved since SMO can determine the quality of flocks to select either the whirling or diving search strategy consciously.

5.3 Quantitative analysis

In this subsection, the performance of the SMO algorithm is analyzed and compared with the state-of-the-art swarm intelligence algorithms: comprehensive learning particle swarm optimizer (CLPSO) [30], artificial bee colony algorithm (ABC) [14], ant colony optimization for continuous domains (ACO_R) [81], Best-so-far ABC [15], krill herd (KH) [39], whale optimization algorithm (WOA) [40], butterfly optimization algorithm (BOA) [19], harris hawks optimization (HHO) [32], henry gas solubility optimization (HGSO) [82] and improved continuous ant colony optimization algorithms (LIACO$_R$) [83]. We performed several experiments to evaluate the ability of SMO to perform exploitation, exploration, local optima avoidance, and convergence. The experimental setup for this quantitative analysis is described as follows.

To ensure a fair comparison, the parameters of the competitive algorithms were set using their original setting shown in Table 2. All algorithms were run 30 times independently, and in each run, the number of population N was set to 200, and the maximum number of iterations (MaxIt) was 3000. Although the appropriate values of SMO's parameters are determined by some pretests reported in Appendix B. Then, all experiments were performed on the multifarious combination of unimodal, multi-modal, hybrid, and composition functions introduced in Subsection 5.1 with different dimensions 30, 50, and 100.

Table 2 Parameters values of competitive algorithms.

Alg.	Year	Ref.	Parameter's settings
CLPSO	2006	[30]	c_1 and c_2 are 1.49445, $PC \in (0.05, 0.5)$, and ω linearly decreases from 0.8 to 0.2.
ABC	2007	[14]	Limit = N×D, food number = N/2.
ACO$_R$	2008	[81]	q =10^{-4}, archive size k =50, speed of convergence = 0.85.
Best-so-far ABC	2011	[15]	Limit = N×D, food number = N/2.
KH	2012	[39]	Maximum diffusion speed = 0.005, the velocity of foraging = 0.02 and maximum induced speed = 0.01.
WOA	2016	[40]	α variable decreases linearly from 2 to 0 α_2 linearly decreases from −1 to −2, b = 1.
BOA	2019	[19]	Sensory modality c is 0.01, power exponent a is increased from 0.1 to 0.3, and p = 0.8.
HHO	2019	[32]	E_0 is a value between [-1, 1], and q and r = [0, 1].
HGSO	2019	[82]	Cluster number = 5, M_1= 0.1, M_2 = 0.2, β = 1, α = 1 and K = 1. Also, l_1=5E−03, l_2=100 and l_3=1E−02 for benchmark test functions, and l_1=1, l_2=10 and l_3=1 for engineering problems.
LIACO$_R$	2019	[83]	Evaporation rate (ξ) = 0.6, and q = 0.2.
SMO			k = 10, λ = 20, μ = 0.5, $\theta, \varphi \in (0, 1.8]$.

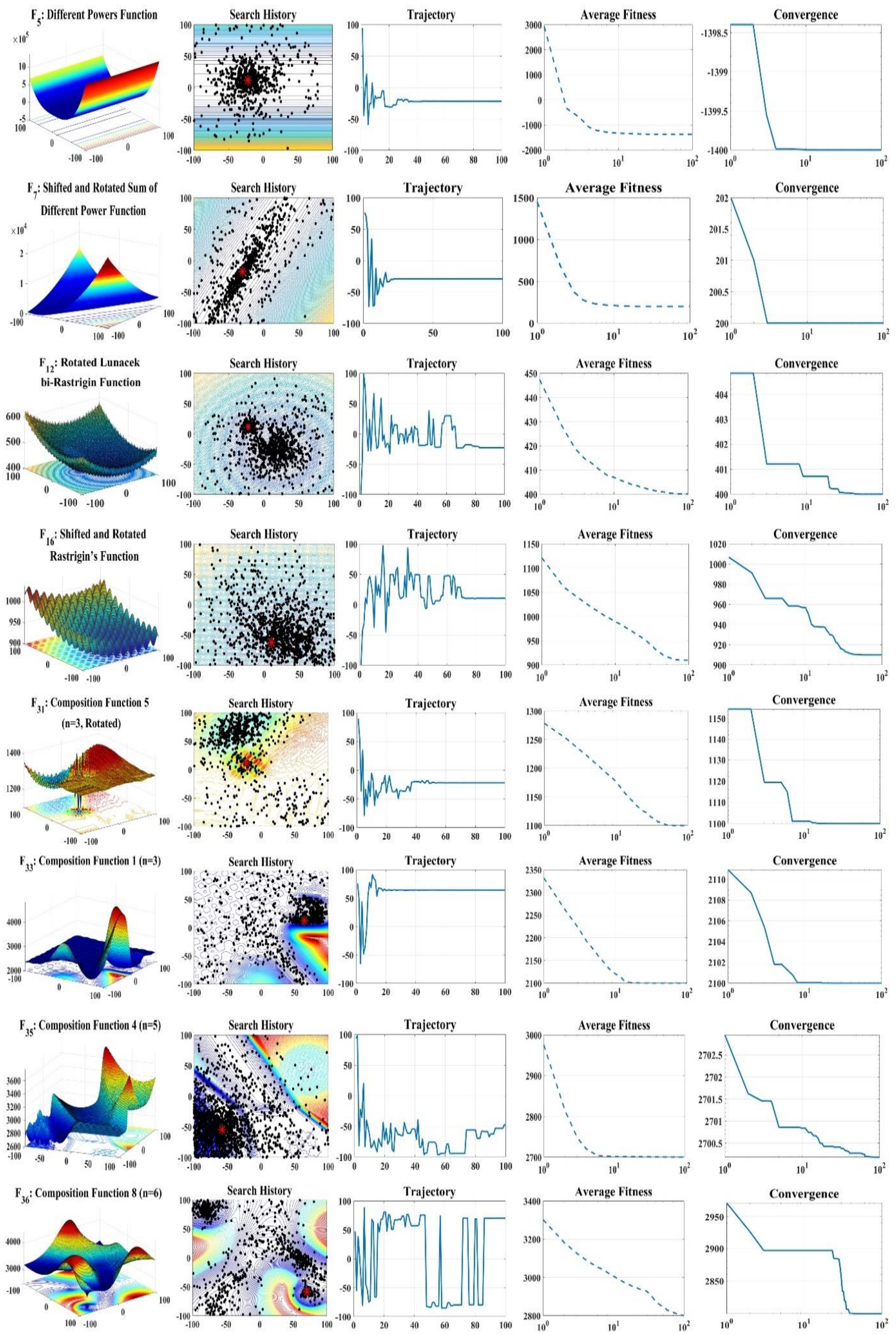

Fig. 8. Qualitative analysis including search history, trajectory, average fitness, and convergence curves.

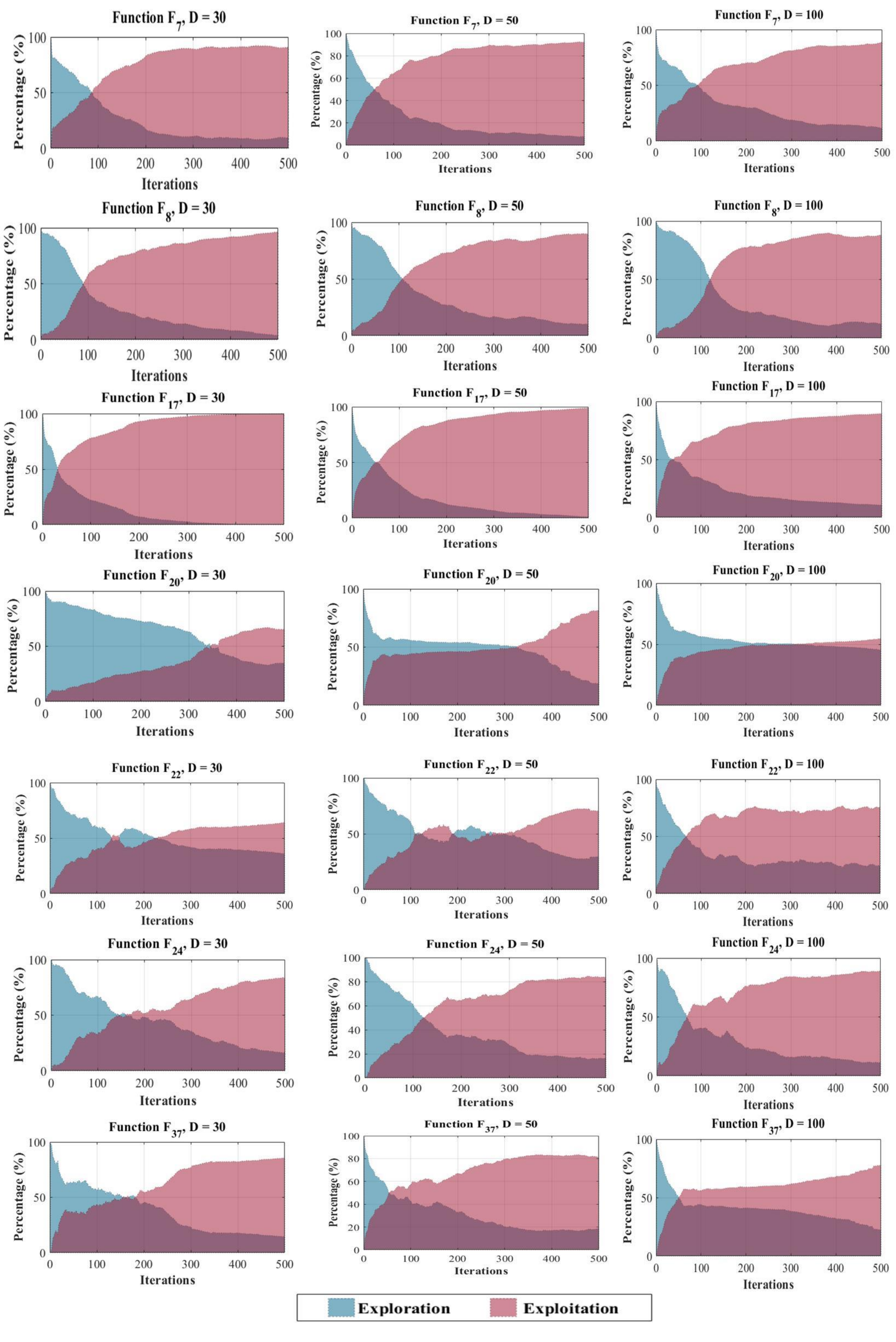

Fig. 9. Exploration and exploitation behavior analysis in some test functions.

In the following subsections, the experiments' results of quantitative analysis are provided in the tables. To facilitate a better understanding, the bold values indicate the best solutions of the winner algorithms, and W, T, and L stand for the number of the win, tie, and loss of each algorithm at the end of these tables, respectively.

5.3.1 Exploitation and exploration evaluation

To evaluate the exploitation ability of SMO, we used the unimodal group including different test functions that have only one global optimum. The overall performance shown in the unimodal section in Table 3 and the detailed results including average (Avg) and minimum (Min) of fitness value tabulated in Table B.3 indicate that our SMO algorithm can approximate the best optimal solution for most of the unimodal functions. These results prove that the SMO is very competitive in terms of exploitation ability. This is due to the whirling search strategy in Eq. (16) encourages the starlings to exploit around the global optimum. The multi-modal test functions are proper for evaluating the exploration capability of an optimization algorithm. The overall performance of the multi-modal section in Table 3 and the results shown in Table B.4 for multi-modal group functions F_9–F_{18}, prove that the SMO algorithm is superior to other comparative algorithms. This is attributed to the use of the quantum random dive operator introduced in Eq. (12) in the diving search strategy, which can guarantee the required exploration for moving toward the global optimum. Using the separating search strategy also provides a notable ability for effectively bypassing the local optima.

5.3.2 The ability of local optima avoidance

The hybrid and composition functions have challenging search spaces with a large number of local optima, which is necessary for evaluating the strength of the proposed algorithm in terms of the local optima avoidance. According to the results shown in the hybrid and composition section of Table 3 and detailed results shown in Tables B.5 and B.6, the SMO algorithm can accurately approximate the global optima solutions and it is very competitive on hybrid and composition functions compared with the other contender algorithms. These results provide evidence that the SMO algorithm can properly avoid local optima. The main reason for this ability is that the separation operator used in the separating search strategy in Eq. (1) can maintain the population diversity via the quantum harmonic oscillator shown in Eq. (2).

Table 3 Overall performance on different group functions.

Functions	D	Metrics	CLPSO (2006)	ABC (2007)	ACO$_R$ (2008)	Best-so-far ABC(2011)	KH (2012)	WOA (2016)	BOA (2019)	HHO (2019)	HGSO (2019)	LIACO$_R$ (2019)	SMO (Proposed)
	30	W|T|L	0|2|6	0|2|6	0|0|8	0|2|6	0|1|7	0|0|8	0|0|8	0|0|8	0|0|8	0|2|6	**6|2|0**
Unimodal	50	W|T|L	0|2|6	0|2|6	0|0|8	0|2|6	0|1|7	0|0|8	0|0|8	0|0|8	0|0|8	1|2|5	**5|2|1**
	100	W|T|L	0|0|8	0|2|6	0|0|8	0|1|7	0|0|8	0|0|8	0|0|8	0|0|8	0|0|8	1|2|5	**5|2|1**
	30	W|T|L	0|2|6	0|2|6	0|0|8	0|2|6	0|1|7	0|0|8	0|0|8	0|0|8	0|0|8	0|2|6	**6|2|0**
Multi-modal	50	W|T|L	0|2|6	0|2|6	0|0|8	0|2|6	0|1|7	0|0|8	0|0|8	0|0|8	0|0|8	1|2|5	**5|2|1**
	100	W|T|L	0|0|8	0|2|6	0|0|8	0|1|7	0|0|8	0|0|8	0|0|8	0|0|8	0|0|8	1|2|5	**5|2|1**
	30	W|T|L	0|2|6	0|2|6	0|0|8	0|2|6	0|1|7	0|0|8	0|0|8	0|0|8	0|0|8	0|2|6	**6|2|0**
Hybrid	50	W|T|L	0|2|6	0|2|6	0|0|8	0|2|6	0|1|7	0|0|8	0|0|8	0|0|8	0|0|8	1|2|5	**5|2|1**
	100	W|T|L	0|0|8	0|2|6	0|0|8	0|1|7	0|0|8	0|0|8	0|0|8	0|0|8	0|0|8	1|2|5	**5|2|1**
	30	W|T|L	0|2|6	0|2|6	0|0|8	0|2|6	0|1|7	0|0|8	0|0|8	0|0|8	0|0|8	0|2|6	**6|2|0**
Composition	50	W|T|L	0|2|6	0|2|6	0|0|8	0|2|6	0|1|7	0|0|8	0|0|8	0|0|8	0|0|8	1|2|5	**5|2|1**
	100	W|T|L	0|0|8	0|2|6	0|0|8	0|1|7	0|0|8	0|0|8	0|0|8	0|0|8	0|0|8	1|2|5	**5|2|1**

5.3.3 Convergence speed evaluation

In this section, the convergence behavior of the SMO algorithm is compared with other competitive algorithms. For such comparisons, the convergence curves on each test function are plotted using the best fitness values obtained by the contender algorithms. Convergence curves of some of unimodal, multi-modal, hybrid, and composition test functions are shown in Figs. 10-13 and convergence curves of the rest of the functions are presented in Figs B.2-B.4 of Appendix B. The curves indicate that the proposed SMO algorithm is faster than other algorithms in solving all functions.

These figures reveal three different convergence behaviors of SMO during the optimizing process. There is a common step in all three behaviors in which SMO converges quickly toward a promising region with a very steep descent slope in the initial iterations. The first behavior of SMO is shown in the convergence curves of test functions D30 {F_2, F_7, F_8, F_{20}, F_{38}}, D50 {F_7, F_8, F_{20}, F_{38}} and D100 {F_2, F_8, F_{38}}. In this behavior, after the common step, it searches in the vicinity of the global optimum and finds the solution before passing half of the iterations. In the second behavior shown on the test functions D50 {F_2, F_{23}, F_{28}} and D100 {F_7, F_{20}, F_{23}} after the common step, the SMO algorithm exploits the promising region and converges to the global optimum by a gentle descent slope. The last behavior registered for D30 and D50 {F_6, F_{12}, F_{13}, F_{14}, F_{17}, F_{18}, F_{21}, F_{27}, F_{28}, F_{29}, F_{31}, F_{33}, F_{37}}, and D100 {F_{21}, F_{27}, F_{29}, F_{31}, F_{33}, F_{37}}, although the SMO algorithm engages to improve the solutions, the best value is seldom decreased.

The results of this experiment show that the convergence behavior of the SMO algorithm is very competitive compared to the other algorithms. The results obtained for unimodal functions F_1-F_8 prove that it has an outstanding exploitation ability, which is due to the use of the whirling search strategy by the flocks located in the potential neighborhoods. Since the multi-modal functions can evaluate the exploration ability, the experimental results of SMO for multi-modal functions F_9 -F_{18} indicates that it provides a superb exploration ability. The main reason is that SMO uses the diving search strategy enriched by a quantum random dive operator defined in Eq. (12), by which the diversity of SMO can be increased to visit more unseen promising regions.

The experimental results of the proposed SMO algorithm for hybrid and composition functions F_{19}-F_{38} prove that SMO can balance between exploration and exploitation and avoid local optima trapping. This is because solving such hybrid and composition functions with a considerable number of local optima requires these abilities. SMO constructs dynamic multi-flocks, whereby the starlings of different flocks use either the diving or whirling search strategy by evaluating the quality of each flock. Thus, it can balance the exploration and exploitation by switching efficiently from a flock trapped in the local optima to a suitable exploration by another flock using the diving search strategy. Meanwhile, the quantum harmonic oscillator defined in Eq. (2) in the separating search strategy can maintain the population diversity and provide the required local optima avoidance for solving these functions.

5.3.4 The overall effectiveness of SMO

Table 4 shows the overall effectiveness (OE) [84] of the SMO algorithm and competitor algorithms based on the results reported in Table 3. The OE of the i-th algorithm is computed by Eq. (24), where N is the total number of test functions, and Li is the number of functions in which the i-th algorithm has lost. As the OE's result shown, the SMO in 86.84 % of the test functions with D=30, 50, and 100 can find the best solutions; however, a few competitors such as the $LIACO_R$ algorithm in some functions are the winner or tie to the SMO.

$$OE_i = \frac{N - L_i}{N} \times 100 \tag{24}$$

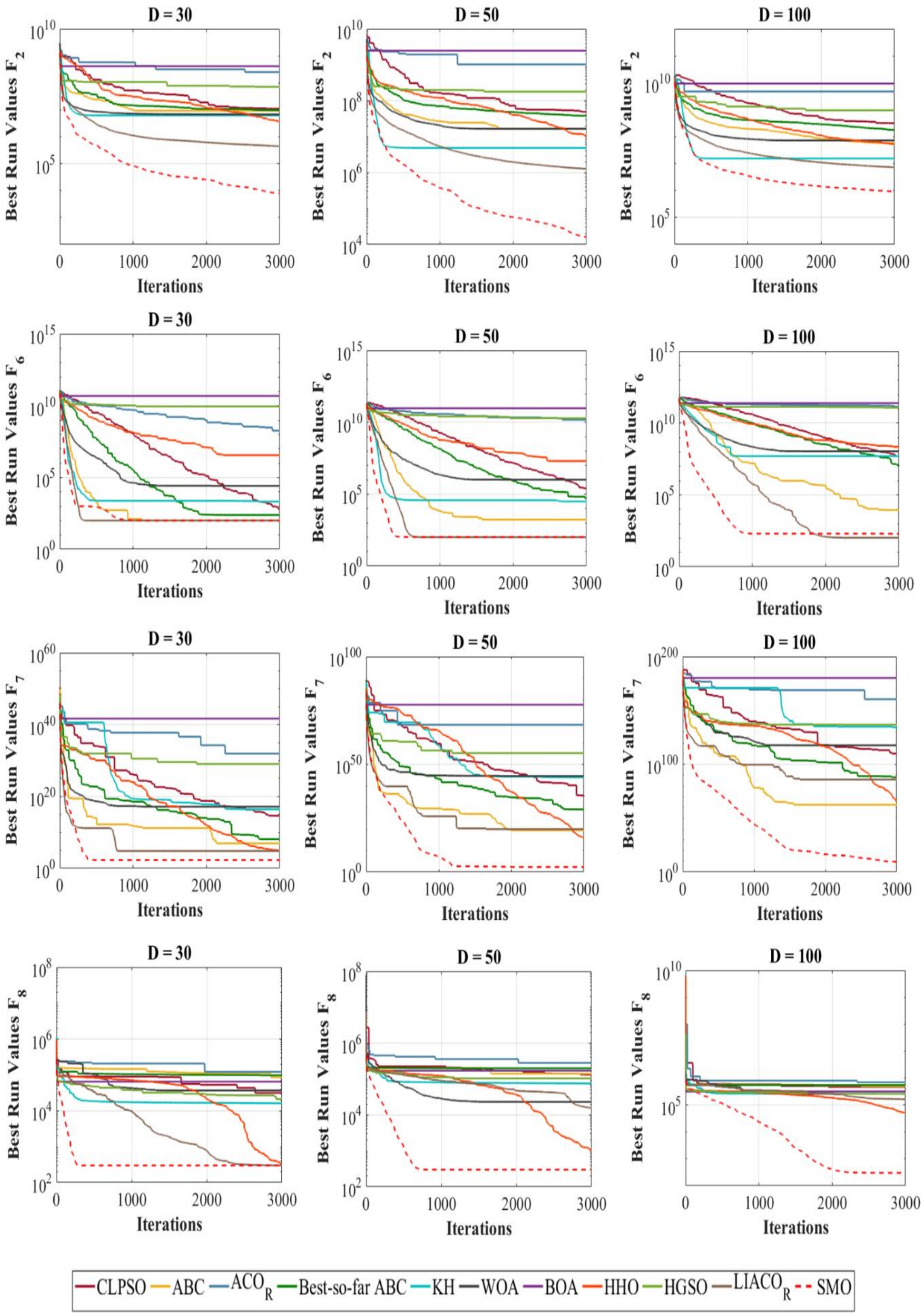

Fig. 10. Convergence curves of SMO and competitive algorithms on the unimodal functions.

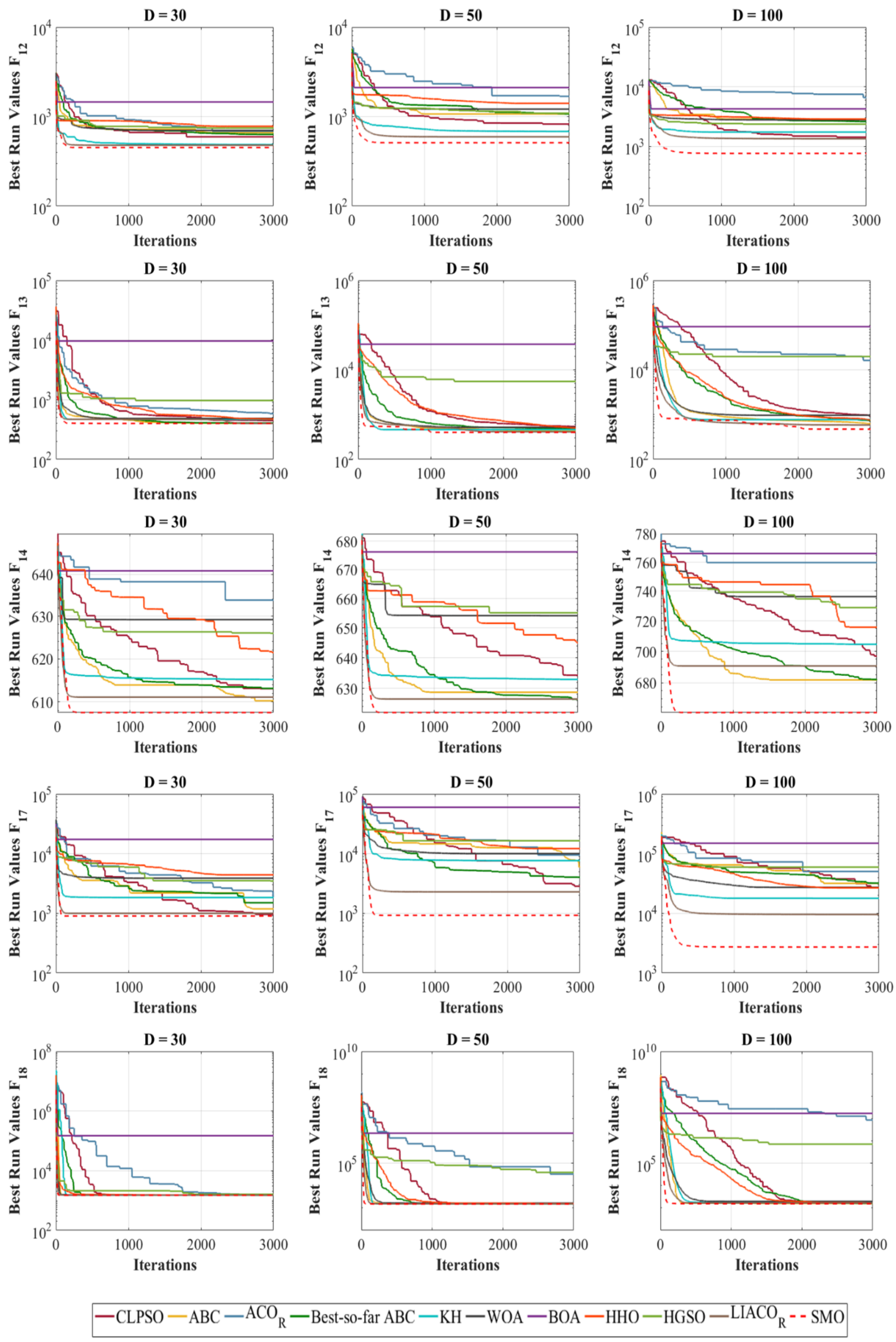

Fig. 11. Convergence curves of SMO and competitive algorithms on the multi-modal functions.

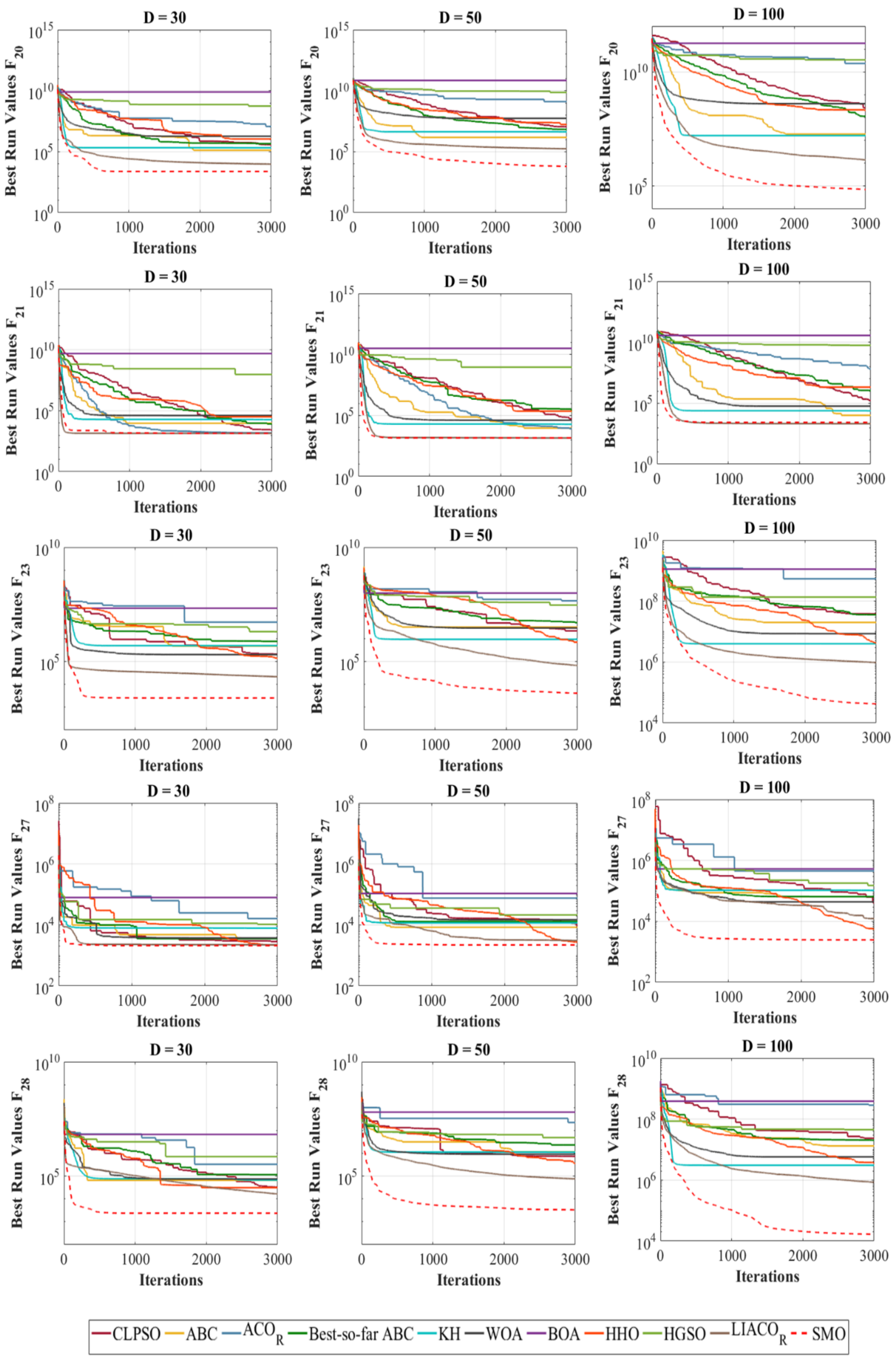

Fig. 12. Convergence curves of SMO and competitive algorithms on the hybrid functions.

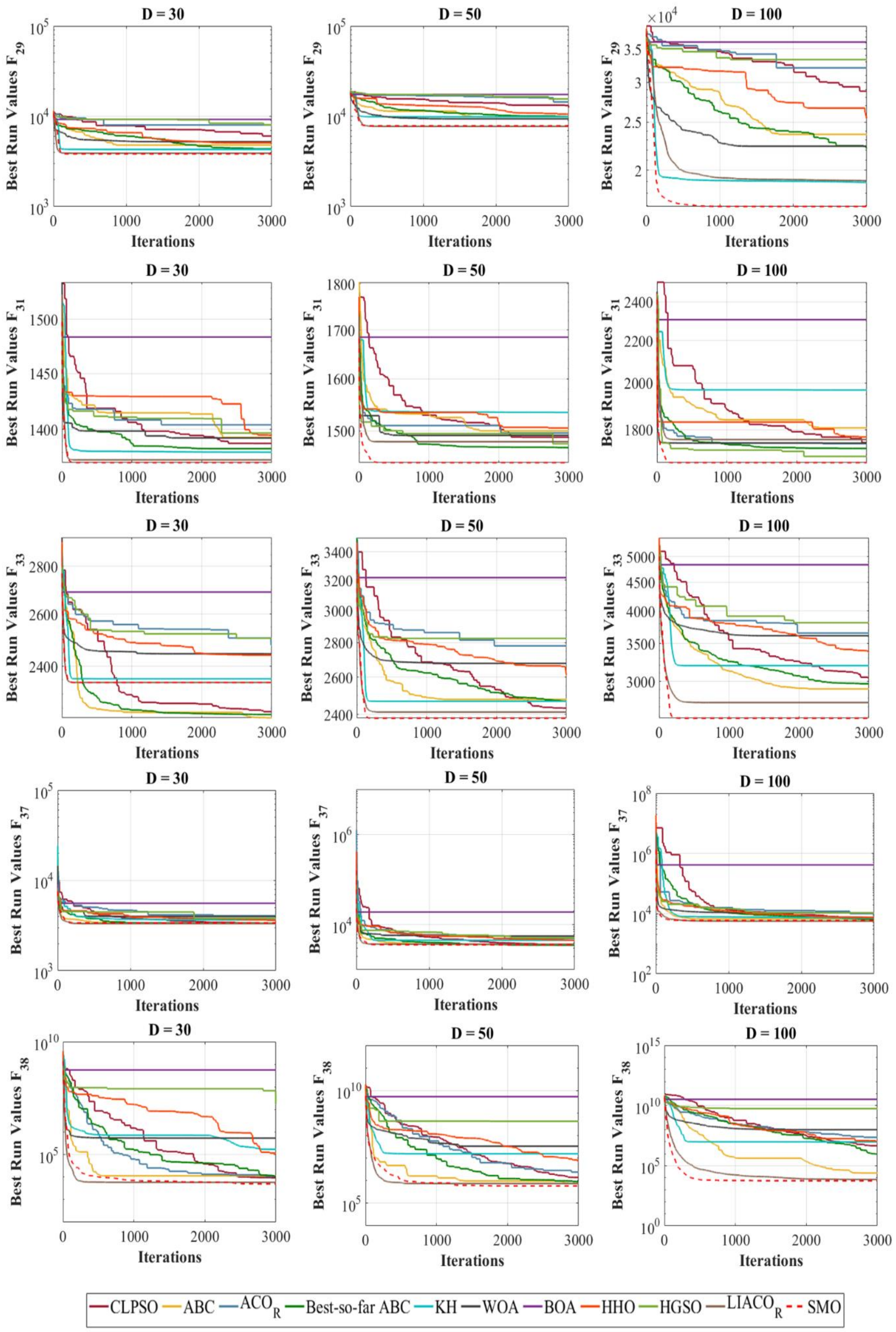

Fig. 13. Convergence curves of SMO and competitive algorithms on the composition functions.

Table 4 Overall effectiveness of the SMO and competitor algorithms.

Algorithms	30 (W|T|L)	50 (W|T|L)	100 (W|T|L)	Total (W|T|L)	OE
CLPSO	0|2|36	0|2|36	0|0|38	0|4|110	3.51%
ABC	1|3|34	0|2|36	1|2|35	2|5|105	7.90%
ACO_R	0|0|38	0|0|38	0|0|38	0|0|114	0%
Best-so-far ABC	0|3|35	1|2|35	0|1|37	1|6|107	6.14%
KH	0|2|36	0|1|37	0|0|38	0|3|111	2.63%
WOA	0|0|38	0|0|38	0|0|38	0|0|114	0%
BOA	0|0|38	0|0|38	0|0|38	0|0|114	0%
HHO	0|0|38	0|0|38	0|0|38	0|0|114	0%
HGSO	0|0|38	0|0|38	0|0|38	0|0|114	0%
$LIACO_R$	2|3|33	5|3|30	5|3|30	12|9|93	18.42%
SMO	32|3|3	29|3|6	29|3|6	**90|9|15**	**86.84%**

5.3.5 Non-parametric statistical test analysis

Besides the aforementioned experimental evaluation, SMO was statistically analyzed by the Wilcoxon signed-rank sum [73] and mean absolute error (MAE) statistical tests to prove its superiority.

First, the Wilcoxon test highlighted the gap between the SMO algorithm results and each comparative algorithm for all benchmark functions with different dimensions. As presented in each row of Table 5, the symbol '>' indicates that the SMO algorithm is significantly superior to the compared algorithm. The results of the Wilcoxon signed-rank sum distinguish the significant superiority of the proposed algorithm. Next, to determine how far the estimated solutions are from the optimal solution, we used mean absolute error (MAE) computed by Eq. (25), where NF is the number of functions, O_i is the global optimum of the function i, and y_i is the best result of the i-th function obtained by the algorithms.

$$MAE = \frac{1}{NF}\sum_{i=1}^{NF} |O_i - y_i| \tag{25}$$

Table 5 Wilcoxon's signed-ranks test.

Functions	Unimodal group		Multi-modal group		Hybrid group		Composition group	
Algorithms	p-value	Significance	p-value	Significance	p-value	Significance	p-value	Significance
SMO vs. CLPSO	1.8916E-49	>	6.1019E-13	>	1.2530E-106	>	3.478E-02	>
SMO vs. ABC	4.6532E-39	>	1.6755E-20	>	3.4420E-136	>	8.658E-07	>
SMO vs. ACO_R	6.1551E-88	>	6.5120E-75	>	4.2047E-117	>	7.911E-19	>
SMO vs. Best-so-far ABC	3.8332E-47	>	6.9970E-28	>	2.4490E-154	>	1.230E-11	>
SMO vs. KH	6.1551E-88	>	8.8832E-17	>	3.8500E-125	>	1.656E-05	>
SMO vs. WOA	3.8332E-47	>	2.3151E-40	>	6.3540E-126	>	3.455E-06	>
SMO vs. BOA	3.5607E-50	>	1.316E-202	>	1.5010E-245	>	5.481E-41	>
SMO vs. HHO	2.0387E-52	>	1.2932E-39	>	8.7420E-109	>	3.665E-05	>
SMO vs. HGSO	4.520E-141	>	3.711E-109	>	2.3150E-200	>	1.373E-11	>
SMO vs. $LIACO_R$	7.9825e-08	>	0.00924601	>	4.3616E-23	>	1.3639E-10	>

Table 6 MAE test of comparative algorithms on all test functions with different dimensions.

Unimodal group functions

Algorithms	MAE D=30	Rank D=30	MAE D=50	Rank D=50	MAE D=100	Rank D=100
CLPSO	5.40E+13	6	1.19E+34	6	8.62E+108	6
ABC	2.49E+07	4	2.67E+18	3	2.66E+61	2
ACO_R	1.06E+31	10	2.80E+67	10	2.81E+159	10
Best-so-far ABC	2.67E+08	5	1.41E+28	5	1.05E+87	5
KH	3.34E+15	7	1.08E+43	7	3.29E+132	7
WOA	1.74E+16	8	4.66E+43	8	4.84E+116	9
BOA	6.20E+40	11	5.65E+76	11	1.71E+179	11
HHO	9.61E+06	2	1.43E+15	2	3.49E+65	3
HGSO	1.39E+28	9	1.98E+54	9	6.30E+135	8
$LIACO_R$	1.65E+06	3	1.012E+19	4	7.77E+84	4
SMO	**1.15E+03**	**1**	**2.26E+04**	**1**	**2.56E+08**	**1**

Multi-modal group functions

Algorithms	MAE D=30	Rank D=30	MAE D=50	Rank D=50	MAE D=100	Rank D=100
CLPSO	6.42E+01	3	3.58E+02	3	3.11E+03	4
ABC	1.03E+02	4	6.97E+02	5	3.89E+03	7
ACO_R	2.67E+02	7	4.88E+03	9	8.69E+05	10
Best-so-far ABC	1.36E+02	5	5.43E+02	4	3.96E+03	8
KH	1.47E+02	6	8.11E+02	6	2.23E+03	3
WOA	5.13E+02	9	1.29E+03	7	3.47E+03	6
BOA	1.84E+04	11	2.31E+05	11	1.73E+06	11
HHO	4.90E+02	8	1.44E+03	8	3.44E+03	5
HGSO	5.60E+02	10	6.35E+03	10	8.08E+04	9
$LIACO_R$	4.63E+01	2	2.22E+02	2	1.23E+03	2
SMO	**2.00E+01**	**1**	**4.84E+01**	**1**	**3.38E+02**	**1**

Hybrid group functions

Algorithms	MAE D=30	Rank D=30	MAE D=50	Rank D=50	MAE D=100	Rank D=100
CLPSO	1.63E+02	3	4.39E+02	3	3.08E+03	4
ABC	2.02E+02	4	7.96E+02	5	3.98E+03	8
ACO_R	1.97E+06	10	1.36E+08	11	2.46E+09	11
Best-so-far ABC	2.35E+02	5	6.29E+02	4	3.59E+03	7
KH	2.47E+02	6	9.11E+02	6	2.31E+03	3
WOA	5.13E+02	8	1.29E+03	7	3.47E+03	5
BOA	1.83E+04	10	2.31E+05	10	1.73E+06	10
HHO	5.89E+02	9	1.54E+03	8	3.51E+03	6
HGSO	4.60E+02	7	6.25E+03	9	8.07E+04	9
$LIACO_R$	4.98E+03	2	3.77E+04	2	3.53E+05	2
SMO	**1.20E+02**	**1**	**1.14E+02**	**1**	**4.38E+02**	**1**

Composition group functions

Algorithms	MAE D=30	Rank D=30	MAE D=50	Rank D=50	MAE D=100	Rank D=100
CLPSO	1.38E+03	4	1.41E+05	5	4.49E+05	5
ABC	1.45E+03	5	7.67E+04	3	5.11E+03	3
ACO_R	1.85E+03	6	2.43E+05	6	2.29E+06	8
Best-so-far ABC	1.34E+03	3	9.09E+04	4	9.54E+04	4
KH	1.75E+04	8	1.57E+06	8	9.50E+05	6
WOA	5.41E+04	9	3.38E+06	9	9.74E+06	9
BOA	5.62E+07	11	5.31E+08	11	3.28E+09	11
HHO	1.20E+04	7	7.07E+05	7	1.03E+06	7
HGSO	1.76E+06	10	4.31E+07	10	5.52E+08	10
$LIACO_R$	8.03E+02	2	7.54E+04	2	2.89E+03	2
SMO	**7.13E+02**	**1**	**5.89E+04**	**1**	**2.49E+03**	**1**

Table 6 tabulates the MAE test results for four groups of the combination benchmark functions with dimensions 30, 50, and 100. The results show that the solutions found by our proposed algorithm rank first for all functions, and thus, SMO is superior to the competitive algorithms.

6. Applicability of SMO for solving mechanical engineering problems

There is a significant interest to optimize the cost, performance, and product lifecycle in mechanical and engineering systems using optimization algorithms [85, 86]. Hence, there have been proposed many optimization algorithms [87, 88] to solve the different engineering problems through which the swarm intelligence algorithms have more simplicity and effectiveness [65, 83, 89, 90]. The applicability of the SMO algorithm for real-world applications was evaluated by a variety of mechanics and engineering design problems of benchmark test-suite CEC 2020 [71] including tension/compression spring design, pressure vessel design (PVD), three-bar truss design, welded beam design (WBD), gas transmission compressor design (GTCD), Himmelblau's function, hydro-static thrust bearing design, optimal design of industrial refrigeration system, and multiple disk clutch brake design. Moreover, the SMO and contender algorithms also compete on the crashworthiness design problem to investigate the vehicle side-impact [72]. These problems have many constraints that should be equipped by a constraint-handling method; therefore, we used a death penalty function to handle constraints. To have a fair comparison, the SMO algorithm and the competitive algorithms were executed for 30 runs with 1500 maximum iteration. In the following, the engineering problems, their objective functions, and experiments results are described in detail.

Problem 1: Tension/compression spring design problem [91, 92]

In this problem, the objective function is to minimize the tension/compression spring weight shown in Fig. 14 [91, 92]. The three decision variables include wire diameter (d), mean coil diameter (D), and the number of active coils (N). This problem with four optimization constraints is formulated by Eq. (26) and the results in comparison with the contender algorithms are reported in Table 7.

Consider $\vec{x} = [x_1 x_2 x_3] = [d\ D\ N],$ (26)

Min $f(\vec{x}) = (x_3 + 2)x_2 x_1^2,$

Subject to $g_1(\vec{x}) = 1 - \frac{x_2^3 x_3}{71785 x_1^4} \leq 0,$

$g_2(\vec{x}) = \frac{4x_2^2 - x_1 x_2}{12566(x_2 x_1^3 - x_1^4)} + \frac{1}{5108 x_1^2} - 1 \leq 0,$

$g_3(\vec{x}) = 1 - \frac{140.45 x_1}{x_2^2 x_3} \leq 0,$

$g_4(\vec{x}) = \frac{x_1 + x_2}{1.5} - 1 \leq 0$

Variable range $0.05 \leq x_1 \leq 2.00, 0.25 \leq x_2 \leq 1.30, 2.00 \leq x_3 \leq 15.0.$

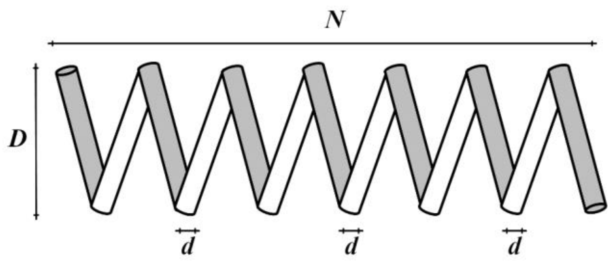

Fig. 14. Tension/compression string design problem [91].

Fig. 14. Tension/compression string design problem [91].

Table 7 Results for tension/compression spring design problem.

Algorithms	Optimal values for variables			Optimum weight
	d	D	N	
CLPSO	0.0528162	0.38365734	9.9234572	0.01276085
ABC	0.0523635	0.37285212	10.499994	0.01272368
ACO_R	0.0544804	0.42765302	8.0861495	0.01280257
Best-so-far ABC	0.0516703	0.35626720	11.315480	0.01266529
KH	0.0594664	0.57340232	4.7633398	0.01371398
WOA	0.0563246	0.47883022	6.5808214	0.01303485
HHO	0.0547934	0.43609241	7.8019335	0.01283342
BOA	0.0513430	0.33487183	12.922705	0.01196561
HGSO	0.0603887	0.60355425	4.3437323	0.01396248
$LIACO_R$	0.051475	0.3515844	11.596387	0.01266607
SMO	0.0516759	0.35640097	11.307562	**0.01266523595**

The results presented in Table 7 show that the SMO algorithm outperformed the other algorithms for finding optimal values for several variables, including wire diameter (d), mean coil diameter (D), and the number of active coils (N), to minimize the weight of a tension/compression spring.

Problem 2: Pressure vessel design (PVD) problem [93]

In the PVD problem, the objective function is to minimize the total cost of the material, forming, and welding of the cylindrical pressure vessel shown in Fig. 15. In this problem, there are four decision variables: x_1 is the thickness of the shell (T_s); x_2 is the thickness of the head (T_h); x_3 is the inner radius (R), and x_4 is the length of the cylindrical section of the vessel without considering the head (L). This problem with four optimization constraints is formulated by Eq. (27) [94], where R and L are continuous variables, and T_s and T_h are integer variables. The obtained results are tabulated in Table 8.

Consider $\vec{x} = [x_1 x_2 x_3 x_4] = [T_s\ T_h\ R\ \ L]$, (27)

Min $f(\vec{x}) = 0.6224x_1x_3x_4 + 1.7781x_2x_3^2 + 3.1661x_1^2x_4 + 19.84\,x_1^2x_3$,

Subject to

$$g_1(\vec{x}) = -x_1 + 0.0193x_3 \leq 0,$$
$$g_2(\vec{x}) = -x_2 + 0.00954x_3 \leq 0,$$
$$g_3(\vec{x}) = -\pi x_3^2 x_4 - \frac{4}{3}\pi x_3^3 + 1{,}296{,}000 \leq 0,$$
$$g_4(\vec{x}) = x_4 - 240 \leq 0$$

Variable range $0 \leq x_i \leq 99, \quad i = 1,2$

$10 \leq x_i \leq 200 \quad i = 3,4$

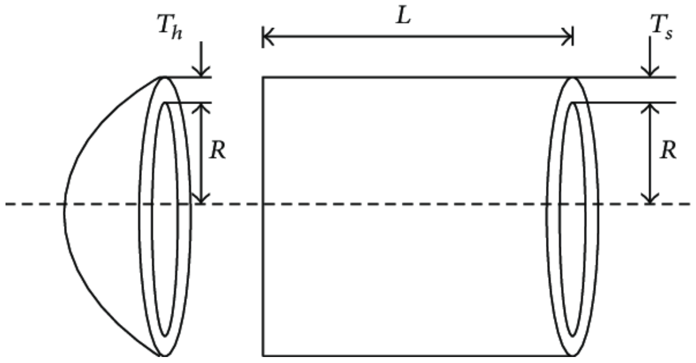

Fig. 15. Design of pressure vessel problem [93].

Table 8 Results for pressure vessel design problem.

Algorithms	Optimal values for variables				Optimum cost
	T_s	T_h	R	L	
CLPSO	0.786479785	0.397687773	40.74157739	196.117575	5.96901674E+03
ABC	0.806649355	0.402195006	41.70908176	181.771366	5.96255160E+03
ACO_R	0.825566300	0.408078882	42.77537419	168.425255	5.97140261E+03
Best-so-far ABC	0.836091135	0.413836022	43.31506689	162.145261	5.99501764E+03
KH	1.213849365	0.605704871	61.61464923	26.5525357	7.24975694E+03
WOA	0.866280219	0.434669925	43.62727532	158.570240	6.22737053E+03
HHO	1.055053881	0.525397724	54.65650724	65.2175661	6.56844058E+03
BOA	3.230015743	0.998879971	22.84511791	48.5777107	2.86020955E+05
HGSO	1.240713421	0.635357139	63.68097157	17.6374751	7.47953364E+03
$LIACO_R$	0.802442245	0.396647617	41.57731838	183.2029920	5.92813207E+03
SMO	0.778168742	0.384649212	40.31962392	199.9999277	**5.88533295E+03**

Table 8 reveals that the optimum cost of the cylindrical pressure vessel obtained by the SMO algorithm is less than other algorithms. Thus, SMO can find the best global solution for optimization variables, i.e., the thickness of the shell (T_s), the thickness of the head (T_h), inner radius (R), and length of the cylindrical section without considering the head (L).

Problem 3: Three-bar truss design problem

This problem is the structural optimization problem in the civil engineering field, in which two parameters should be optimized to obtain the minimum weight. The schematic design of the three-bar truss problem is shown in Fig. 16. Also, the formulation of this optimization problem is computed by Eq. (28). The results shown in Table 9 indicate that the SMO algorithm can optimize two parameters x_1 and x_2 for the three-bar truss problem better than the other algorithms.

Consider $\vec{x} = [x_1 x_2] = [A_1\ A_2]$, (28)

Min $f(\vec{x}) = \left(2\sqrt{2x_1} + x_2\right) \times l$,

Subject to

$$g_1(\vec{x}) = \frac{\sqrt{2}x_1 + x_2}{\sqrt{2}\,x_1^2 + 2x_1x_2} P - \sigma \le 0,$$

$$g_2(\vec{x}) = \frac{x_2}{\sqrt{2}x_1^2 + 2x_1x_2} P - \sigma \le 0,$$

$$g_3(\vec{x}) = \frac{1}{\sqrt{2}x_2 + x_1} P - \sigma \le 0,$$

Variable range $0 \le x_i \le 1, \quad i = 1,2$

$l = 100cm, P = 2\ kN/cm^2, and\ \ \sigma = 2\ kN/cm^2$

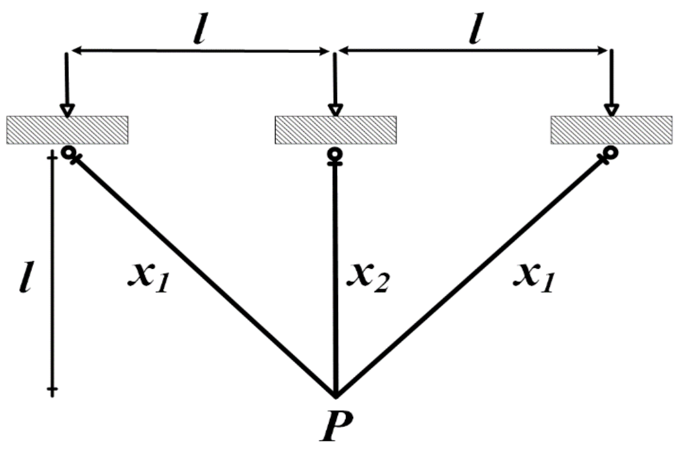

Fig. 16. Three-bar truss problem.

Table 9 Results for the three-bar truss problem.

Algorithms	Optimal values for variables		Optimal weight
	x_1	x_2	
CLPSO	0.788649321036270	0.408321420128666	2.63895855166E+02

ABC	0.791921803261280	0.399165678741402	2.63897235896E+02
ACO$_R$	0.788653773999128	0.408308723410851	2.63895844982E+02
Best-so-far ABC	0.788806481834012	0.407890932774407	2.63897258217E+02
KH	0.785125499417041	0.420705357829172	2.64137561671E+02
WOA	0.807624796411589	0.357126765175809	2.64143464596E+02
HHO	0.792284872646965	0.398132978987478	2.63905300331E+02
BOA	0.823331535298134	0.313381441824923	2.66734135381E+02
HGSO	0.784495397132808	0.420605145026335	2.63949320552E+02
LIACO$_R$	0.788670011025545	0.408262782880504	2.63895843454E+02
SMO	0.788676944913215	0.408243170134184	**2.63895843378E+02**

Problem 4: Welded beam design (WBD) problem [93]

In this problem, the objective function is designed to minimize the fabrication cost of a welded beam based on Eq. (29). There are four decision variables: h (x_1) is the thickness of weld; l (x_2) is the length of the clamped bar; t (x_3) is the height of the bar, and b (x_4) is the thickness of the bar. The schematic design of the welded beam is shown in Fig. 17 and formulated by Eq. (B.4). This optimization problem contains four variables thickness of weld (h), length (l), height (t), and thickness of the bar (b) with seven constraints. Moreover, the obtained results are reported in Table 10.

Consider $\vec{x} = [x_1, x_2, x_3, x_4] = [h, l, t, b]$, (29)

Min $f(\vec{x}) = 1.10471 x_1^2 x_2 + 0.04811 x_3 x_4 (14.0 + x_2)$,

Subject to

$$g_1(\vec{x}) = \tau(\vec{x}) - \tau_{max} \le 0,$$
$$g_2(\vec{x}) = \sigma(\vec{x}) - \sigma_{max} \le 0,$$
$$g_3(\vec{x}) = x_1 - x_4 \le 0,$$
$$g_4(\vec{x}) = 1.10471 x_1^2 + 0.04811 x_3 x_4 (14.0 + x_2) - 5.0 \le 0,$$
$$g_5(\vec{x}) = 0.125 - x_1 \le 0,$$
$$g_6(\vec{x}) = \delta(\vec{x}) - \delta_{max} \le 0,$$
$$g_7(\vec{x}) = P - P_c \le 0,$$

Variable range $0.1 \le x_i \le 2,\ i = 1,4, \qquad 0.1 \le x_i \le 10,\ i = 2,3$

Where $\tau(\vec{x}) = \sqrt{(\tau')^2 + 2\tau'\tau''\frac{x_2}{2R} + (\tau'')^2},\ \tau' = \frac{P}{\sqrt{2}\,x_1 x_2},\ \tau'' = \frac{MR}{J},\ M = P\left(L + \frac{x_2}{2}\right),\ R = \sqrt{\frac{x_2^2}{4} + (\frac{x_1 + x_3}{2})^2}, \quad J = 2\left\{\sqrt{2}\,x_1 x_2\left[\frac{x_2^2}{12} + \left(\frac{x_1 + x_3}{2}\right)^2\right]\right\},\ \sigma(\vec{x}) = \frac{6PL}{x_4 x_3^2},\ \delta(\vec{x}) = \frac{6PL^3}{E\,x_3^2\,x_4},$

$P_c(\vec{x}) = \frac{4.013E\sqrt{\frac{x_3^2\,x_4^6}{36}}}{E\,x_3^2\,x_4}\left(1 - \frac{x_3}{2L}\sqrt{\frac{E}{4G}}\right), P = 6000\,lb, L = 14\,in., E = 30 \times 1^6 psi, G = 12 \times 10^6 psi,\ \tau_{max} = 13{,}600\,psi,\ \sigma_{max} = 30{,}000\,psi,\ \delta_{max} = 0.25\,in.$

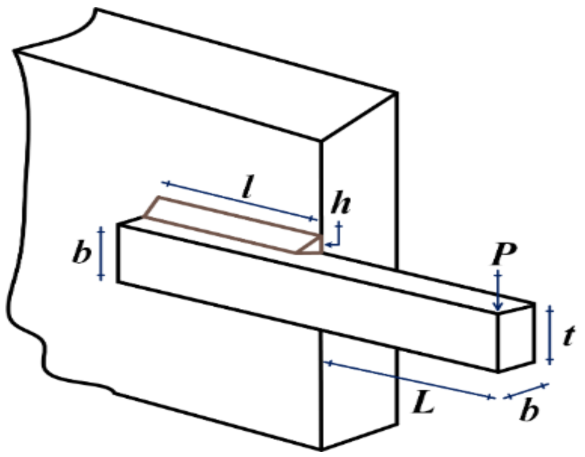

Fig. 17. Welded beam design (WBD) problem [93, 95].

Table 10 further proves that the SMO and LIACO$_R$ can find the optimum cost better than the other algorithms by finding the optimum values for the design variables, including weld thickness (h), length (l), height (t), and thickness of the bar (b).

Table 10 Results of the welded beam design problem.

Algorithms	Optimal values for variables				Optimum cost
	h	l	t	b	
CLPSO	0.20043684951	3.61781217135	9.12632634245	0.205392564	1.749360118249957
ABC	0.21601066079	3.21817385411	9.19315650531	0.218132255	1.803929558372931
ACO$_R$	0.20572961534	3.47048910478	9.03662418450	0.205729640	1.724852376184159
Best-so-far ABC	0.22781912459	3.22228585497	8.55433193633	0.229649894	1.812469010983658
KH	0.22685002867	3.49887858194	8.60029213677	0.298971192	2.363561357410289
WOA	0.18660545086	3.96352297459	9.02318604844	0.206342866	1.761542689738283
HHO	0.20718794648	3.45481153594	8.99630131487	0.207712428	1.733028379140158
BOA	0.16370033515	3.18982074389	6.53810915088	0.184186629	2.552269551814868
HGSO	0.17500325946	4.67821274646	8.95647311732	0.211263389	1.858603007057090
LIACO$_R$	0.20572963979	3.47048866563	9.03662391036	0.205729640	**1.724852308597364**
SMO	0.20572963979	3.47048866563	9.03662391036	0.205729640	**1.724852308597364**

Problem 5: Gas transmission compressor design (GTCD) problem [96]

The gas transmission compressor design is a well-known optimization problem that determines the minimum cost for a gas pipeline transmission system per day as shown in Fig. 18. This problem consists of four decision variables: L (x_1) length between compressor stations, r (x_2) compression ratio denoting inlet pressure to the compressor, D (x_3) is the pipe inside diameter (inches), and x_4 (x^2-1). The total annual cost of the transmission system and its operation is defined by Eq. (30). The results are tabulated in Table 11 indicate that the proposed can be effectively applied to solve mechanical engineering problems.

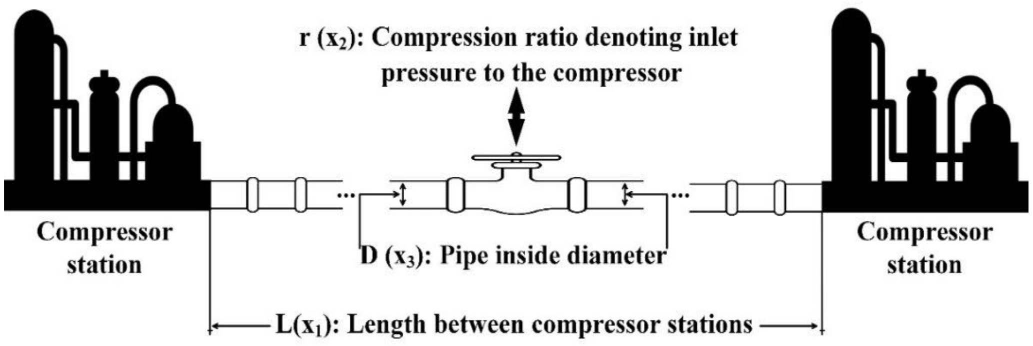
r (x_2): Compression ratio denoting inlet pressure to the compressor
Compressor station
D (x_3): Pipe inside diameter
Compressor station
L(x_1): Length between compressor stations

Fig. 18. Gas transmission compressor design (GTCD) problem.

Minimize $f(\bar{x}) = 8.61 \times 10^5 x_1^{1/2} x_2 x_3^{-2/3} x_4^{-1/2} + (3.69) \times 10^4 x_3 + (7.72) \times 10^8 x_1^{-1}\, x_2^{0.219} - (765.43) \times\ 10^6 x_1^{-1}$ (30)

Subject to $x_4 x_2^{-2} + x_2^{-2} - 1 \leq 0$

Variable range $20 \leq x_1 \leq 50, 1 \leq x_2 \leq 10, 20 \leq x_3 \leq 45, 0.1 \leq x_4 \leq 60.$

Table 11 Results of the gas transmission compressor design (GTCD) problem.

Algorithms	Optimal values for variables				Optimum cost
	x_1	x_2	x_3	x_4	
CLPSO	45.8830	1.571778	27.18201	1.45592	3.7381430E+06
ABC	50.0000	1.185882	24.89145	0.39507	2.9845610E+06
ACO_R	49.6067	1.174456	23.92940	0.37862	2.9671090E+06
Best-so-far ABC	50.0000	1.207839	24.49319	0.45792	2.9755610E+06
KH	35.6206	1.092393	31.99460	1.10937	3.4608480E+06
WOA	49.7095	1.178115	24.72718	0.38796	2.9650350E+06
HHO	49.9844	1.180801	24.20547	0.39429	2.9650910E+06
BOA	20.0000	1.000000	20.00000	0.16475	3.1364520E+06
HGSO	50.0000	1.164785	25.72731	0.35606	2.9689110E+06
$LIACO_R$	50.0000	1.178480	24.58628	0.38882	2.9648960E+06
SMO	50.0000	1.178284	24.59259	0.38835	**2.9648954E+06**

Problem 6: The crashworthiness design problem to investigate the vehicle side-impact [72]

The crashworthiness design problem is formulated to optimize the vehicle side crashworthiness by minimizing the weight with eleven design variables and ten constraints. The design variables including, thicknesses of B-Pillar inner, B-Pillar reinforcement, floor side inner, cross members, door beam, door beltline reinforcement and roof rail (x_1–x_7), materials of B-Pillar inner and floor side inner (x_8 and x_9), and barrier height, and hitting position (x_{10} and x_{11}). This problem is defined by Eq. (31) [97, 98] and shown in Fig. 19. The results are reported in Table 12 and indicate that the SMO algorithm is superior for approximating the optimal solutions for the decision variables of the crashworthiness design problem.

Minimize (31)

$$F(x) = 1.98 + 4.90x_1 + 6.67x_2 + 6.98x_3 + 4.01x_4 + 1.78x_5 + 2.73x_7$$

Subject to:

$$\begin{aligned}
g_1(x) &= 1.16 - 0.3717x_2x_4 - 0.00931x_2x_{10} - 0.484x_3x_9 + 0.01343x_6x_{10} \leq 1, \\
g_2(x) &= 0.261 - 0.0159x_1x_2 - 0.188x_1x_8 - 0.019x_2x_7 + 0.0144x_3x_5 + 0.0008757x_5x_{10} \\
&\quad + 0.080405x_6x_9 + 0.00139x_8x_{11} + 0.00001575x_{10}x_{11} \leq 0.32, \\
g_3(x) &= 0.214 + 0.00817x_5 - 0.131x_1x_8 - 0.0704x_1x_9 + 0.03099x_2x_6 - 0.018x_2x_7 \\
&\quad + 0.0208x_3x_8 + 0.121x_3x_9 - 0.00364x_5x_6 + 0.0007715x_5x_{10} \\
&\quad - 0.0005354x_6x_{10} + 0.00121x_8x_{11} \leq 0.32, \\
g_4(x) &= 0.074 - 0.061x_2 - 0.163x_3x_8 + 0.001232x_3x_{10} - 0.166x_7x_9 + 0.227x_2^2 \leq 0.32, \\
g_5(x) &= 28.98 + 3.818x_3 - 4.2x_1x_2 + 0.0207x_5x_{10} + 6.63x_6x_9 - 7.7x_7x_8 + 0.32x_9x_{10} \leq 32, \\
g_6(x) &= 33.86 + 2.95x_3 + 0.1792x_{10} - 5.057x_1x_2 - 11.0x_2x_8 - 0.0215x_5x_{10} - 9.98x_7x_8 + 22.0x_8x_9 \\
&\quad \leq 32 \\
g_7(x) &= 46.36 - 9.9x_2 - 12.9x_1x_8 + 0.1107x_3x_{10} \leq 32, \\
g_8(x) &= 4.72 - 0.5x_4 - 0.19x_2x_3 - 0.0122x_4x_{10} + 0.009325x_6x_{10} + 0.000191x_{11}^2 \leq 4, \\
g_9(x) &= 10.58 - 0.674x_1x_2 - 1.95x_2x_8 + 0.02054x_3x_{10} - 0.0198x_4x_{10} + 0.028x6x_{10} \leq 9.9, \\
g_{10}(x) &= 16.45 - 0.489x_3x_7 - 0.843x_5x_6 + 0.0432x_9x_{10} - 0.0556x_9x_{11} - 0.000786x_{11}^2 \\
&\quad \leq 15.7.
\end{aligned}$$

Variable range

$$0.5 \leq x_1 \dots x_7 \leq 1.5, x_8, x_9 \in \{0.192, 0.345\}, and - 30 \leq x_{10} \dots x_{11} \leq 30.$$

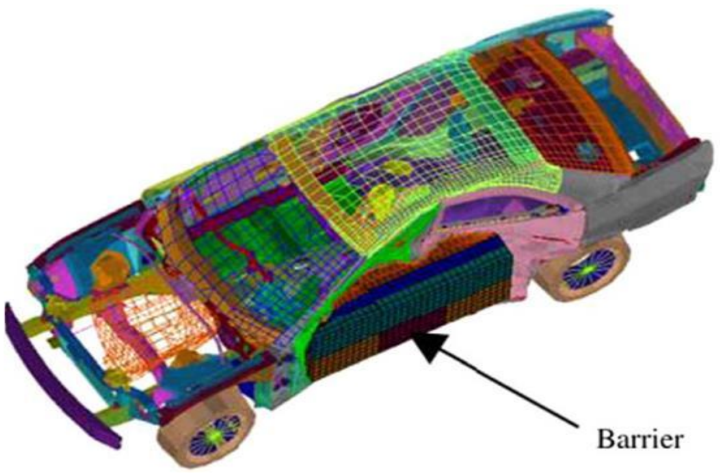

Fig. 19. The crashworthiness design problem [99].

Table 12 Optimization results for the crashworthiness design problem to investigate the vehicle side impact.

Algorithms	Optimal values for variables											Optimum cost
	x_1	x_2	x_3	x_4	x_5	x_6	x_7	x_8	x_9	x_{10}	x_{11}	
CLPSO	0.5061	1.17379	0.5013	1.24706	0.5037	1.4956	0.5000	0.3450	0.3450	-9.5985	3.3627	23.06244
ABC	0.5000	1.13863	0.5000	1.29027	0.5000	1.5000	0.5403	0.3450	0.1920	-16.047	5.0767	22.94362
ACO_R	0.5000	1.12004	0.5000	1.29627	0.5000	1.5000	0.5000	0.3450	0.1920	-18.905	-0.0008	22.84371
Best-so-far ABC	0.5000	1.30539	0.5000	1.10312	0.5000	0.5000	0.5000	0.3450	0.3450	14.213	20.3306	22.88605
KH	0.5000	1.14747	0.5000	1.26118	0.5000	1.5000	0.5000	0.3450	0.3450	-13.998	-0.8984	22.88596
WOA	0.5000	1.09276	0.5000	1.41233	0.5000	1.45497	0.5000	0.3450	0.1920	-24.038	-3.1789	23.12717
HHO	0.5000	1.15627	0.5000	1.27133	0.5000	1.4777	0.5000	0.3450	0.1920	-14.592	-2.4898	22.98537
BOA	0.8246	1.03224	0.54007	1.35639	0.6377	1.26889	0.5854	0.1920	0.3450	-5.7333	0.4352	25.06573
HGSO	0.5000	1.22375	0.5000	1.27111	0.5000	1.31085	0.5000	0.3450	0.3450	-4.3235	2.93676	23.43457

LIACO$_R$	0.5000	1.11593	0.5000	1.30293	0.5000	1.50000	0.5000	0.1920	0.3450	-19.640	-0.000003	22.84299
SMO	0.5000	1.11634	0.5000	1.30224	0.5000	1.50000	0.5000	0.3450	0.3450	-19.566	0.000001	**22.84298**

Problem 7: Himmelblau's function [100]

This problem contains six nonlinear constraints and five decision variables to analyze the non-linear constrained optimization algorithms using Eq. (32). The results are tabulated in Table 13.

Minimize (32)

$$f(\bar{x}) = 5.3578547x_3^2 + 0.8356891x_1x_5 + 37.293239x_1 - 40792.141$$

Subject to:

$$g_1(\bar{x}) = -G_1 \le 0,$$
$$g_2(\bar{x}) = G_1 - 92 \le 0,$$
$$g_3(\bar{x}) = 90 - G_2 \le 0,$$
$$g_4(\bar{x}) = G_2 - 110 \le 0,$$
$$g_5(\bar{x}) = 20 - G_3 \le 0,$$
$$g_6(\bar{x}) = G_3 - 25 \le 0,$$

Where

$$G_1 = 85.334407 + 0.0056858x_2x_5 + 0.0006262x_1x_4 - 0.0022053x_3x_5,$$
$$G_2 = 80.51249 + 0.0071317x_2x_5 + 0.0029955x_1x_2 + 0.0021813x_3^2,$$
$$G_3 = 9.300961 + 0.0047026x_3x_3 + 0.00125447x_1x_3 + 0.0019085x_3x_4.$$

Variable range

$$78 \le x_1 \le 102, 33 \le x_2 \le 45, 27 \le x_3 \le 45, 27 \le x_4 \le 45, 27 \le x_5 \le 45.$$

Table 13 Results of the Himmelblau's function.

Algorithms	Optimal values for variables					Optimum cost
	x1	x2	x3	x4	x5	
CLPSO	86.35114	34.27649	31.27986	44.57583	32.75833	-2.996561E+04
ABC	78	33.27290	30.65216	44.30402	36.49082	-3.051574E+04
ACO$_R$	78	33	30.04808	44.93806	36.70563	-3.065312E+04
Best-so-far ABC	78	33	30.19617	45	36.35274	-3.062832E+04
KH	78.99892	33.00575	30.67021	43.63579	35.53123	-3.046036E+04
WOA	79.36031	33	30.04906	42.54110	37.27498	-3.052259E+04
HHO	78	33	30.00757	44.99297	36.74753	-3.066342E+04
BOA	78	33	30.31139	39.59049	31.58397	-3.015535E+04
HGSO	78	33	3.109831	4.002299	3.623523	-3.033971E+04
LIACO$_R$	78	33	29.99526	45.00000	36.77581	**-3.066554E+04**
SMO	78	33	29.99526	45.00000	36.77581	**-3.066554E+04**

Problem 8: Hydro-static thrust bearing design problem

The Hydro-static thrust bearing design problem was defined by Siddall [101] to optimize the bearing power loss using four design variables and seven inequality constraints. This problem is defined using Eq. (33) where μ is the oil viscosity, R is the bearing radius, Q is the flow rate, and R_o is the recess radius. The schematic of this problem is shown in Fig. (20). Table 14 reports the results of the proposed algorithm and other optimization algorithms in which the SMO and LIACO$_R$ algorithms are superior to other comparative algorithms.

Minimize (33)

$$f(\bar{x}) = \frac{\varrho P_0}{0.7} + E_f$$

Subject to:

$$g_1(\bar{x}) = 101000 - W \leq 0,$$
$$g_2(\bar{x}) = P_0 - 1000 \leq 0,$$
$$g_3(\bar{x}) = \Delta T - 50 \leq 0,$$
$$g_4(\bar{x}) = 0.001 - h \leq 0,$$
$$g_5(\bar{x}) = R - R_0 \leq 0,$$
$$g_6(\bar{x}) = 0.0307\left(\frac{386.4}{P_0}\right) \times \left(\frac{\varrho}{2\pi R h}\right) - 0.001 \leq 0,$$
$$g_7(\bar{x}) = \left(\frac{W}{\pi \times (R^2 - R_0^2)}\right) - 5000 \leq 0$$

Where

$$W = \frac{\pi P_0}{2} \times \frac{R^2 - R_0^2}{ln\left(\frac{R}{R_0}\right)},$$

$$P_0 = \frac{6\mu\varrho}{\pi h^3} ln\left(\frac{R}{R_0}\right),$$
$$E_f = 9336\varrho \times 0.0307 \times 0.5\Delta T \quad \Delta T = 2(10^P - 559.7),$$
$$P = \frac{log_{10} log_{10}(8.122 \times 10^6 \mu + 0.8) - 10.04}{-3.55},$$
$$h = \left(\frac{2\pi \times 750}{60}\right)^2 \frac{2\pi\mu}{E_f}\left(\frac{R^4}{4} - \frac{R_0^4}{4}\right)$$

Variable range

$$1 \leq R \leq 16, \; 1 \leq R_0 \leq 16$$
$$1 \times 10^{-6} \leq \mu \leq 16 \times 10^{-6}, \; 1 \leq \varrho \leq 16$$

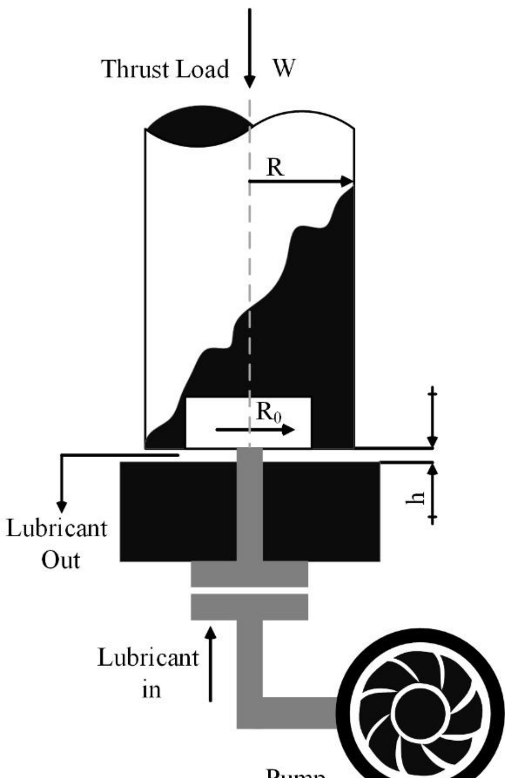

Fig. 20. The schematic of the hydro-static thrust bearing design problem

Table 14 Results of solving the hydro-static thrust bearing design problem.

Algorithms	Optimal values for variables				Optimum value
	R	R_0	μ	Q	
CLPSO	7.0766281	5.7799332	8.30E-06	13.976341	3.97E+03
ABC	6.248404	5.690787	5.80E-06	2.899149	1.81E+03
ACO_R	6.893258	6.360649	6.89E-06	5.069318	2.23E+03
Best-so-far ABC	6.734411	6.172581	5.58E-06	3.129316	2.03E+03
KH	6.287436	5.750665	6.81E-06	4.070802	1.90E+03
WOA	5.963189	5.391826	5.45E-06	2.339102	1.64E+03
HHO	5.957047	5.387234	7.25E-06	4.378191	1.85E+03
BOA	8.296644	6.665785	7.32E-06	14.97732	5.57E+03
HGSO	6.272983	5.690010	5.64E-06	2.814452	1.84E+03
$LIACO_R$	5.955511	5.388716	5.36E-06	2.256638	**1.62E+03**
SMO	5.955511	5.388716	5.36E-06	2.256638	**1.62E+03**

Problem 9: Optimal design of industrial refrigeration system

This is a non-linear inequality constrained optimization problem which is defined by Eq. (34) [102, 103]. Table 15 tabulates results for solving this problem in which the SMO is superior to other comparative algorithms.

Minimize (34)

$$f(\bar{x}) = 63098.88x_2\, x_4\, x_{12} + 5441.5\, x_2^2\, x_{12} + 115055.5\, x_2^{1.664} x_6 + 6172.27 x_2^2\, x_6 + 63098.88\, x_1\, x_3\, x_{11} + 5441.5\, x_1^2\, x_{11} + 115055.5\, x_1^{1.664} x_5 + 6172.27 x_1^2\, x_5 + 140.53\, x_1\, x_{11} + 281.29\, x_3\, x_{111} + 70.26\, x_1^2 + 281.29\, x_1\, x_3 + 281.29\, x_3^2 + 14437\, x_8^{1.8812}\, x_{12}^{0.3424}\, x_{10}\, x_{14}^{-1}\, x_1^2 x_7\, x_9^{-1} + 20470.2\, x_7^{2.893} x_{11}^{0.316} x_1^2$$

Subject to:

$$g_1(\bar{x}) = 1.5240\, x_7^{-1} \le 1,$$
$$g_2(\bar{x}) = 1.5240\, x_8^{-1} \le 1,$$
$$g_3(\bar{x}) = 0.07789\, x_1 - 2\, x_7^{-1}\, x_9 - 1 \le 0,$$
$$g_4(\bar{x}) = 7.05305\, x_9^{-1}\, x_1^2\, x_{10}\, x_8^{-1} x_2^{-1} x_1^{-1} - 1 \le 0,$$
$$g_5(\bar{x}) = 0.0833\, x_{13}^{-1}\, x_{14} \le 0,$$
$$g_6(\bar{x}) = 47.136\, x_2^{0.333} x_{10}^{-1}\, x_{12} - 1.333\, x_8\, x_{13}^{2.1195} + 62.08 x_{13}^{2.1195}\, x_{12}^{-1}\, x_8^{0.2}\, x_{10}^{-1} - 1 \le 0,$$
$$g_7(\bar{x}) = 0.04771\, x_{10}\, x_8^{1.8812} x_{12}^{0.3424} - 1 \le 0$$
$$g_8(\bar{x}) = 0.0488\, x_9\, x_7^{1.893} x_{11}^{0.316} - 1 \le 0$$
$$g_9(\bar{x}) = 0.0099\, x_1\, x_3^{-1} - 1 \le 0$$
$$g_{10}(\bar{x}) = 0.0193\, x_2\, x_4^{-1} - 1 \le 0$$
$$g_{11}(\bar{x}) = 0.0298\, x_1\, x_5^{-1} - 1 \le 0$$
$$g_{12}(\bar{x}) = 0.056\, x_2\, x_6^{-1} - 1 \le 0$$
$$g_{13}(\bar{x}) = 2\, x_9^{-1} - 1 \le 0$$
$$g_{14}(\bar{x}) = 2\, x_{10}^{-1} - 1 \le 0$$
$$g_{15}(\bar{x}) = x_{12}\, x_{11}^{-1} - 1 \le 0$$

Variable range

$$0.001 \le x_2 \le 5, \qquad i = 1 \ldots 14.$$

Table 15 Results for the optimal design of the industrial refrigeration system.

Alg.	CLPSO	ABC	ACO_R	Best-so-far ABC	KH	WOA	HHO	$LIACO_R$	SMO
X_1	0.0010	0.0010	0.0010	0.0010	0.0010	0.0010	0.0010	0.0010	0.0010
X_2	0.0014	0.0010	0.0010	0.0010	0.0010	0.0011	0.0010	0.0010	0.0010
X_3	0.0011	0.0010	0.0010	0.0010	0.0010	0.0010	0.0010	0.0010	0.0010

X_4	0.0010	0.0010	0.0010	0.0010	1.9345	0.0028	0.0010	0.0010	0.0010
X_5	0.0011	0.0010	0.0010	0.0010	1.7837	0.0011	0.0010	0.0010	0.0010
X_6	0.0010	0.0010	0.0010	0.0010	2.0031	0.0010	0.0010	0.0010	0.0010
X_7	1.5546	1.5240	1.5249	1.5240	2.4043	1.5265	1.5963	1.5240	1.5240
X_8	1.5296	1.5240	1.5252	1.5240	2.3534	1.5263	1.5240	1.5240	1.5240
X_9	4.9841	5.0000	5.0000	5.0000	2.7000	5.0000	5.0000	5.0000	5.0000
X_{10}	2.3945	2.1033	2.0016	2.0230	4.0368	2.0000	2.1777	2.000034	2.0000
X_{11}	0.0021	0.0010	0.0010	0.0010	1.8600	0.0011	0.0010	0.0010	0.0010
X_{12}	0.0020	0.0010	0.0010	0.0010	0.0048	0.0010	0.0010	0.0010	0.0010
X_{13}	0.0095	0.0073	0.0073	0.0073	0.0201	0.0062	0.0076	0.0073	0.0073
X_{14}	0.1135	0.0792	0.0874	0.0880	0.2357	0.0740	0.0912	0.0876	0.0876
F(X)	0.041400	0.034900	0.032400	0.032300	6.45100	0.03680	0.035300	0.032214235	**0.032213001**

Problem 10: Multiple disk clutch brake design

The multiple disk clutch brake design problem is defined using Eq. (35) to minimize the mass of the multiple disk clutch brake. This problem contains nine non-linear constraints and five discrete design variables include inner radius (x_1), outer radius (x_2), disk thickness (x_3), a force of actuators (x_4), and the number of frictional surfaces (x_5). The schematic of this problem is shown in Fig. 21. Table 16 reports obtained results of optimization algorithms for this problem in which SMO, ACO_R, Best-so-far ABC, HHO, and LIACO_R algorithms outperform other comparative algorithms.

Minimize (35)

$$f(\bar{x}) = \pi\,(x_2^2 - x_1^2)\,x_3(x_5 + 1)\rho$$

Subject to:

$$g_1(\bar{x}) = -x_2 + x_1 + \Delta\mathrm{R} \le 0,$$
$$g_2(\bar{x}) = (x_5 + 1) \times (x_5 + \Delta) - L_{max} \le 0,$$
$$g_3(\bar{x}) = \mathrm{p_{rz}} - p_{max} \le 0,$$
$$g_4(\bar{x}) = \mathrm{p_{rz}} \times V_{sr} - p_{max} \times V_{sr,max} \le 0,$$
$$g_5(\bar{x}) = V_{sr} - V_{sr,max} \le 0,$$
$$g_6(\bar{x}) = T - T_{max} \le 0,$$
$$g_7(\bar{x}) = S \times M_S - M_h \le 0,$$
$$g_8(\bar{x}) = -T \le 0,$$

where

$$M_h = \frac{2}{3}\mu\, x_4 x_5 (x_2^3 - x_1^3)/(x_2^2 - x_1^2)\mathrm{mm}$$
$$R_{sr} = \frac{2}{3}(x_2^3 - x_1^3)/(x_2^2 - x_1^2)\mathrm{mm}$$
$$V_{sr} = \frac{\pi \times R_{sr} \times \mathrm{n}}{30}\mathrm{mm/s}$$
$$A = \pi \times (x_2^2 - x_1^2)\ \mathrm{N/m}m^2$$
$$\mathrm{p_{rz}} = \frac{x_4}{A}\ \mathrm{N/m}m^2$$
$$\omega = \frac{\pi \times \mathrm{n}}{30}\mathrm{rad/s},$$
$$T = \frac{I_Z \times \omega}{M_h + M_f}$$
$$\Delta R = 20\,mm, L_{max} = 30, \mu = 0.6, \Delta = 50$$
$$V_{sr,max} = 10\,m/s,\ \delta = 0.5\,mm,\ s = 1.5,$$
$$T_{max} = 15\,s, n = 250\,rpm,\ I_Z = 55Kg.m^2$$
$$M_S = 40\,Nm, M_f = 3\,Nm, p_{max} = 1, \rho = 0.0000078$$

Variable range

$60 \le x_1 \le 80$, $90 \le x_2 \le 110$, $1 \le x_3 \le 3$, $0 \le x_4 \le 1000$, $2 \le x_5 \le 9$.

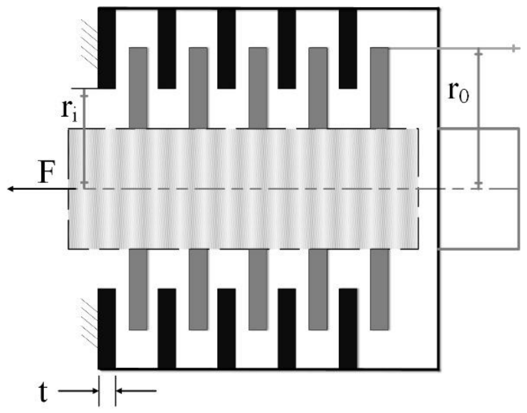

Fig. 21. The schematic of the multiple disk clutch brake design

Table 16 Results for the optimal design of the multiple disk clutch brake.

Alg.	Optimal values for variables					Optimum value
	x_1	x_2	x_3	x_4	x_5	
CLPSO	75.95932	97.06936	1.01058	909.47864	2.09723	0.280152637613733
ABC	69.99974	90.00000	1.00000	697.47983	2.00000	0.235242474598156
ACO_R	70.00000	90.00000	1.00000	718.00397	2.00000	**0.235242457900804**
Best-so-far ABC	70.00000	90.00000	1.00000	317.17055	2.00000	**0.235242457900804**
KH	70.00000	90.00000	1.00000	481.07988	2.00000	0.235242458886112
WOA	70.00000	90.00000	1.00000	182.35543	2.00000	0.235242457901052
HHO	70.00000	90.00000	1.00000	304.20738	2.00000	**0.235242457900804**
BOA	67.72699	90.00000	1.00000	673.06921	2.00000	0.248171278270212
HGSO	69.99945	90.00000	1.00000	8.73600	2.00000	0.235248138956563
$LIACO_R$	70.00000	90.00000	1.00000	169.99845	2.00000	**0.235242457900804**
SMO	70.00000	90.00000	1.00000	999.99899	2.00000	**0.235242457900804**

7. Conclusion and future work

This work modeled the starlings' behaviors during their stunning murmuration to propose a novel, population-based swarm intelligence algorithm named SMO. In this model, the separating search strategy enriched using the separating operator defined in Definition 1 guarantees the population diversity for complex problems. Next, the murmuration M is initially formed by constructing the dynamic multi-flock introduced in Definition 2, the quality of the flocks is computed by Definition 3. Finally, using the quality of each flock, if it is located in a promising region, its starlings exploit this region by the whirling search strategy. Otherwise, the starlings of this flock explore the search space using a quantum random dive operator defined by Definition 4 in the diving search strategy.

A comprehensive evaluation was designed to analyze the SMO algorithm's performance and behavior. In this evaluation, first, a multifarious combination of the benchmark test functions was provided. Then, the SMO algorithm was qualitatively and quantitatively analyzed by several experiments on this combination of benchmark functions. Finally, the applicability of the proposed algorithm for real-world applications was evaluated by mechanical engineering problems. Moreover, SMO was statistically analyzed by different statistical tests, including Wilcoxon signed-rank sum and mean absolute error (MAE).

The comparison of the experimental and statistical results of SMO with the state-of-the-art algorithms and the associated discussions confirm the following conclusions:

– Using the topology of the dynamic multi-flock provides the covering of different landscapes, which results in a meaningful search to converge the global optimum faster than the compared algorithms.
– Generating the candidate solutions using the new quantum random dive operator in the diving search strategy enhances the exploration ability and diversity of the proposed algorithm.
– The experimental results shown in unimodal section of Table 3, Table B.3, and Fig. 10 prove that using the whirling search strategy provides high exploitation with less chance for the local optima trapping.
– The results shown in hybrid and composition sections of Table 3, Tables B.5 and B.6, and Figs. 12 and 13 verify that combining the diving and whirling search strategies with the separating strategy enriches the movement strategy to bypass the local optima in the hybrid and composition problems. Moreover, these results and switching between the exploration and exploitation, as shown in Fig. 9, prove that these introduced strategies and the quality of flocks achieve an efficient balance between local and global search in the complex landscape.
– The applicability tests on various mechanical engineering problems in Section 6 show that the proposed SMO algorithm can solve these real-world problems more precisely than the other contender algorithms.
– The comprehensive evaluation's experimental and statistical results prove that the proposed SMO algorithm is superior to the state-of-the-art algorithms.

We proposed a standard version of the SMO algorithm to solve single-objective continuous and engineering optimization problems. Thus, developing the SMO algorithm for solving different real-world and large-scale optimization problems is a promising further direction. Furthermore, different probability distributions, chaotic maps, different flock construction techniques, and other search strategies can be integrated to introduce improved versions of the SMO and cover more problems' complexity. Furthermore, the SMO can be developed for multi-objective and binary problems.

Acknowledgment

The authors would like to thank the editor and anonymous reviewers for improving this paper with their valuable comments and suggestions.

Conflict of Interest

The authors declare that there is no conflict of interest regarding the publication of the paper.

Appendix A

Table A.1 The description of unimodal group functions.

Function's name	Function	F_{min}(x)	Source
F_1: Sphere	$F_1(z) = \sum_{i=1}^{D} z_i^2$	-1400	CEC 2013, F_1
F_2: Rotated High Conditioned Elliptic	$F_2(z) = \sum_{i=1}^{D} (10^6)^{\frac{i-1}{D-1}} z_i^2$	-1300	CEC 2013, F_2
F_3: Rotated Bent Cigar	$F_3(z) = z_1^2 + 10^6 \sum_{i=1}^{D} z_i^2$	-1200	CEC 2013, F_3
F_4: Rotated Discus	$F_4(x) = 10^6 z_1^2 + \sum_{i=1}^{D} z_i^2$ $z = M_2 T_{asy}^{0.5}(M_1(x-o))$	-1100	CEC 2013, F_4
F_5: Different Powers	$F_5(x) = \sqrt{\sum_{i=1}^{D} \lvert z_i \rvert^{2+4\frac{i-1}{D-1}}}$	-1000	CEC 2013, F_5
F_6: Shifted and Rotated Bent Cigar	$F_6(x) = x_1^2 + 10^6 \sum_{i=1}^{D} x_i^2$	100	CEC 2017, F_1
F_7: Shifted and Rotated Sum of Different Power	$F_7(x) = \sum_{i=1}^{D} \lvert x_i \rvert^{i+1}$	200	CEC 2017, F_2
F_8: Shifted and Rotated Zakharov	$F_8(x) = \sum_{i=1}^{D} x_i^2 + (\sum_{i=1}^{D} 0.5x_i)^2 + (\sum_{i=1}^{D} 0.5x_i)^4$	300	CEC 2017, F_3

Table A.2 The description of multi-modal group functions.

Function's name	Function	$F_{min}(x)$	Sources
F_9: Rotated Griewank's Function	$F_9(x) = \sum_{i=1}^{D} \frac{z_i^2}{4000} - \prod_{i=1}^{D} \cos\left(\frac{z_i}{\sqrt{i}}\right) + 1 + f_{10}^*, \quad z = \Lambda^{100} M_1 \frac{600(x-o)}{100}$	-500	CEC 2013, F_{10}
F_{10}: Rotated Rastrigin's Function	$F_{10}(x) = \sum_{i=1}^{D} (z_i^2 - 10\cos(2\pi z_i) + 10) + f_{12}^*, \; z = M_1 \Lambda^{10} M_2 T_{asy}^{0.2}(T_{osz}(M_1 \frac{5.12(x-o)}{100}))$	-300	CEC 2013, F_{12}
F_{11}: Non-Continuous Rotated Rastrigin's Function	$F_{11}(x) = \sum_{i=1}^{D} (z_i^2 - 10\,cos(2\pi z_i) + 10) + f_{13}^*$ $\hat{x} = M_1 \frac{5.12(x-o)}{100}, \; y_i = \begin{cases} \hat{x_i} & if\ \lvert\hat{x_i}\rvert \le 0.5 \\ round(2\hat{x_i})/2 & if\ \lvert\hat{x_i}\rvert > 0.5 \end{cases} for\ i = 1.2. \ldots .D$ $z = M_1 \Lambda^{10} M_2 T_{asy}^{0.2}(T_{osz}(y))$	-200	CEC 2013, F_{13}
F_{12}: Rotated Lunacek bi-Rastrigin Function	$F_{12}(x) = min\,(\sum_{i=1}^{D}(\hat{x_i} - \mu_0)^2, dD + s\sum_{i=1}^{D}(\hat{x_i} - \mu_1)^2 + 10(D - \sum_{i=1}^{D}\cos(2\pi \hat{z_i})) + F_{18}{}^*$ $\mu_0 = 2.5, \; \mu_1 = -\sqrt{\frac{{\mu_0}^2 - d}{s}}, s = 1 - \frac{1}{2\sqrt{D+20} - 8.2}$, d =1 $y = \frac{10(x-o)}{100}, \hat{x_i} = 2sign(y_i{}^*)y_i + \mu_0$, for i=1, 2, …, D, $z = M_2 \Lambda^{100}(M_1(\hat{x} - \mu_0))$	400	CEC 2013, F_{18}
F_{13}: Shifted and Rotated Rosenbrock's Function	$F_{13}(X) = f_{11}'\left(M\left(\frac{2.048(X-O)}{100}\right) + 1\right), \; F_{11}'(x) = \sum_{i=1}^{D-1}(100(x_i^2 - x_{i+1})^2 + (x_i - 1)^2)$	400	CEC 2014, F_4
F_{14}: Shifted and Rotated Weierstrass Function	$F_{14}(X) = \sum_{i=1}^{D}\left(\sum_{k=0}^{k\,max}\left[a^k \cos\left(2\pi b^k(x_i + 0.5)\right)\right]\right) - D\sum_{k=0}^{kmax}[a^k \cos(2\pi b^k . 0.5)]$ $a = 0.5. b = 3, \; kmax = 20$	600	CEC 2014, F_6
F_{15}: Shifted and Rotated Griewank's Function	$F_{15}(X) = \sum_{i=1}^{D} \frac{x_i^2}{4000} - \prod_{i=1}^{D} \cos\left(\frac{x_i}{\sqrt{i}}\right) + 1$	700	CEC 2014, F_7
F_{16}: Shifted and Rotated Rastrigin's Function	$F_{16}(X) = 418.9829 \times D - \sum_{i=1}^{D} g(z_i), \; z_i = x_i + 4.209687462275036e + 002$ $g(z_i) = \begin{cases} z_i \sin(\lvert z_i\rvert^{1/2}) & if\ \lvert z_i\rvert \le 500 \\ \left(500 - mod(z_i, 500)\right)\sin\left(\sqrt{\lvert 500 - mod(z_i, 500)\rvert}\right) - \frac{(z_i - 500)^2}{10000D} & if\ z_i > 500 \\ (mod(\lvert z_i\rvert, 500) - 500)\sin(\sqrt{\lvert mod(\lvert z_i\rvert, 500) - 500\rvert}) - \frac{(z_i + 500)^2}{10000D} & if\ z_i < -500 \end{cases}$	900	CEC 2014, F_9
F_{17}: Shifted and Rotated Levy Function	$F_{17}(X) = sin^2(\pi w_1) + \sum_{i=1}^{D-1}(w_i - 1)^2[1 + 10sin^2(\pi w_i + 1)] + (w_D - 1)^2[1 + sin^2(2\pi w_D)] \; where\ w_i = 1 + \frac{x_i - 1}{4}. \forall\, i = 1. \ldots .D$	900	CEC 2017, F_9
F_{18}: Shifted and Rotated Expanded Griewank's plus Rosenbrock's Function	$F_{18}(X) = f_{13}\left(M\left(\frac{5(x - o_{15})}{100}\right) + 1\right) + F_{15}^*$	1500	CEC 2014, F_{15}

Table A.3 The description of hybrid group functions.

Function's name	Function	$F_{min}(x)$	Sources
F_{19}: Hybrid Function 1	n = 3, p = [0.2, 0.4, 0.4] g_1: Zakharov Function F_3, g_2: Rosenbrock Function F_4 g_3: Rastrigin's Function F_5	1100	CEC 2017, F_{11}

F_{20}: Hybrid Function 2	n = 3, p = [0.3, 0.3, 0.4] g_1: High Conditioned Elliptic Function F_{11} g_2: Modified Schwefel's Function F_{10} g_3: Bent Cigar Function F_1	1200	CEC 2017, F_{12}
F_{21}: Hybrid Function 3	n = 3, p = [0.3, 0.3, 0.4] g_1: Bent Cigar Function F_1 g_2: Rosenbrock Function F_4 g_3: Lunache Bi-Rastrigin Function F_7	1300	CEC 2017, F_{13}
F_{22}: Hybrid Function 4	n = 4, p = [0.2, 0.2, 0.2, 0.4] g_1: High Conditioned Elliptic Function F_{11} g_2: Ackley's Function F_{13} g_3: Schaffer's F_7 Function F_{20} g_4: Rastrigin's Function F_5	1400	CEC 2017, F_{14}
F_{23}: Hybrid Function 1	n = 3, p = [0.3,0.3,0.4] g_1: Modified Schwefel's Function F_9 g_2: Rastrigin's Function F_8 g_3: High Conditioned Elliptic Function F_1	1700	CEC 2014, F_{17}
F_{24}: Hybrid Function 8	n = 5, p = [0.2, 0.2, 0.2, 0.2, 0.2] g_1: High Conditioned Elliptic Function F_1 g_2: Ackley's Function F_{13} g_3: Rastrigin's Function F_5 g_4: HGBat Function F_{18} g_5: Discus Function F_{12}	1800	CEC 2017, F_{18}
F_{25}: Hybrid Function 2	n = 3, p = [0.3,0.3,0.4] g_1: Bent Cigar Function F_2 g_2: HGBat Function F_{12} g_3: Rastrigin's Function F_8	1800	CEC 2014, F_{18}
F_{26}: Hybrid Function 3	n = 4, p = [0.2, 0.2, 0.3, 0.3] g_1: Griewank's Function F_7 g_2: Weierstrass Function F_6 g_3: Rosenbrock's Function F_4 g_4: Scaffer's F_6 Function F_{14}	1800	CEC 2014, F_{19}
F_{27}: Hybrid Function 4	n = 4, p = [0.2, 0.2, 0.3, 0.3] g_1: HGBat Function F_{12} g_2: Discus Function F_3 g_3: Expanded Griewank's plus Rosenbrock's Function F_{13} g_4: Rastrigin's Function F_8	2000	CEC 2014, F_{20}
F_{28}: Hybrid Function 5	n = 5, p = [0.1, 0.2, 0.2, 0.2, 0.3] g_1: Scaffer's F_6 Function F_{14} g_2: HGBat Function F_{12} g_3: Rosenbrock's Function F_4 g_4: Modified Schwefel's Function F_9 g_5: High Conditioned Elliptic Function F_1	2100	CEC 2014, F_{21}

Table A.4 The description of composition group functions.

Function's name	Function	$F_{min}(x)$	Sources
F_{29}: Composition Function 3 (n=3, Rotated)	n = 3, σ = [20, 20, 20] λ = [1, 1, 1] *bias* = [0, 100, 200] $g_{1\text{-}3}$: Rotated Schwefel's Function F_{15}'	900	CEC 2013, F_{23}
F_{30}: Composition Function 4 (n=3, Rotated)	n = 3, σ = [20, 20, 20] λ = [0.25, 1, 2.5] *bias* = [0, 100, 200] g_1: Rotated Schwefel's Function F_{15}' g_2: Rotated Rastrigin's Function F_{12}' g_3: Rotated Weierstrass Function F_9'	1000	CEC 2013, F_{24}

F_{31}: Composition Function 5 (n=3, Rotated)	$n = 3$, $\sigma = [10, 30, 50]$ $\lambda = [0.25, 1, 2.5]$ $bias = [0, 100, 200]$ g_1: Rotated Schwefel's Function F_{15}' g_2: Rotated Rastrigin's Function F_{12}' g_3: Rotated Weierstrass Function F_9'	1100	CEC 2013, F_{25}
F_{32}: Composition Function 6 (n=5, Rotated)	$n = 5$, $\sigma = [10, 10, 10, 10, 10]$, $\lambda = [0.25, 1, 1e-7, 2.5, 10]$ $bias = [0, 100, 200, 300, 400]$, g_1: Schwefel's Function F_{15}', g_2: Rotated Rastrigin's Function F_{12}', g_3 High Conditioned Elliptic Function F_2' g_4: Rotated Weierstrass Function F_9' g_5: Rotated Griewank's Function F_{10}'	1200	CEC 2013, F_{26}
F_{33}: Composition Function 1 (n=3)	$n = 3$, $\sigma = [10, 20, 30]$, $\lambda = [1, 1e-6, 1]$ $bias = [0, 100, 200]$, g_1: Rosenbrock's Function F_4', g_2: High Conditioned Elliptic Function F_{11}' g_3: Rastrigin's Function F_4'	2100	CEC 2017, F_{21}
F_{34}: Composition Function 5 (n=5)	$n = 5$, $\sigma = [10, 20, 30, 40, 50]$, $\lambda = [10, 1, 10, 1e-6, 1]$, $bias = [0, 100, 200,300, 400]$, g_1: Rastrigin 's Function F_5' g_2: Happycat Function F_{17}' g_3: Ackley Function F_{13}' g_4: Discus Function F_{12}' g_5: Rosenbrock's Function F_4'	2500	CEC 2017, F_{25}
F_{35}: Composition Function 4 (n=5)	$n = 5$, $\sigma= [10, 10, 10, 10, 10]$ $\lambda= [0.26, 1, 1e-7, 2.5, 10]$ $bias = [0, 100, 200, 300, 400]$, g_1: Rotated Schwefel's Function F_{11}' g_2: Rotated HappyCat Function F_{13}' g_3: Rotated High Conditioned Elliptic Function F_1', g_4: Rotated Weierstrass Function F_6', g_5: Rotated Griewank's Function F_7'	2600	CEC 2014, F_{26}
F_{36}: Composition Function 8 (n=6)	$n = 6$, $\sigma= [10, 20, 30, 40, 50, 60]$ $\lambda= [10, 10, 1e-6, 1, 1, 5e-4]$ $bias = [0, 100, 200, 300, 400, 500]$ g_1: Ackley's Function F_{13}' g_2: Griewank's Function F_{15}' g_3: Discus Function F_{12}' g_4: Rosenbrock's Function F_4' g_5: HappyCat Function F_{17}' g_6: Expanded Scaffer's F_6 Function F_6'	2800	CEC 2017, F_{28}
F_{37}: Composition Function 9 (n=3)	$n = 3$, $\sigma= [10, 30, 50]$, $\lambda= [1, 1, 1]$ $bias = [0, 100, 200]$ g_1: Hybrid Function 5 F_5' g_2: Hybrid Function 6 F_6' g_3: Hybrid Function 7 F_7'	2900	CEC 2017, F_{29}
F_{38}: Composition Function 10 (n=3)	$n = 3$, $\sigma= [10, 30, 50]$, $\lambda= [1, 1, 1]$ $bias = [0, 100, 200]$ g_1: Hybrid Function 5 F_5' g_2: Hybrid Function 8 F_8' g_3: Hybrid Function 9 F_9'	3000	CEC 2017, F_{30}

Appendix B

This appendix is to show detailed results of some pretests and experiments. First, experimental results of tuning pretests of the SMO's control parameters are presented in Fig B.1 and Tables B.1 and B.2. Then, the obtained results of experiments of Subsections 5.3.1 and 5.3.2 are reported in Tables B.3-B.6. Finally, convergence curves of the rest of the functions used in experiments of Subsection 5.3.4 are illustrated in Figs B.2- B.4.

Tuning of SMO's control parameters: The performance of the metaheuristic algorithms strongly depends upon the suitable setting of user-dependent parameters. Therefore, parameters of the SMO algorithm are tuned and set using the offline parameter tuning method. Fig. B.1 shows the impact of using different values for parameters λ and μ on the inverse Gaussian distribution used in the SMO. Then, to set these parameters by appropriate values, the performance of SMO was assessed using different combinations of values for λ and μ. The performance results gained by combinations were reported in Table. B.1 where the last row shows their rank using Friedman statistical test. The rank indicates the highest performance of SMO when λ=20 and μ=0.5.

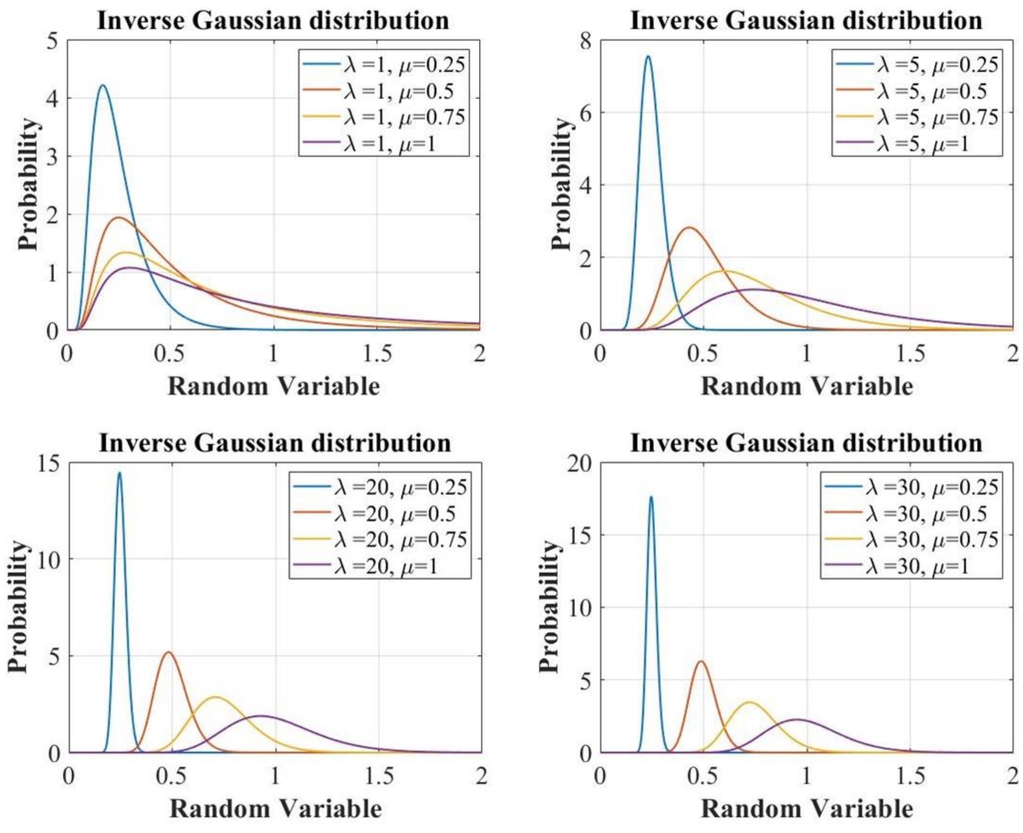

Fig. B.1. The inverse Gaussian distribution with different values of λ, and μ.

Table B.1 Performance results of SMO using different combinations of values for λ, and μ.

Func.	λ = 1	λ = 5

	μ = 0.25	μ = 0.5	μ = 0.75	μ = 1	μ = 0.25	μ = 0.5	μ = 0.75	μ = 1
F_1	-1.4000E+03	-1.4000E+03	-1.4000E+03	-1.4000E+03	-1.4000E+03	-1.4000E+03	-1.4000E+03	-1.4000E+03
F_2	2.9241E+05	4.0129E+05	3.0934E+05	4.4356E+05	2.4748E+05	5.1872E+05	4.4179E+05	3.4293E+05
F_3	2.0495E+06	2.3532E+06	1.2511E+06	8.1996E+05	5.8133E+05	3.7890E+05	6.0191E+05	1.0064E+05
F_4	-1.0988E+03	-1.0980E+03	-1.0996E+03	-1.0987E+03	-1.0986E+03	-1.0987E+03	-1.0995E+03	-1.0995E+03
F_5	-1.0000E+03	-1.0000E+03	-1.0000E+03	-1.0000E+03	-1.0000E+03	-1.0000E+03	-1.0000E+03	-1.0000E+03
F_6	1.0679E+02	1.0006E+02	1.0026E+02	1.0089E+02	1.0039E+02	1.0006E+02	1.0044E+02	1.0044E+02
F_7	3.1700E+02	2.0000E+02	2.0400E+02	6.5800E+02	4.9100E+02	3.1800E+02	2.0000E+02	2.0000E+02
F_8	3.0000E+02	3.0000E+02	3.0000E+02	3.0000E+02	3.0000E+02	3.0000E+02	3.0000E+02	3.0000E+02
F_9	-4.9999E+02	-4.9997E+02	-4.9999E+02	-4.9998E+02	-4.9998E+02	-4.9999E+02	-4.9998E+02	-4.9999E+02
F_{10}	-1.8260E+02	-2.1344E+02	-2.1244E+02	-1.9851E+02	-1.8160E+02	-2.0349E+02	-2.2836E+02	-2.4428E+02
F_{11}	4.2964E+01	-2.3182E+01	4.6255E+00	-4.8627E+01	-1.5775E+01	-3.9542E+01	-3.7385E+01	-6.5015E+01
F_{12}	5.1342E+02	5.2764E+02	5.1895E+02	5.0929E+02	5.2188E+02	5.0132E+02	5.1102E+02	5.0588E+02
F_{13}	4.0966E+02	4.1123E+02	4.0012E+02	4.0121E+02	4.0049E+02	4.0467E+02	4.1034E+02	4.1001E+02
F_{14}	6.1126E+02	6.1009E+02	6.0869E+02	6.1187E+02	6.1266E+02	6.0770E+02	6.0619E+02	6.0407E+02
F_{15}	7.0000E+02	7.0000E+02	7.0000E+02	7.0000E+02	7.0000E+02	7.0000E+02	7.0000E+02	7.0000E+02
F_{16}	1.0075E+03	9.8756E+02	9.8159E+02	9.6666E+02	9.8258E+02	9.6169E+02	9.6467E+02	9.5174E+02
F_{17}	9.2926E+02	9.0854E+02	9.0317E+02	9.0399E+02	9.0790E+02	9.0372E+02	9.0190E+02	9.0190E+02
F_{18}	1.5065E+03	1.5054E+03	1.5051E+03	1.5050E+03	1.5065E+03	1.5051E+03	1.5050E+03	1.5049E+03
F_{19}	1.1550E+03	1.1839E+03	1.1909E+03	1.1716E+03	1.1869E+03	1.1550E+03	1.1790E+03	1.1790E+03
F_{20}	8.1393E+03	1.5122E+04	1.3811E+04	1.9666E+04	1.8678E+04	1.8470E+04	3.0082E+04	3.0082E+04
F_{21}	1.8787E+03	1.3781E+03	1.3720E+03	1.4168E+03	1.3936E+03	1.3847E+03	1.4254E+03	1.4254E+03
F_{22}	1.4879E+03	1.5009E+03	1.4756E+03	1.4844E+03	1.4746E+03	1.4949E+03	1.4822E+03	1.4822E+03
F_{23}	4.1041E+03	3.6501E+03	3.5095E+03	3.1258E+03	3.1711E+03	3.3009E+03	3.2435E+03	3.2763E+03
F_{24}	1.8851E+03	1.8897E+03	1.8923E+03	1.8835E+03	1.8772E+03	1.8668E+03	1.8955E+03	1.8955E+03
F_{25}	1.9191E+03	1.9443E+03	1.9784E+03	1.9937E+03	1.9928E+03	1.9545E+03	2.0354E+03	1.8906E+03
F_{26}	1.9079E+03	1.9074E+03	1.9072E+03	1.9079E+03	1.9077E+03	1.9065E+03	1.9056E+03	1.9062E+03
F_{27}	2.0993E+03	2.0448E+03	2.0704E+03	2.0567E+03	2.0647E+03	2.0638E+03	2.0871E+03	2.0611E+03
F_{28}	2.6233E+03	2.5765E+03	2.8290E+03	2.6585E+03	2.8128E+03	2.5008E+03	2.8628E+03	2.5437E+03
F_{29}	6.5415E+03	6.0848E+03	5.1514E+03	6.9927E+03	6.8742E+03	6.2775E+03	6.5835E+03	6.8842E+03
F_{30}	1.2727E+03	1.2637E+03	1.2780E+03	1.2677E+03	1.2740E+03	1.2658E+03	1.2549E+03	1.2574E+03
F_{31}	1.3910E+03	1.4104E+03	1.4018E+03	1.4115E+03	1.4128E+03	1.3976E+03	1.4002E+03	1.3948E+03
F_{32}	1.4001E+03	1.4000E+03	1.4000E+03	1.4000E+03	1.4000E+03	1.4001E+03	1.4000E+03	1.4000E+03
F_{33}	2.4087E+03	2.3724E+03	2.3701E+03	2.3668E+03	2.3759E+03	2.3594E+03	2.3456E+03	2.3456E+03
F_{34}	2.9617E+03	2.9604E+03	2.9612E+03	2.9603E+03	2.9703E+03	2.9605E+03	2.9608E+03	2.9608E+03
F_{35}	2.7002E+03	2.7002E+03	2.7002E+03	2.7002E+03	2.7002E+03	2.7002E+03	2.7002E+03	2.7002E+03
F_{36}	3.2588E+03	3.2588E+03	3.2539E+03	3.2588E+03	3.2588E+03	3.2588E+03	3.2588E+03	3.2588E+03
F_{37}	3.3551E+03	3.3588E+03	3.4167E+03	3.3479E+03	3.4497E+03	3.2835E+03	3.2706E+03	3.2706E+03
F_{38}	5.8244E+05	5.8249E+05	5.8243E+05	5.8243E+05	5.8256E+05	5.8251E+05	5.8243E+05	5.8243E+05
Rank	10.455	7.993	8.016	9.361	10.001	6.669	4.977	4.621

Table B.1 Continued.

Func.	λ = 20				λ = 30			
	μ = 0.25	μ = 0.5	μ = 0.75	μ = 1	μ = 0.25	μ = 0.5	μ = 0.75	μ = 1
F_1	-1.4000E+03	-1.4000E+03	-1.4000E+03	-1.4000E+03	-1.4000E+03	-1.4000E+03	-1.4000E+03	-1.4000E+03
F_2	3.4107E+05	1.6303E+04	3.9360E+05	3.0839E+05	3.0791E+05	4.5244E+05	2.3298E+05	2.9854E+05
F_3	3.9236E+06	1.6167E+05	9.2876E+05	4.2533E+05	1.7748E+06	1.3630E+06	1.6241E+05	1.0080E+05
F_4	-1.0972E+03	-1.1000E+03	-1.0996E+03	-1.0996E+03	-1.0981E+03	-1.0994E+03	-1.0991E+03	-1.0994E+03
F_5	-1.0000E+03	-1.0000E+03	-1.0000E+03	-1.0000E+03	-1.0000E+03	-1.0000E+03	-1.0000E+03	-1.0000E+03
F_6	1.0044E+02	1.0266E+02	1.0044E+02	1.0094E+02	1.0034E+02	1.0135E+02	1.0000E+02	1.0012E+02
F_7	2.0000E+02	2.0000E+02	2.0000E+02	2.2400E+02	2.6000E+02	2.0100E+02	2.1700E+02	2.1000E+02
F_8	3.0000E+02	3.0000E+02	3.0000E+02	3.0000E+02	3.0000E+02	3.0000E+02	3.0000E+02	3.0000E+02
F_9	-4.9997E+02	-4.9999E+02	-4.9999E+02	-4.9999E+02	-4.9999E+02	-4.9998E+02	-4.9999E+02	-4.9999E+02
F_{10}	-1.8359E+02	-2.2040E+02	-2.3234E+02	-2.4826E+02	-2.0548E+02	-2.4528E+02	-2.3632E+02	-2.3433E+02
F_{11}	-4.6401E+00	-3.4470E+01	-5.5719E+01	-4.9095E+01	-2.1750E+00	-3.4928E+01	-5.6127E+01	-8.5320E+01
F_{12}	5.1773E+02	5.1030E+02	5.1593E+02	5.0472E+02	5.3952E+02	5.0835E+02	5.0747E+02	4.9759E+02
F_{13}	4.0619E+02	4.0000E+02	4.0940E+02	4.0021E+02	4.0326E+02	4.0000E+02	4.0976E+02	4.0001E+02
F_{14}	6.1456E+02	6.2210E+02	6.0513E+02	6.0456E+02	6.1054E+02	6.0725E+02	6.0496E+02	6.0402E+02
F_{15}	7.0000E+02	7.0000E+02	7.0000E+02	7.0000E+02	7.0000E+02	7.0000E+02	7.0000E+02	7.0000E+02
F_{16}	9.8059E+02	9.7562E+02	9.6069E+02	9.5472E+02	9.9950E+02	9.6567E+02	9.5174E+02	9.5373E+02
F_{17}	9.0190E+02	9.2442E+02	9.0190E+02	9.0063E+02	9.0742E+02	9.0296E+02	9.0072E+02	9.0045E+02
F_{18}	1.5067E+03	1.5064E+03	1.5047E+03	1.5051E+03	1.5055E+03	1.5062E+03	1.5052E+03	1.5054E+03
F_{19}	1.1790E+03	1.1398E+03	1.1790E+03	1.1531E+03	1.1709E+03	1.1597E+03	1.1567E+03	1.1537E+03
F_{20}	3.0082E+04	6.1510E+03	3.0082E+04	1.7618E+04	1.2029E+04	2.4108E+04	1.5900E+04	1.3781E+04
F_{21}	1.4254E+03	1.4330E+03	1.4254E+03	1.4924E+03	1.3812E+03	1.3992E+03	1.3793E+03	1.5398E+03
F_{22}	1.4822E+03	1.6015E+03	1.4822E+03	1.4907E+03	1.4463E+03	1.5064E+03	1.4869E+03	1.4621E+03
F_{23}	3.2188E+03	4.0961E+03	3.8672E+03	3.2261E+03	3.6055E+03	3.3910E+03	3.2132E+03	3.6542E+03
F_{24}	1.8955E+03	2.0622E+03	1.8955E+03	1.8789E+03	1.8817E+03	1.8539E+03	1.8794E+03	1.8789E+03
F_{25}	2.0960E+03	1.9630E+03	1.8731E+03	1.9587E+03	1.9690E+03	1.9372E+03	2.0111E+03	1.9225E+03
F_{26}	1.9070E+03	1.9056E+03	1.9048E+03	1.9069E+03	1.9083E+03	1.9065E+03	1.9063E+03	1.9068E+03

F_{27}	2.0417E+03	2.2035E+03	2.0437E+03	2.0508E+03	2.0638E+03	2.0785E+03	2.0703E+03	2.0654E+03
F_{28}	3.0092E+03	3.3369E+03	2.5971E+03	2.6770E+03	2.6889E+03	2.7069E+03	2.8331E+03	2.5755E+03
F_{29}	6.6686E+03	7.8262E+03	6.2083E+03	7.2932E+03	6.3759E+03	6.4027E+03	6.5286E+03	6.2726E+03
F_{30}	1.2725E+03	1.3258E+03	1.2520E+03	1.2510E+03	1.2813E+03	1.2718E+03	1.2649E+03	1.2478E+03
F_{31}	1.4149E+03	1.4419E+03	1.3972E+03	1.3912E+03	1.4050E+03	1.3977E+03	1.3910E+03	1.3926E+03
F_{32}	1.4000E+03	1.4000E+03	1.4000E+03	1.4000E+03	1.4001E+03	1.4000E+03	1.4000E+03	1.4000E+03
F_{33}	2.3456E+03	2.3811E+03	2.3456E+03	2.3630E+03	2.3824E+03	2.3613E+03	2.3603E+03	2.3460E+03
F_{34}	2.9608E+03	2.9599E+03	2.9608E+03	2.9589E+03	2.9609E+03	2.9608E+03	2.9560E+03	2.9513E+03
F_{35}	2.7002E+03	2.7002E+03	2.7002E+03	2.7002E+03	2.7002E+03	2.7002E+03	2.7002E+03	2.7002E+03
F_{36}	3.2588E+03	3.2588E+03	3.2588E+03	3.2588E+03	3.2534E+03	3.2588E+03	3.2588E+03	3.2588E+03
F_{37}	3.2706E+03	3.5850E+03	3.2706E+03	3.3660E+03	3.3040E+03	3.2973E+03	3.2544E+03	3.2494E+03
F_{38}	5.8243E+05	5.8242E+05	5.8243E+05	5.8242E+05	5.8243E+05	5.8243E+05	5.8243E+05	5.8253E+05
Rank	9.739	1.040	4.552	2.695	10.135	5.135	3.058	1.314

Tuning of the number of flocks (k): In this experiment, the impact of k on SMO's performance was assessed using different values of 3, 5, 10, 15, and 20. The obtained results on all test functions for dimension 50 are reported in Table B.2 where the last row shows the Freidman rank. The rank recommends us to set k by 10 to gain the best SMO's performance.

Table B.2 Impact of the number of flocks (k) on SMO's performance on all test functions for dimension 50.

Func.	k = 3		k = 5		k = 10		k = 15		k = 20	
	Avg.	Min	Avg.	Min	Avg.	Min	Avg.	Min	Avg.	Min
F_1	-1.4000E+03	**-1.4000E+03**	-1.4000E+03	**-1.4000E+03**	-1.4000E+03	**-1.4000E+03**	-1.4000E+03	**-1.4000E+03**	-1.4000E+03	**-1.4000E+03**
F_2	7.9285E+05	2.9985E+05	1.0771E+06	4.9741E+05	2.3686E+05	**1.6303E+04**	6.3578E+05	1.1640E+05	5.3191E+05	2.3333E+05
F_3	2.1008E+07	9.2181E+05	1.1662E+07	4.1319E+05	9.2489E+06	1.6167E+05	1.3056E+07	1.1440E+06	9.6949E+06	**1.1237E+05**
F_4	-1.0895E+03	-1.0973E+03	-1.0960E+03	-1.0992E+03	-1.1000E+03	**-1.1000E+03**	-1.0988E+03	**-1.0998E+03**	-1.0985E+03	-1.0998E+03
F_5	-1.0000E+03	**-1.0000E+03**	-1.0000E+03	**-1.0000E+03**	-1.0000E+03	**-1.0000E+03**	-1.0000E+03	**-1.0000E+03**	-1.0000E+03	**-1.0000E+03**
F_6	6.3667E+02	1.0737E+02	6.4416E+02	**1.0000E+02**	1.4052E+03	1.0266E+02	1.4528E+02	1.0053E+02	1.1668E+02	**1.0002E+02**
F_7	5.2330E+16	2.4134E+05	1.1332E+12	4.1040E+03	2.0513E+02	**2.0000E+02**	2.7490E+10	**2.0000E+02**	1.2823E+05	2.1200E+02
F_8	3.1516E+02	3.0250E+02	3.0019E+02	**3.0003E+02**	3.0000E+02	**3.0000E+02**	3.0000E+02	**3.0000E+02**	3.0000E+02	**3.0000E+02**
F_9	-4.9996E+02	**-4.9999E+02**	-4.9995E+02	**-4.9999E+02**	-4.9996E+02	**-4.9999E+02**	-4.9993E+02	**-4.9999E+02**	-4.9995E+02	-4.9998E+02
F_{10}	-1.9523E+02	-2.2836E+02	-2.0762E+02	**-2.4528E+02**	-1.6203E+02	-2.2040E+02	-1.9200E+02	-2.2737E+02	-1.8031E+02	**-2.4528E+02**
F_{11}	-1.7403E+01	**-9.2497E+01**	-1.0925E+00	-8.2072E+01	6.6467E+01	-3.4470E+01	2.5526E+01	-4.1955E+01	5.3278E+01	-5.3951E+01
F_{12}	5.4102E+02	5.0404E+02	5.3415E+02	**4.9731E+02**	5.5805E+02	5.1030E+02	5.4102E+02	5.0796E+02	5.3788E+02	5.0898E+02
F_{13}	4.6876E+02	4.1570E+02	4.6158E+02	4.0321E+02	4.0395E+02	**4.0000E+02**	4.3798E+02	**4.0057E+02**	4.4073E+02	4.0011E+02
F_{14}	6.0685E+02	**6.0206E+02**	6.0751E+02	6.0359E+02	6.4040E+02	6.2210E+02	6.1061E+02	6.0656E+02	6.1186E+02	6.0651E+02
F_{15}	7.0001E+02	**7.0000E+02**	7.0001E+02	**7.0000E+02**	7.0000E+02	**7.0000E+02**	7.0000E+02	**7.0000E+02**	7.0001E+02	**7.0000E+02**
F_{16}	9.9666E+02	9.5174E+02	9.8900E+02	**9.4975E+02**	1.0459E+03	9.7562E+02	9.9681E+02	9.5273E+02	1.0034E+03	9.6169E+02
F_{17}	9.0318E+02	**9.0009E+02**	9.0325E+02	9.0018E+02	1.2489E+03	9.2442E+02	9.1828E+02	9.0190E+02	9.2668E+02	9.0560E+02
F_{18}	1.5071E+03	**1.5045E+03**	1.5076E+03	**1.5041E+03**	1.5099E+03	1.5064E+03	1.5089E+03	1.5051E+03	1.5099E+03	1.5072E+03
F_{19}	1.1641E+03	**1.1289E+03**	1.1804E+03	1.1481E+03	1.2078E+03	1.1398E+03	1.2382E+03	1.1800E+03	1.2361E+03	1.1879E+03
F_{20}	5.3394E+04	1.3122E+04	6.8961E+04	1.2782E+04	1.5422E+04	**6.1510E+03**	5.4707E+04	8.1472E+03	4.6298E+04	1.6801E+04
F_{21}	5.6589E+03	1.6201E+03	7.9351E+03	**1.3928E+03**	3.6486E+03	1.4330E+03	6.4385E+03	1.5198E+03	4.8414E+03	**1.3546E+03**
F_{22}	1.4701E+03	**1.4344E+03**	1.4851E+03	1.4542E+03	1.7595E+03	1.6015E+03	1.5606E+03	1.4829E+03	1.5964E+03	1.5368E+03
F_{23}	3.9032E+03	3.3079E+03	3.7598E+03	**2.7837E+03**	8.7564E+03	4.0961E+03	7.7064E+03	3.7110E+03	1.0044E+04	3.3267E+03
F_{24}	1.8992E+03	1.8630E+03	1.8983E+03	**1.8515E+03**	5.4535E+03	2.0622E+03	2.0852E+03	1.8930E+03	2.0329E+03	1.9307E+03
F_{25}	2.5185E+03	**1.8348E+03**	2.0907E+03	1.8363E+03	2.3451E+03	1.9630E+03	2.3064E+03	1.9168E+03	2.4836E+03	1.9355E+03
F_{26}	1.9109E+03	1.9067E+03	1.9106E+03	1.9071E+03	1.9078E+03	**1.9056E+03**	1.9104E+03	1.9061E+03	1.9098E+03	1.9068E+03
F_{27}	2.0684E+03	2.0425E+03	2.0680E+03	**2.0299E+03**	2.3685E+03	2.2035E+03	2.1671E+03	2.0824E+03	2.1807E+03	2.0917E+03
F_{28}	3.0595E+03	2.5989E+03	2.9836E+03	**2.4036E+03**	4.9980E+03	3.3369E+03	3.2941E+03	2.8011E+03	3.7045E+03	2.6914E+03
F_{29}	8.4638E+03	7.3251E+03	8.2444E+03	**5.6879E+03**	9.6003E+03	7.8262E+03	8.4981E+03	7.3580E+03	8.4300E+03	6.3719E+03
F_{30}	1.2724E+03	1.2533E+03	1.2724E+03	**1.2406E+03**	1.3544E+03	1.3258E+03	1.2857E+03	1.2661E+03	1.2813E+03	1.2629E+03
F_{31}	1.4080E+03	1.3813E+03	1.4091E+03	**1.3736E+03**	1.4800E+03	1.4419E+03	1.4187E+03	1.3977E+03	1.4236E+03	1.4047E+03
F_{32}	1.4322E+03	**1.4000E+03**	1.4703E+03	**1.4000E+03**	1.4913E+03	**1.4000E+03**	1.4466E+03	**1.4000E+03**	1.5024E+03	**1.4000E+03**
F_{33}	2.3925E+03	**2.3354E+03**	2.3981E+03	2.3593E+03	2.4558E+03	2.3811E+03	2.3876E+03	2.3397E+03	2.3991E+03	2.3578E+03
F_{34}	3.0345E+03	2.9802E+03	3.0292E+03	2.9619E+03	3.0346E+03	**2.9599E+03**	3.0226E+03	**2.9602E+03**	3.0283E+03	2.9603E+03
F_{35}	2.7004E+03	**2.7003E+03**	2.7003E+03	**2.7003E+03**	2.7003E+03	**2.7002E+03**	2.7103E+03	**2.7002E+03**	2.7153E+03	**2.7002E+03**
F_{36}	3.2751E+03	**3.2569E+03**	3.2760E+03	3.2588E+03	3.2842E+03	3.2588E+03	3.2952E+03	3.2588E+03	3.2742E+03	3.2588E+03
F_{37}	3.5625E+03	**3.2328E+03**	3.5176E+03	3.2364E+03	4.3394E+03	3.5850E+03	3.6197E+03	3.2576E+03	3.6708E+03	3.3392E+03
F_{38}	6.6355E+05	5.9133E+05	6.8806E+05	5.8490E+05	7.4394E+05	**5.8242E+05**	6.6958E+05	**5.8241E+05**	6.8692E+05	5.8322E+05
Rank	2.8263		2.7875		2.1901		3.0362		3.1599	

Table B.3 Results comparison of unimodal group functions.

F	D	Metrics	CLPSO (2006)	ABC (2007)	ACO_R (2008)	Best-so-far ABC (2011)	KH (2012)	WOA (2016)	BOA (2019)	HHO (2019)	HGSO (2019)	$LIACO_R$ (2019)	SMO
F_1	30	Avg	-1.4000E+03	-1.4000E+03	-1.2988E+03	-1.4000E+03	-1.4000E+03	-1.39997E+03	5.3296E+04	-1.3961E+03	1.0356E+04	-1.4000E+03	-1.4000E+03
		Min	**-1.4000E+03**	**-1.4000E+03**	-1.3237E+03	**-1.4000E+03**	**-1.4000E+03**	-1.39998E+03	4.2784E+04	-1.3980E+03	3.5655E+03	**-1.4000E+03**	**-1.4000E+03**
	50	Avg	-1.4000E+03	-1.4000E+03	1.0894E+04	-1.4000E+03	-1.4000E+03	-1.3989E+03	7.9398E+04	-1.3809E+03	2.3957E+04	-1.4000E+03	-1.4000E+03
		Min	**-1.4000E+03**	**-1.4000E+03**	7.5004E+03	**-1.4000E+03**	**-1.4000E+03**	-1.3997E+03	7.1261E+04	-1.3888E+03	1.3238E+04	**-1.4000E+03**	**-1.4000E+03**
	100	Avg	-1.3965E+03	-1.4000E+03	1.0480E+05	-1.3999E+03	-1.1323E+03	-1.3452E+03	1.8288E+05	-1.2559E+03	9.8512E+04	-1.4000E+03	-1.4000E+03
		Min	-1.3971E+03	**-1.4000E+03**	9.3768E+04	**-1.4000E+03**	-1.3697E+03	-1.3822E+03	1.6811E+05	-1.2879E+03	6.2606E+04	**-1.4000E+03**	**-1.4000E+03**
F_2	30	Avg	2.3166E+07	1.3524E+07	3.3763E+08	1.7193E+07	1.0116E+07	2.2161E+07	1.2291E+09	7.7974E+06	1.2330E+08	9.2712E+05	4.4149E+04
		Min	1.0949E+07	9.2948E+06	2.5168E+08	9.6225E+06	6.1665E+06	6.7446E+06	4.1552E+08	3.6281E+06	7.0771E+07	4.4127E+05	**7.9314E+03**
	50	Avg	7.3572E+07	2.7766E+07	1.4601E+09	5.4587E+07	9.3850E+06	3.3738E+07	3.3834E+09	1.8823E+07	3.3458E+08	2.2109E+06	2.3686E+05
		Min	4.9368E+07	1.6751E+07	1.0382E+09	3.8133E+07	4.8612E+06	1.6622E+07	2.4945E+09	1.0264E+07	1.7970E+08	1.2754E+06	**1.6303E+04**
	100	Avg	4.0803E+08	9.1472E+07	6.3594E+09	2.2758E+08	2.8549E+07	1.2891E+08	1.3867E+10	7.6232E+07	1.9726E+09	1.2812E+07	1.3339E+06
		Min	3.1230E+08	5.8621E+07	4.7729E+09	1.7341E+08	1.5519E+07	7.2462E+07	9.4139E+09	5.2181E+07	9.6251E+08	7.2854E+06	**9.2768E+05**
F_3	30	Avg	9.9975E+08	7.9705E+08	6.2137E+09	3.9086E+09	6.6065E+10	1.1376E+10	1.0591E+20	1.1024E+09	4.1887E+10	2.7544E+08	4.0660E+05
		Min	3.8110E+08	1.8111E+08	4.9440E+09	2.0058E+09	1.6548E+09	1.1814E+09	7.6014E+12	6.9535E+07	2.3153E+10	1.2652E+07	**-1.2000E+03**
	50	Avg	1.4586E+10	5.3855E+09	1.0375E+11	3.5799E+10	1.9294E+11	1.9416E+10	1.8732E+18	2.6431E+09	7.3763E+10	6.7819E+08	9.2489E+06
		Min	8.6546E+09	1.2344E+09	8.4581E+10	1.9312E+10	3.4506E+10	4.0770E+09	2.5471E+13	6.5631E+08	5.2199E+10	4.8509E+07	**1.6167E+05**
	100	Avg	2.0607E+11	6.3794E+10	5.6381E+11	2.3728E+11	1.8309E+18	1.2528E+11	1.2603E+26	3.7743E+10	4.9571E+16	2.2358E+10	2.3773E+08
		Min	1.4013E+11	3.5167E+10	4.6110E+11	1.9852E+11	9.2050E+15	4.8053E+10	3.0547E+23	1.4969E+10	1.7409E+15	9.2379E+09	**1.1237E+07**
F_4	30	Avg	4.2869E+04	6.4159E+04	1.0182E+05	9.1570E+04	3.6124E+04	3.1878E+04	7.2052E+04	3.5423E+02	3.4108E+04	1.8694E+04	-1.1000E+03
		Min	3.2845E+04	3.9050E+04	8.3427E+04	6.1939E+04	2.6005E+04	1.1328E+04	6.1428E+04	-4.3869E+02	2.1901E+04	5.3573E+03	**-1.1000E+03**
	50	Avg	8.4619E+04	1.3154E+05	2.0149E+05	1.6318E+05	5.7232E+04	2.4767E+04	9.6693E+04	1.3805E+03	7.2309E+04	4.8942E+04	-1.1000E+03
		Min	6.3459E+04	1.1425E+05	1.7704E+05	1.3299E+05	3.8726E+04	1.4485E+04	8.2545E+04	2.0838E+02	6.4446E+04	3.0548E+04	**-1.1000E+03**
	100	Avg	2.3255E+05	3.3778E+05	4.6242E+05	3.7501E+05	1.7538E+05	3.8301E+05	3.7513E+05	3.5259E+04	1.8533E+05	9.7821E+04	-1.0985E+03
		Min	1.9623E+05	2.9008E+05	3.8791E+05	3.1611E+05	1.4712E+05	1.5315E+05	2.2822E+05	2.1060E+04	1.6073E+05	6.6847E+04	**-1.0999E+03**
F_5	30	Avg	-1.0000E+03	-1.0000E+03	-9.6482E+02	-1.0000E+03	-9.9981E+02	-9.7473E+02	2.8853E+04	-9.9845E+02	1.5986E+03	-1.0000E+03	-1.0000E+03
		Min	**-1.0000E+03**	**-1.0000E+03**	-9.7199E+02	**-1.0000E+03**	-9.9997E+02	-9.9810E+02	8.0007E+03	-9.9910E+02	4.2974E+02	**-1.0000E+03**	**-1.0000E+03**
	50	Avg	-9.9999E+02	-1.0000E+03	-2.9438E+02	-1.0000E+03	-9.9366E+02	-9.0759E+02	2.6781E+04	-9.9458E+02	1.9401E+03	-1.0000E+03	-1.0000E+03
		Min	**-1.0000E+03**	**-1.0000E+03**	-4.6256E+02	**-1.0000E+03**	-9.9970E+02	-9.6766E+02	1.5712E+04	-9.9628E+02	8.2139E+02	**-1.0000E+03**	**-1.0000E+03**
	100	Avg	-9.9277E+02	-1.0000E+03	7.9682E+03	-9.9991E+02	-7.5630E+02	-6.9059E+02	8.3446E+04	-9.5982E+02	1.6478E+04	-1.0000E+03	-1.0000E+03
		Min	-9.9427E+02	**-1.0000E+03**	6.0123E+03	-9.9996E+02	-8.9593E+02	-7.8906E+02	6.0191E+04	-9.6938E+02	1.1763E+04	**-1.0000E+03**	**-1.0000E+03**
F_6	30	Avg	9.6742E+02	2.6751E+02	3.8911E+08	9.6133E+02	7.6704E+03	3.7518E+05	5.6197E+10	5.8696E+06	1.3430E+10	1.9950E+03	1.0000E+02
		Min	6.0333E+02	1.0421E+02	1.8125E+08	2.4350E+02	2.0993E+03	2.6656E+04	4.7482E+10	3.5972E+06	8.9550E+09	1.0117E+02	**1.0000E+02**
	50	Avg	4.8111E+05	5.6494E+03	2.0239E+10	1.3694E+05	1.0457E+05	5.2129E+06	1.0805E+11	3.2430E+07	4.3670E+10	1.2565E+03	1.4052E+03
		Min	2.5206E+05	1.6877E+03	1.5251E+10	5.1301E+04	3.0587E+04	1.0128E+06	9.4326E+10	1.9959E+07	1.9217E+10	**1.0008E+02**	1.0266E+02
	100	Avg	5.9227E+07	3.7811E+04	1.5654E+11	2.0350E+07	8.7027E+08	2.1930E+08	2.6373E+11	2.4988E+08	1.5831E+11	4.5279E+03	4.0077E+03
		Min	4.7148E+07	8.6697E+03	1.3997E+11	1.0721E+07	4.9840E+07	1.0979E+08	2.4310E+11	2.0473E+08	1.1802E+11	**1.0385E+02**	1.9904E+02
F_7	30	Avg	1.5430E+16	1.7237E+10	1.2649E+36	4.2608E+12	1.4805E+27	1.4639E+23	4.0705E+50	5.1272E+08	4.2712E+33	7.2826E+13	2.0000E+02
		Min	4.3216E+14	8.7019E+06	8.4496E+31	1.2058E+08	2.6745E+16	1.3933E+17	4.9626E+41	8.7447E+04	1.1146E+29	6.5765E+04	**2.0000E+02**
	50	Avg	2.6990E+40	1.4691E+26	6.6869E+72	8.5645E+32	4.2816E+62	9.3586E+56	6.4743E+88	3.5111E+22	3.5189E+60	8.9313E+45	2.0513E+02
		Min	9.5120E+34	2.1340E+19	2.2421E+68	1.1313E+29	8.6786E+43	3.7261E+44	4.5162E+77	1.1400E+16	1.5816E+55	8.0978E+19	**2.0000E+02**
	100	Avg	3.9871E+116	1.0208E+81	3.5032E+168	5.0695E+100	1.9460E+166	2.7377E+156	1.4446E+192	1.2013E+85	2.5603E+147	1.6019E+116	9.9560E+21
		Min	6.8982E+109	2.1279E+62	2.2476E+160	8.3748E+87	2.6317E+133	3.8723E+117	1.3668E+180	2.7910E+66	5.0404E+136	6.2166E+85	**2.0374E+09**
F_8	30	Avg	4.3324E+04	1.0567E+05	1.5808E+05	1.2647E+05	2.9994E+04	1.0251E+05	8.3747E+04	3.8019E+02	3.4548E+04	7.1246E+02	3.0000E+02
		Min	3.1619E+04	8.5433E+04	1.2173E+05	9.7263E+04	1.6214E+04	3.6822E+04	6.4722E+04	3.2157E+02	2.1310E+04	3.0039E+02	**3.0000E+02**
	50	Avg	1.6311E+05	2.1241E+05	3.6731E+05	2.5448E+05	1.0683E+05	5.8009E+04	2.2499E+05	1.8795E+03	1.3368E+05	4.7124E+04	3.0000E+02
		Min	1.3340E+05	1.4255E+05	2.8195E+05	2.0009E+05	7.5633E+04	2.3182E+04	1.7175E+05	1.0223E+03	1.0521E+05	1.5731E+04	**3.0000E+02**
	100	Avg	5.3614E+05	5.5762E+05	9.0173E+05	6.4287E+05	3.3609E+05	6.6315E+05	3.6587E+05	7.1018E+04	3.0499E+05	2.2690E+05	3.0074E+02
		Min	4.6934E+05	4.9190E+05	6.8732E+05	5.4783E+05	2.6021E+05	2.5691E+05	3.1606E+05	4.9445E+04	2.5828E+05	1.6291E+05	**3.0013E+02**

Table B.4 Results comparison of multi-modal group functions.

F	D	Metrics	CLPSO (2006)	ABC (2007)	ACO$_R$ (2008)	Best-so-far ABC (2011)	KH (2012)	WOA (2016)	BOA (2019)	HHO (2019)	HGSO (2019)	LIACO$_R$ (2019)	SMO
F_9	30	Avg	-4.8977E+02	-4.9823E+02	2.0102E+02	-4.8541E+02	-4.9882E+02	-4.7687E+02	9.0086E+03	-4.9465E+02	1.2541E+03	-4.9955E+02	-4.9996E+02
		Min	-4.9360E+02	-4.9863E+02	-1.9946E+01	-4.9428E+02	-4.9978E+02	-4.9270E+02	6.6582E+03	-4.9652E+02	5.1400E+02	-4.9991E+02	-4.9999E+02
	50	Avg	-3.8579E+02	-4.9248E+02	5.8329E+03	-3.8576E+02	-4.9311E+02	-3.8734E+02	1.4419E+04	-4.7846E+02	2.7754E+03	-4.9969E+02	-4.9996E+02
		Min	-4.0523E+02	-4.9518E+02	4.4275E+03	-4.2764E+02	-4.9767E+02	-4.4628E+02	1.2123E+04	-4.8681E+02	1.7529E+03	-4.9994E+02	-4.9999E+02
	100	Avg	2.7851E+02	-4.7183E+02	2.7671E+04	6.6748E+02	-2.8998E+02	8.3396E+00	4.2186E+04	-3.2191E+02	1.3254E+04	-4.9420E+02	-4.9995E+02
		Min	1.5415E+02	-4.8562E+02	2.4762E+04	3.6084E+02	-4.2362E+02	-1.9301E+02	3.7298E+04	-3.6856E+02	9.7179E+03	-4.9594E+02	-5.0000E+02
F_{10}	30	Avg	-1.5328E+02	-5.5114E+01	-4.2533E+01	-3.2544E+01	-1.3977E+02	1.3688E+02	7.8355E+02	2.1613E+02	7.8349E+01	-1.8289E+02	-2.3032E+02
		Min	-1.7595E+02	-1.4628E+02	-7.0321E+01	-1.0299E+02	-1.9146E+02	-4.7928E+01	4.6274E+02	4.4951E+01	-4.5351E+00	-2.1841E+02	-2.6816E+02
	50	Avg	9.9495E+01	4.2477E+02	4.3317E+02	4.3608E+02	7.4462E+01	5.4745E+02	1.3412E+03	6.2227E+02	4.3261E+02	-4.3551E+01	-1.6203E+02
		Min	6.7818E+01	1.9223E+02	3.7790E+02	1.9948E+02	2.6450E+00	3.1807E+02	1.0669E+03	3.8690E+02	3.0621E+02	-1.5175E+02	-2.2040E+02
	100	Avg	7.6450E+02	2.1378E+03	2.0916E+03	2.0451E+03	9.6151E+02	1.9360E+03	3.3051E+03	2.2176E+03	1.7535E+03	7.3131E+02	9.8977E+01
		Min	7.1949E+02	1.8357E+03	1.8821E+03	1.6155E+03	7.7958E+02	1.3343E+03	3.0233E+03	1.9454E+03	1.4414E+03	5.2979E+02	-6.4880E+00
F_{11}	30	Avg	-3.0806E+01	9.7693E+01	5.6039E+01	1.0659E+02	7.5834E+01	2.7512E+02	9.9595E+02	3.6600E+02	1.9854E+02	1.1797E+01	-8.4187E+01
		Min	-5.7123E+01	4.2007E+01	3.2317E+01	3.7580E+01	-1.1900E+01	1.2098E+02	7.0044E+02	2.0804E+02	1.3212E+02	-6.3567E+01	-1.2823E+02
	50	Avg	2.1844E+02	5.8081E+02	5.3615E+02	6.5344E+02	3.8164E+02	7.7149E+02	1.6983E+03	8.6993E+02	5.1666E+02	2.2506E+02	6.6467E+01
		Min	1.7424E+02	4.2297E+02	4.3005E+02	5.5633E+02	2.8042E+02	5.9882E+02	1.3685E+03	6.8992E+02	4.2618E+02	1.1003E+02	-3.4470E+01
	100	Avg	8.6887E+02	2.4452E+03	2.2229E+03	2.3381E+03	1.6105E+03	2.2716E+03	3.8363E+03	2.5607E+03	1.8961E+03	1.1059E+03	4.9338E+02
		Min	7.9708E+02	2.0912E+03	2.0823E+03	2.0409E+03	1.3912E+03	1.6486E+03	3.0966E+03	2.1817E+03	1.4968E+03	8.6338E+02	3.0610E+02
F_{12}	30	Avg	6.1505E+02	7.0993E+02	7.1607E+02	6.8185E+02	5.2682E+02	9.2432E+02	1.7272E+03	1.0674E+03	8.1875E+02	5.1979E+02	4.7825E+02
		Min	5.9445E+02	6.6232E+02	6.8568E+02	6.3254E+02	4.8624E+02	7.0102E+02	1.4578E+03	7.7827E+02	7.4356E+02	4.7873E+02	4.5138E+02
	50	Avg	8.5272E+02	1.2199E+03	1.8299E+03	1.1611E+03	7.4354E+02	1.4745E+03	2.3640E+03	1.5391E+03	1.2457E+03	7.0597E+02	5.5805E+02
		Min	8.2566E+02	1.0693E+03	1.6863E+03	1.0708E+03	6.8212E+02	1.2114E+03	2.1111E+03	1.4052E+03	1.0914E+03	5.9442E+02	5.1030E+02
	100	Avg	1.4950E+03	3.2439E+03	7.5203E+03	3.3058E+03	1.9058E+03	3.2411E+03	4.7296E+03	3.2844E+03	2.8590E+03	1.6211E+03	8.8135E+02
		Min	1.4281E+03	2.8748E+03	6.5879E+03	2.6072E+03	1.7362E+03	2.7895E+03	4.2665E+03	2.8787E+03	2.3677E+03	1.3414E+03	7.6468E+02
F_{13}	30	Avg	4.8804E+02	4.1246E+02	6.0438E+02	4.5619E+02	5.0480E+02	5.6468E+02	1.7236E+04	5.2661E+02	1.3986E+03	4.5678E+02	4.0000E+02
		Min	4.4595E+02	4.0120E+02	5.8353E+02	4.0644E+02	4.6827E+02	4.8413E+02	9.6320E+03	4.7337E+02	9.6843E+02	4.0001E+02	4.0000E+02
	50	Avg	5.7647E+02	4.6305E+02	1.6161E+03	5.0185E+02	5.5036E+02	6.4086E+02	5.1879E+04	6.0145E+02	8.6841E+03	5.1176E+02	4.0395E+02
		Min	5.4066E+02	4.2515E+02	1.4045E+03	4.8642E+02	4.6152E+02	5.1929E+02	3.7461E+04	5.0178E+02	5.5239E+03	4.1159E+02	4.0000E+02
	100	Avg	9.9397E+02	6.7023E+02	1.8966E+04	7.8239E+02	8.8293E+02	1.0761E+03	1.1261E+05	8.9821E+02	2.6917E+04	7.3339E+02	5.2312E+02
		Min	9.4943E+02	6.2599E+02	1.6322E+04	7.3408E+02	7.7303E+02	9.6373E+02	9.2681E+04	7.5588E+02	1.9802E+04	5.8661E+02	4.7319E+02
F_{14}	30	Avg	6.1493E+02	6.1467E+02	6.3716E+02	6.1446E+02	6.2006E+02	6.3500E+02	6.4628E+02	6.2889E+02	6.3054E+02	6.1530E+02	6.1989E+02
		Min	6.1307E+02	6.1029E+02	6.3380E+02	6.1314E+02	6.1519E+02	6.2918E+02	6.4081E+02	6.2143E+02	6.2594E+02	6.1111E+02	6.0758E+02
	50	Avg	6.3723E+02	6.3302E+02	6.7263E+02	6.3174E+02	6.4299E+02	6.6443E+02	6.8200E+02	6.5358E+02	6.6105E+02	6.3510E+02	6.4040E+02
		Min	6.3427E+02	6.2870E+02	6.6692E+02	6.2642E+02	6.3290E+02	6.5419E+02	6.7620E+02	6.4503E+02	6.5519E+02	6.2651E+02	6.2210E+02
	100	Avg	7.0555E+02	6.9075E+02	7.6302E+02	6.8521E+02	7.1363E+02	7.5058E+02	7.7364E+02	7.3151E+02	7.3773E+02	7.0341E+02	7.0194E+02
		Min	6.9698E+02	6.8183E+02	7.5975E+02	6.8176E+02	7.0458E+02	7.3628E+02	7.6607E+02	7.1579E+02	7.2884E+02	6.9071E+02	6.6162E+02
F_{15}	30	Avg	7.0000E+02	7.0000E+02	7.0302E+02	7.0000E+02	7.0002E+02	7.0059E+02	1.4927E+03	7.0106E+02	8.8403E+02	7.0002E+02	7.0001E+02
		Min	7.00001E+02	7.0000E+02	7.0264E+02	7.0000E+02	7.0000E+02	7.0025E+02	1.3334E+03	7.0103E+02	8.0876E+02	7.0000E+02	7.0000E+02
	50	Avg	7.0020E+02	7.0001E+02	8.5014E+02	7.0006E+02	7.0005E+02	7.0113E+02	2.3434E+03	7.0133E+02	1.2766E+03	7.0001E+02	7.0000E+02
		Min	7.0014E+02	7.00002E+02	8.2876E+02	7.0002E+02	7.0003E+02	7.0103E+02	2.0216E+03	7.0123E+02	1.1247E+03	7.0000E+02	7.0000E+02
	100	Avg	7.0165E+02	7.0005E+02	1.9254E+03	7.0109E+02	7.2735E+02	7.0400E+02	3.9984E+03	7.0342E+02	2.4088E+03	7.0003E+02	7.0000E+02
		Min	7.0150E+02	7.0002E+02	1.8212E+03	7.0102E+02	7.0441E+02	7.0241E+02	3.6203E+03	7.0305E+02	1.9683E+03	7.0000E+02	7.0000E+02
F_{16}	30	Avg	9.6688E+02	9.7761E+02	1.1455E+03	9.7857E+02	1.0136E+03	1.1313E+03	1.4259E+03	1.0685E+03	1.1430E+03	9.8054E+02	9.7296E+02
		Min	9.4697E+02	9.6160E+02	1.1214E+03	9.5503E+02	9.5274E+02	1.0504E+03	1.3529E+03	1.0360E+03	1.1177E+03	9.4875E+02	9.3582E+02
	50	Avg	1.0981E+03	1.0945E+03	1.4389E+03	1.0998E+03	1.1340E+03	1.3061E+03	1.8784E+03	1.2527E+03	1.4480E+03	1.0644E+03	1.0459E+03
		Min	1.0749E+03	1.0156E+03	1.4071E+03	1.0718E+03	1.0582E+03	1.2047E+03	1.7501E+03	1.2006E+03	1.3760E+03	1.0075E+03	9.7562E+02
	100	Avg	1.6677E+03	1.6472E+03	2.2708E+03	1.6224E+03	1.5358E+03	1.6605E+03	2.8010E+03	1.6620E+03	2.1198E+03	1.3653E+03	1.2808E+03
		Min	1.4836E+03	1.5533E+03	2.2063E+03	1.5219E+03	1.4271E+03	1.5295E+03	2.6730E+03	1.5671E+03	2.0139E+03	1.2831E+03	1.1179E+03
F_{17}	30	Avg	1.0096E+03	1.7344E+03	2.4565E+03	2.0245E+03	2.6638E+03	6.8239E+03	2.6770E+04	5.4017E+03	5.2103E+03	1.2903E+03	9.0589E+02
		Min	9.5959E+02	1.1848E+03	1.8569E+03	1.5058E+03	1.8367E+03	3.8784E+03	1.7365E+04	4.4054E+03	3.4773E+03	9.9940E+02	9.0000E+02
	50	Avg	3.8064E+03	9.3125E+03	1.1981E+04	6.5379E+03	9.4788E+03	1.8580E+04	7.8144E+04	1.5228E+04	2.6111E+04	3.6058E+03	1.2489E+03
		Min	2.8419E+03	5.8941E+03	9.5083E+03	4.0319E+03	7.6570E+03	1.0015E+04	6.0048E+04	1.2187E+04	1.6461E+04	2.2867E+03	9.2442E+02
	100	Avg	3.2268E+04	4.9805E+04	6.0371E+04	3.8734E+04	2.2380E+04	4.0131E+04	1.7597E+05	3.3290E+04	6.6600E+04	1.3164E+04	7.6435E+03
		Min	2.6946E+04	3.1820E+04	5.0318E+04	3.2137E+04	1.7845E+04	2.7272E+04	1.4999E+05	2.6747E+04	5.9545E+04	9.5503E+03	2.7226E+03
F_{18}	30	Avg	1.5099E+03	1.5104E+03	1.5978E+03	1.5083E+03	1.5175E+03	1.5664E+03	3.7872E+05	1.5404E+03	2.7523E+03	1.5125E+03	1.5042E+03
		Min	1.5082E+03	1.5072E+03	1.5428E+03	1.5051E+03	1.5103E+03	1.5253E+03	1.4867E+05	1.5260E+03	1.6200E+03	1.5072E+03	1.5019E+03
	50	Avg	1.5278E+03	1.5270E+03	7.1948E+04	1.5245E+03	1.5606E+03	1.7382E+03	5.0287E+06	1.5928E+03	1.1488E+05	1.5531E+03	1.5099E+03
		Min	1.5240E+03	1.5203E+03	3.2506E+04	1.5181E+03	1.5343E+03	1.6355E+03	2.1994E+06	1.5616E+03	3.9139E+04	1.5348E+03	1.5064E+03
	100	Avg	1.6050E+03	1.5930E+03	1.4029E+07	1.6356E+03	1.7871E+03	2.4939E+03	2.6680E+07	1.7247E+03	1.6218E+06	1.7305E+03	1.5597E+03
		Min	1.5927E+03	1.5807E+03	8.5862E+06	1.6110E+03	1.7275E+03	1.9647E+03	1.6974E+07	1.6644E+03	7.1375E+05	1.6566E+03	1.5396E+03

Table B.5 Results comparison of hybrid group functions.

F	D	Metrics	CLPSO (2006)	ABC (2007)	ACO_R (2008)	Best-so-far ABC(2011)	KH (2012)	WOA (2016)	BOA (2019)	HHO (2019)	HGSO (2019)	$LIACO_R$ (2019)	SMO
F_{19}	30	Avg	1.2187E+03	1.6103E+03	1.6827E+03	1.7860E+03	1.4980E+03	1.3243E+03	8.1182E+03	1.2305E+03	2.4061E+03	1.1705E+03	1.1710E+03
		Min	1.1832E+03	1.2954E+03	1.4971E+03	1.1937E+03	1.2914E+03	1.1907E+03	5.0473E+03	1.1577E+03	1.5984E+03	1.1286E+03	**1.1100E+03**
	50	Avg	1.5153E+03	3.6224E+03	6.8535E+03	6.2173E+03	5.8668E+03	1.5532E+03	2.5818E+04	1.4166E+03	5.5159E+03	1.2228E+03	1.2078E+03
		Min	1.3954E+03	1.5952E+03	3.8906E+03	1.9296E+03	2.9429E+03	1.4002E+03	1.8140E+04	1.2888E+03	3.0612E+03	1.1650E+03	**1.1398E+03**
	100	Avg	5.2800E+04	7.0774E+04	2.8817E+05	8.6604E+04	8.4583E+04	1.4099E+04	2.9979E+05	3.0470E+03	1.2832E+05	2.9424E+03	1.7255E+03
		Min	3.6864E+04	4.7979E+04	2.0521E+05	4.9218E+04	6.0365E+04	8.4785E+03	1.7482E+05	2.5443E+03	1.1173E+05	2.0508E+03	**1.3432E+03**
F_{20}	30	Avg	8.0864E+05	8.0564E+05	3.1462E+07	1.1702E+06	2.5485E+06	2.1209E+07	1.4392E+10	6.0554E+06	1.1670E+09	3.5477E+04	8.8850E+03
		Min	3.2525E+05	1.3006E+05	1.1687E+07	4.5159E+05	2.0746E+05	1.8229E+06	7.6859E+09	1.0989E+06	5.4588E+08	9.3174E+03	**2.3433E+03**
	50	Avg	1.9750E+07	5.6216E+06	1.8594E+09	1.2051E+07	1.4003E+07	1.7274E+08	8.3672E+10	5.5412E+07	1.4324E+10	6.9979E+05	1.5422E+04
		Min	1.1004E+07	1.4818E+06	1.2699E+09	6.7299E+06	4.2194E+06	5.3985E+07	6.9303E+10	1.5630E+07	7.1716E+09	1.7231E+05	**6.1510E+03**
	100	Avg	3.4698E+08	4.1403E+07	3.1000E+10	2.0155E+08	1.2238E+08	8.6739E+08	1.9782E+11	3.6522E+08	6.5678E+10	3.1603E+06	1.8856E+05
		Min	2.6421E+08	1.8983E+07	2.3410E+10	1.1398E+08	1.6249E+07	4.0657E+08	1.7866E+11	2.0602E+08	3.3626E+10	1.4030E+06	**7.1275E+04**
F_{21}	30	Avg	6.4426E+03	2.4187E+04	8.9060E+03	4.5916E+04	4.0696E+04	1.5096E+05	1.3101E+10	1.2402E+05	3.2206E+08	7.8307E+03	2.0240E+03
		Min	2.6495E+03	9.3709E+03	1.5357E+03	8.1508E+03	1.8288E+04	4.0779E+04	4.9367E+09	3.1744E+04	9.5281E+07	1.4011E+03	**1.3887E+03**
	50	Avg	2.0888E+05	3.3745E+04	1.3819E+04	6.1497E+05	4.7935E+04	2.1564E+05	5.0134E+10	9.9279E+05	2.6051E+09	4.1751E+03	3.6486E+03
		Min	5.2100E+04	9.2254E+03	8.2106E+03	1.9472E+05	1.8734E+04	4.0642E+04	3.1648E+10	2.2447E+05	9.1502E+08	**1.4091E+03**	1.4330E+03
	100	Avg	5.8069E+05	4.1924E+04	1.4556E+08	2.6546E+06	3.6406E+04	1.5226E+05	4.5797E+10	3.8434E+06	1.1465E+10	5.1325E+03	4.8931E+03
		Min	1.6650E+05	1.0177E+04	6.5965E+07	1.0939E+06	2.3723E+04	5.7507E+04	3.5926E+10	2.0669E+06	5.5684E+09	**2.0858E+03**	2.6468E+03
F_{22}	30	Avg	1.7698E+04	1.0576E+05	1.8968E+05	1.5869E+05	1.8672E+05	3.7197E+05	5.6332E+06	2.5001E+04	3.0283E+05	1.1410E+04	1.5918E+03
		Min	3.3812E+03	2.1312E+04	4.8333E+04	1.2547E+04	3.9929E+03	2.1848E+04	1.5552E+06	3.3104E+03	4.2204E+04	2.0287E+03	**1.5216E+03**
	50	Avg	4.9540E+05	1.0402E+06	2.8296E+06	9.2776E+05	9.8895E+05	5.8129E+05	1.4333E+08	2.3246E+05	3.6036E+06	5.0999E+04	1.7595E+03
		Min	1.4324E+05	4.2880E+05	6.4965E+05	3.1824E+05	7.4663E+04	7.2261E+04	2.8323E+07	4.2240E+04	1.3914E+06	1.1268E+04	**1.6015E+03**
	100	Avg	9.1433E+06	1.1348E+07	1.1703E+08	1.4991E+07	5.3970E+06	2.4992E+06	1.8885E+08	1.1601E+06	1.6977E+07	2.7945E+05	6.2997E+03
		Min	3.4494E+06	6.1625E+06	7.1888E+07	4.8436E+06	2.8338E+06	4.5559E+05	7.3749E+07	3.8063E+05	1.1079E+07	8.0640E+04	**2.3670E+03**
F_{23}	30	Avg	1.2140E+06	2.0055E+06	1.0761E+07	2.2182E+06	1.3974E+06	2.3435E+06	1.3370E+08	8.7723E+05	4.6944E+06	1.5056E+05	3.1596E+03
		Min	2.1001E+05	4.7621E+05	5.3006E+06	7.6430E+05	4.9611E+05	2.0163E+05	2.1575E+07	1.3711E+05	2.0178E+06	2.1698E+04	**2.5462E+03**
	50	Avg	7.0953E+06	7.2860E+06	7.8390E+07	1.0279E+07	2.0800E+06	1.5179E+07	7.2129E+08	2.3720E+06	4.9294E+07	2.4607E+05	8.7564E+03
		Min	2.1440E+06	3.2293E+06	4.5554E+07	4.9982E+06	9.3876E+05	2.9272E+06	9.9228E+07	7.0373E+05	2.9478E+07	6.7203E+04	**4.0961E+03**
	100	Avg	6.3265E+07	3.5276E+07	7.6918E+08	5.4918E+07	7.2221E+06	1.8648E+07	1.8570E+09	1.0355E+07	2.3343E+08	1.8577E+06	1.2845E+05
		Min	3.7997E+07	1.9880E+07	5.3811E+08	3.5453E+07	3.9546E+06	8.5318E+06	1.1162E+09	4.1626E+06	1.3497E+08	9.5926E+05	**4.2002E+04**
F_{24}	30	Avg	1.5691E+05	2.1877E+05	9.9808E+06	2.8270E+05	2.9230E+05	1.7275E+06	9.0759E+07	3.1811E+05	1.5665E+06	1.1359E+05	1.9943E+03
		Min	6.9132E+04	7.2571E+04	2.3077E+06	5.7395E+04	4.4749E+04	1.0782E+05	1.5397E+07	6.8016E+04	2.7827E+05	7.8661E+03	**1.8843E+03**
	50	Avg	1.4246E+06	1.5739E+06	4.2753E+07	2.3801E+06	2.4575E+06	4.6428E+06	2.5718E+08	1.6917E+06	9.3091E+06	1.7033E+05	5.4535E+03
		Min	3.8534E+05	5.6894E+05	1.8584E+07	9.7073E+05	8.4147E+05	8.1591E+05	4.3178E+07	5.9130E+05	3.6983E+06	5.6562E+04	**2.0622E+03**
	100	Avg	1.0284E+07	8.2595E+06	2.1750E+08	1.1484E+07	3.0265E+06	2.5706E+06	3.4129E+08	2.5818E+06	2.1688E+07	6.7153E+05	7.9758E+04
		Min	6.0713E+06	2.2553E+06	1.3708E+08	6.6678E+06	1.4776E+06	9.0446E+05	2.1034E+08	6.6547E+05	1.1542E+07	2.2716E+05	**1.8971E+04**
F_{25}	30	Avg	2.0139E+03	9.6783E+03	3.2158E+03	1.1723E+04	2.6434E+03	6.3484E+03	4.5119E+09	2.1461E+04	6.6600E+07	2.3369E+03	2.0846E+03
		Min	1.9350E+03	3.2407E+03	1.8960E+03	5.3548E+03	2.0295E+03	2.1265E+03	1.5282E+09	2.9327E+03	1.9012E+07	1.8580E+03	**1.8277E+03**
	50	Avg	6.9109E+03	2.0077E+04	2.5769E+03	2.5434E+04	3.7191E+03	7.9588E+03	1.9453E+10	3.2642E+05	1.7360E+09	3.1388E+03	2.3451E+03
		Min	3.0983E+03	9.8480E+03	2.0892E+03	1.1169E+04	2.2521E+03	2.5224E+03	1.3455E+10	1.9309E+04	9.0091E+08	**1.8766E+03**	1.9630E+03
	100	Avg	6.5321E+05	2.6999E+05	1.5013E+08	2.3936E+06	5.9528E+03	4.9790E+04	4.1534E+10	6.9801E+06	7.7426E+09	3.0810E+03	2.6607E+03
		Min	3.2235E+05	1.8023E+04	8.5165E+07	9.4564E+05	3.2408E+03	1.4966E+04	3.3683E+10	2.3541E+06	3.0755E+09	**2.1130E+03**	2.2636E+03
F_{26}	30	Avg	1.9093E+03	1.9072E+03	1.9140E+03	1.9077E+03	1.9148E+03	1.9534E+03	2.5153E+03	1.9207E+03	2.0134E+03	1.9059E+03	1.9047E+03
		Min	1.9070E+03	1.9060E+03	1.9128E+03	1.9055E+03	1.9110E+03	1.9178E+03	2.3262E+03	1.9089E+03	1.9914E+03	1.9041E+03	**1.9024E+03**
	50	Avg	1.9262E+03	1.9171E+03	1.9633E+03	1.9236E+03	1.9429E+03	1.9730E+03	4.8139E+03	1.9570E+03	2.2954E+03	1.9143E+03	1.9078E+03
		Min	1.9189E+03	1.9133E+03	1.9579E+03	1.9189E+03	1.9212E+03	1.9334E+03	3.1911E+03	1.9198E+03	2.2184E+03	1.9101E+03	**1.9056E+03**
	100	Avg	2.0572E+03	1.9869E+03	2.2447E+03	2.0198E+03	2.0273E+03	2.1164E+03	1.3047E+04	2.0580E+03	3.7521E+03	2.0107E+03	1.9640E+03
		Min	2.0273E+03	1.9514E+03	2.1982E+03	2.0023E+03	1.9834E+03	2.0533E+03	9.2759E+03	2.0061E+03	3.1356E+03	1.9642E+03	**1.9151E+03**
F_{27}	30	Avg	4.9213E+03	6.0462E+03	3.3801E+04	8.5554E+03	1.5899E+04	1.2503E+04	3.0514E+05	2.6646E+03	2.6653E+04	3.2501E+03	2.2029E+03
		Min	2.8399E+03	3.6278E+03	1.6219E+04	3.5530E+03	7.8477E+03	3.7455E+03	7.9522E+04	2.1590E+03	1.0479E+04	2.2354E+03	**2.0915E+03**
	50	Avg	1.7853E+04	1.9084E+04	1.7007E+05	2.9521E+04	2.1896E+04	6.8685E+04	3.4816E+05	3.5366E+03	4.4081E+04	9.0650E+03	2.3685E+03
		Min	9.1190E+03	8.3840E+03	7.5871E+04	1.2886E+04	1.1642E+04	1.4770E+04	1.0817E+05	2.7388E+03	2.1201E+04	3.0647E+03	**2.2035E+03**
	100	Avg	8.6338E+04	8.3430E+04	8.2079E+05	9.5219E+04	1.4698E+05	9.6836E+04	1.2748E+06	8.4662E+03	2.5390E+05	5.1663E+04	2.6686E+03
		Min	4.1069E+04	6.4805E+04	4.5177E+05	6.4952E+04	1.0395E+05	4.3618E+04	5.2615E+05	5.5657E+03	1.5108E+05	1.2323E+04	**2.4716E+03**
F_{28}	30	Avg	9.8177E+04	3.4713E+05	1.8688E+06	4.5506E+05	3.3996E+05	7.9226E+05	4.9786E+07	2.1829E+05	1.7587E+06	1.0014E+05	2.8642E+03
		Min	3.2851E+04	6.5721E+04	3.2863E+05	1.1582E+05	6.7443E+04	7.4562E+04	6.6586E+06	3.1153E+04	7.1529E+05	1.6583E+04	**2.3816E+03**
	50	Avg	2.6338E+06	3.2932E+06	3.7495E+07	5.2542E+06	2.6514E+06	4.8109E+06	1.2402E+08	9.8087E+05	8.3083E+06	2.6005E+05	4.9980E+03
		Min	7.3566E+05	1.1527E+06	2.2192E+07	2.3073E+06	1.1187E+06	9.0970E+05	6.2662E+07	3.5016E+05	4.8510E+06	7.5936E+04	**3.3369E+03**
	100	Avg	3.4335E+07	2.2133E+07	3.7010E+08	3.7125E+07	6.4243E+06	1.2315E+07	6.1569E+08	7.0743E+06	9.3411E+07	1.5607E+06	4.1374E+04
		Min	2.3469E+07	1.3252E+07	2.8732E+08	2.0304E+07	3.0734E+06	5.7919E+06	3.8861E+08	3.5894E+06	4.5194E+07	9.1146E+05	**1.6690E+04**

Table B.6 Results comparison of composition group functions.

F	D	Metrics	CLPSO (2006)	ABC (2007)	ACO_R (2008)	Best-so-far ABC (2011)	KH (2012)	WOA (2016)	BOA (2019)	HHO (2019)	HGSO (2019)	$LIACO_R$ (2019)	SMO
F_{29}	30	Avg	6.8984E+03	5.7917E+03	8.5282E+03	5.4233E+03	6.5591E+03	7.2418E+03	1.0533E+04	6.9560E+03	8.5355E+03	5.5119E+03	5.3167E+03
		Min	6.0388E+03	4.7945E+03	8.0074E+03	4.3554E+03	4.2930E+03	5.2242E+03	9.2235E+03	5.0784E+03	8.0627E+03	3.8986E+03	**3.8304E+03**
	50	Avg	1.3820E+04	1.1208E+04	1.5371E+04	1.0576E+04	1.2004E+04	1.3125E+04	1.8336E+04	1.2649E+04	1.6622E+04	1.0065E+04	9.6003E+03
		Min	1.2440E+04	9.8642E+03	1.4398E+04	9.9334E+03	9.8760E+03	9.3627E+03	1.7433E+04	1.0468E+04	1.5577E+04	**7.7321E+03**	7.8262E+03
	100	Avg	3.0872E+04	2.4726E+04	3.3460E+04	2.4259E+04	2.3951E+04	2.9045E+04	3.7295E+04	2.9059E+04	3.4424E+04	2.2598E+04	2.0338E+04
		Min	2.8829E+04	2.2835E+04	3.2103E+04	2.2125E+04	1.8912E+04	2.2364E+04	3.6155E+04	2.5419E+04	3.3351E+04	1.9065E+04	**1.6928E+04**
F_{30}	30	Avg	1.2736E+03	1.2865E+03	1.3045E+03	1.2830E+03	1.2736E+03	1.3101E+03	1.4934E+03	1.3186E+03	1.3044E+03	1.2562E+03	1.2756E+03
		Min	1.2645E+03	1.2778E+03	1.2971E+03	1.2713E+03	1.2383E+03	1.2884E+03	1.4023E+03	1.2925E+03	1.2955E+03	1.2302E+03	**1.2265E+03**
	50	Avg	1.3561E+03	1.3708E+03	1.3922E+03	1.3628E+03	1.3691E+03	1.4010E+03	1.8621E+03	1.4216E+03	1.3878E+03	1.3289E+03	1.3544E+03
		Min	1.3443E+03	1.3562E+03	1.3880E+03	1.3497E+03	1.3269E+03	1.3718E+03	1.5350E+03	1.3831E+03	1.3806E+03	**1.3032E+03**	1.3258E+03
	100	Avg	1.5536E+03	1.6255E+03	1.6225E+03	1.5842E+03	1.8687E+03	1.6613E+03	4.4433E+03	1.7028E+03	1.6122E+03	1.5536E+03	1.5749E+03
		Min	1.5321E+03	1.5985E+03	1.6023E+03	1.5559E+03	1.7020E+03	1.6180E+03	3.5209E+03	1.6441E+03	1.5992E+03	**1.5042E+03**	1.5148E+03
F_{31}	30	Avg	1.3961E+03	1.4015E+03	1.4092E+03	1.3923E+03	1.4204E+03	1.4153E+03	1.5389E+03	1.4272E+03	1.4195E+03	1.3954E+03	1.3903E+03
		Min	1.3878E+03	1.3929E+03	1.4040E+03	1.3832E+03	1.3801E+03	1.3924E+03	1.4835E+03	1.3943E+03	1.3968E+03	1.3734E+03	**1.3711E+03**
	50	Avg	1.4988E+03	1.5130E+03	1.5027E+03	1.4858E+03	1.5673E+03	1.5164E+03	1.7472E+03	1.5371E+03	1.5591E+03	1.5062E+03	1.4800E+03
		Min	1.4863E+03	1.5000E+03	1.4960E+03	1.4691E+03	1.5347E+03	1.4914E+03	1.6847E+03	1.5052E+03	1.4761E+03	1.4800E+03	**1.4419E+03**
	100	Avg	1.7744E+03	1.8248E+03	1.7522E+03	1.7495E+03	2.0949E+03	1.8055E+03	2.4789E+03	1.8599E+03	1.7058E+03	1.8129E+03	1.7379E+03
		Min	1.7476E+03	1.7928E+03	1.7437E+03	1.7249E+03	1.9679E+03	1.7459E+03	2.3062E+03	1.7703E+03	1.6943E+03	1.7600E+03	**1.6706E+03**
F_{32}	30	Avg	1.4018E+03	1.4008E+03	1.5347E+03	1.4015E+03	1.4003E+03	1.5015E+03	1.6202E+03	1.5363E+03	1.4112E+03	1.4147E+03	1.4000E+03
		Min	1.4011E+03	1.4005E+03	1.4709E+03	1.4009E+03	1.4002E+03	1.4003E+03	1.5266E+03	1.4001E+03	1.4060E+03	1.40002E+03	**1.4000E+03**
	50	Avg	1.4091E+03	1.4026E+03	1.6891E+03	1.4055E+03	1.4928E+03	1.6778E+03	1.7533E+03	1.6682E+03	1.5800E+03	1.5770E+03	1.4913E+03
		Min	1.4058E+03	1.4019E+03	1.6838E+03	1.4036E+03	1.4006E+03	1.6538E+03	1.5825E+03	1.4024E+03	1.4233E+03	1.4003E+03	**1.4000E+03**
	100	Avg	1.4642E+03	1.4069E+03	1.9125E+03	1.4255E+03	1.8506E+03	1.8967E+03	2.3260E+03	1.8950E+03	1.9071E+03	1.8267E+03	1.8396E+03
		Min	1.4443E+03	**1.4049E+03**	1.9046E+03	1.4197E+03	1.8126E+03	1.8564E+03	2.0274E+03	1.8468E+03	1.8752E+03	1.7817E+03	1.7672E+03
F_{33}	30	Avg	2.3182E+03	2.2511E+03	2.5241E+03	2.3236E+03	2.3968E+03	2.5330E+03	2.8182E+03	2.5187E+03	2.5518E+03	2.3727E+03	2.3809E+03
		Min	2.2377E+03	**2.2162E+03**	2.4792E+03	2.2276E+03	2.3539E+03	2.4462E+03	2.6910E+03	2.4415E+03	2.5060E+03	2.3407E+03	2.3404E+03
	50	Avg	2.5046E+03	2.5145E+03	2.8117E+03	2.5150E+03	2.5180E+03	2.8562E+03	3.3709E+03	2.7845E+03	2.9101E+03	2.4594E+03	2.4558E+03
		Min	2.4330E+03	2.4788E+03	2.7799E+03	2.4673E+03	2.4693E+03	2.6782E+03	3.2176E+03	2.6130E+03	2.8251E+03	2.4126E+03	**2.3811E+03**
	100	Avg	3.1111E+03	3.0406E+03	3.7076E+03	3.0701E+03	3.3584E+03	3.9016E+03	5.1972E+03	3.7968E+03	4.1448E+03	2.8323E+03	2.7205E+03
		Min	3.0427E+03	2.9074E+03	3.6553E+03	2.9699E+03	3.1982E+03	3.6148E+03	4.8364E+03	3.3773E+03	3.8136E+03	2.7496E+03	**2.5782E+03**
F_{34}	30	Avg	2.8882E+03	2.8840E+03	2.9460E+03	2.8861E+03	2.9158E+03	2.9306E+03	6.1738E+03	2.9030E+03	3.2733E+03	2.8933E+03	2.8870E+03
		Min	2.8875E+03	2.8836E+03	2.9337E+03	2.8841E+03	2.8879E+03	2.8901E+03	5.1218E+03	2.8842E+03	3.1835E+03	2.8837E+03	**2.8835E+03**
	50	Avg	3.1136E+03	3.0145E+03	4.2175E+03	3.0385E+03	3.0935E+03	3.1395E+03	1.7227E+04	3.1232E+03	6.4299E+03	3.0691E+03	3.0346E+03
		Min	3.0801E+03	2.9896E+03	3.8363E+03	3.0076E+03	3.0363E+03	3.0579E+03	1.4365E+04	3.0310E+03	5.3679E+03	3.0170E+03	**2.9599E+03**
	100	Avg	3.7325E+03	3.3568E+03	3.1798E+04	3.5736E+03	3.5315E+03	3.7619E+03	3.1234E+04	3.5671E+03	1.3653E+04	3.3307E+03	3.3008E+03
		Min	3.6908E+03	3.2565E+03	2.6957E+04	3.5144E+03	3.4216E+03	3.5919E+03	2.8734E+04	3.4255E+03	1.0661E+04	3.2023E+03	**3.1565E+03**
F_{35}	30	Avg	2.7004E+03	2.7004E+03	2.7007E+03	2.7003E+03	2.7119E+03	2.7005E+03	2.7892E+03	2.7369E+03	2.7528E+03	2.7003E+03	2.7003E+03
		Min	2.7003E+03	2.7003E+03	2.7006E+03	2.7002E+03	2.7004E+03	2.7003E+03	2.7141E+03	2.7002E+03	2.7024E+03	2.7002E+03	**2.7001E+03**
	50	Avg	2.7005E+03	2.7005E+03	2.7289E+03	2.7005E+03	2.7912E+03	2.7004E+03	2.8260E+03	2.7801E+03	2.7971E+03	2.7154E+03	2.7003E+03
		Min	2.7004E+03	2.7003E+03	2.7009E+03	2.7004E+03	2.7078E+03	2.7003E+03	2.7511E+03	2.7003E+03	2.7119E+03	2.7003E+03	**2.7002E+03**
	100	Avg	2.7531E+03	2.7364E+03	3.0902E+03	2.7006E+03	2.8003E+03	2.8000E+03	2.9028E+03	2.8000E+03	2.8000E+03	2.8004E+03	2.7968E+03
		Min	2.7040E+03	2.7005E+03	2.7061E+03	2.7006E+03	2.8002E+03	2.8000E+03	2.8059E+03	2.8000E+03	2.8000E+03	2.8002E+03	**2.7004E+03**
F_{36}	30	Avg	3.2491E+03	3.1988E+03	3.3139E+03	3.2331E+03	3.2357E+03	3.2817E+03	8.1988E+03	3.2371E+03	3.5540E+03	3.1345E+03	3.1145E+03
		Min	3.2307E+03	3.1939E+03	3.3032E+03	3.2232E+03	3.1963E+03	3.2558E+03	6.0494E+03	3.1970E+03	3.3000E+03	**3.1000E+03**	**3.1000E+03**
	50	Avg	3.4581E+03	3.2921E+03	6.6946E+03	3.3892E+03	3.3492E+03	3.4216E+03	1.4548E+04	3.3497E+03	6.1091E+03	3.3194E+03	3.2842E+03
		Min	3.4312E+03	3.2667E+03	6.0887E+03	3.3284E+03	3.2716E+03	3.3122E+03	9.9414E+03	3.2763E+03	3.3000E+03	3.2589E+03	**3.2588E+03**
	100	Avg	5.3626E+03	3.5110E+03	1.7256E+04	5.0916E+03	3.9678E+03	3.9378E+03	3.8504E+04	3.6043E+03	1.8826E+04	3.4254E+03	3.3469E+03
		Min	4.9962E+03	3.4547E+03	1.6755E+04	4.0281E+03	3.6358E+03	3.7646E+03	3.5692E+04	3.5129E+03	1.5189E+04	3.3565E+03	**3.2915E+03**
F_{37}	30	Avg	3.4507E+03	3.4865E+03	4.2620E+03	3.4933E+03	4.0600E+03	4.7490E+03	9.5342E+03	4.1340E+03	4.0308E+03	3.6223E+03	3.6766E+03
		Min	3.3507E+03	3.3603E+03	4.0665E+03	3.3471E+03	3.6497E+03	3.9913E+03	5.5893E+03	3.6194E+03	3.7995E+03	**3.3293E+03**	3.3813E+03
	50	Avg	3.8129E+03	4.0254E+03	5.5941E+03	3.8106E+03	5.1198E+03	6.7858E+03	1.5422E+05	5.1736E+03	6.3958E+03	4.2941E+03	4.3394E+03
		Min	3.5891E+03	3.6254E+03	4.9625E+03	**3.5250E+03**	4.4950E+03	5.5855E+03	1.9047E+04	4.4310E+03	5.0897E+03	3.6823E+03	3.5850E+03
	100	Avg	7.8152E+03	7.1188E+03	1.1528E+04	7.1287E+03	9.1351E+03	1.3768E+04	8.8665E+05	8.9024E+03	1.7213E+04	6.7734E+03	6.7111E+03
		Min	7.3744E+03	6.1294E+03	1.0070E+04	6.6061E+03	7.1268E+03	1.0695E+04	4.1818E+05	7.5602E+03	1.0706E+04	**5.6439E+03**	5.8741E+03
F_{38}	30	Avg	1.4228E+04	1.9007E+04	1.6545E+04	2.1863E+04	1.5764E+06	5.6602E+06	1.7143E+09	5.9704E+05	5.2100E+07	6.8620E+03	5.3492E+03
		Min	9.3983E+03	1.1404E+04	1.0977E+04	1.0703E+04	1.7176E+05	5.3611E+05	5.6230E+08	1.1615E+05	1.7576E+07	5.8715E+03	**4.9942E+03**
	50	Avg	1.9673E+06	9.2928E+05	7.6425E+06	1.1397E+06	5.1112E+07	7.1930E+07	8.8020E+09	1.0903E+07	5.8641E+08	8.8240E+05	7.4394E+05
		Min	1.4006E+06	7.5808E+05	2.4078E+06	9.0003E+05	1.5649E+07	3.3773E+07	5.3096E+09	7.0569E+06	4.3085E+08	7.4712E+05	**5.8242E+05**
	100	Avg	8.1518E+06	4.4526E+04	4.0001E+07	2.1813E+06	3.0882E+07	2.9972E+08	4.0643E+10	2.5103E+07	9.0539E+09	1.2301E+04	7.7060E+03
		Min	4.4550E+06	2.4317E+04	2.2770E+07	9.2702E+05	9.4799E+06	9.7378E+07	3.2811E+10	1.0272E+07	5.5172E+09	7.0904E+03	**5.4974E+03**

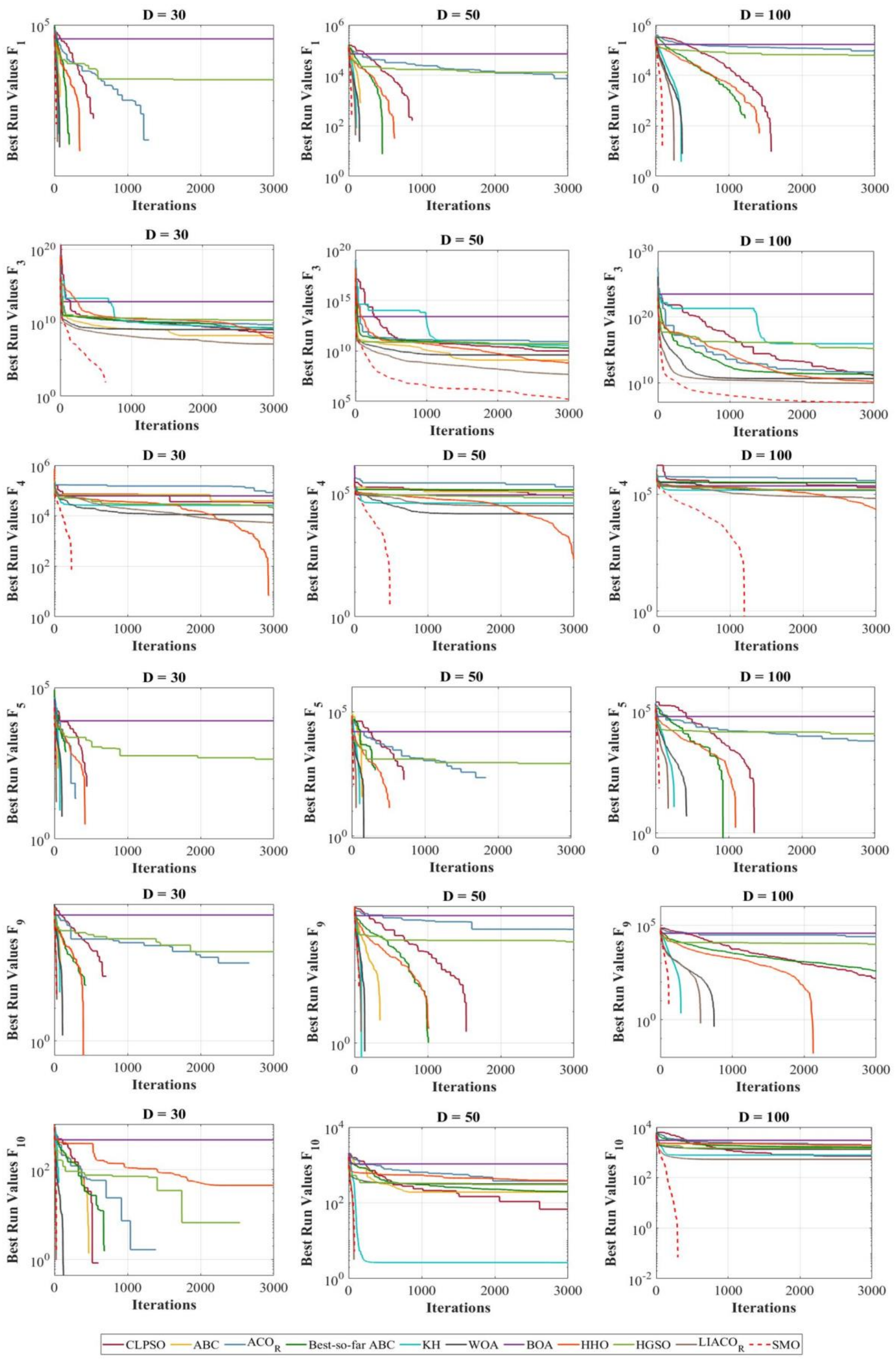

Fig. B.2. Convergence curves of SMO and competitive algorithms on the rest of test functions.

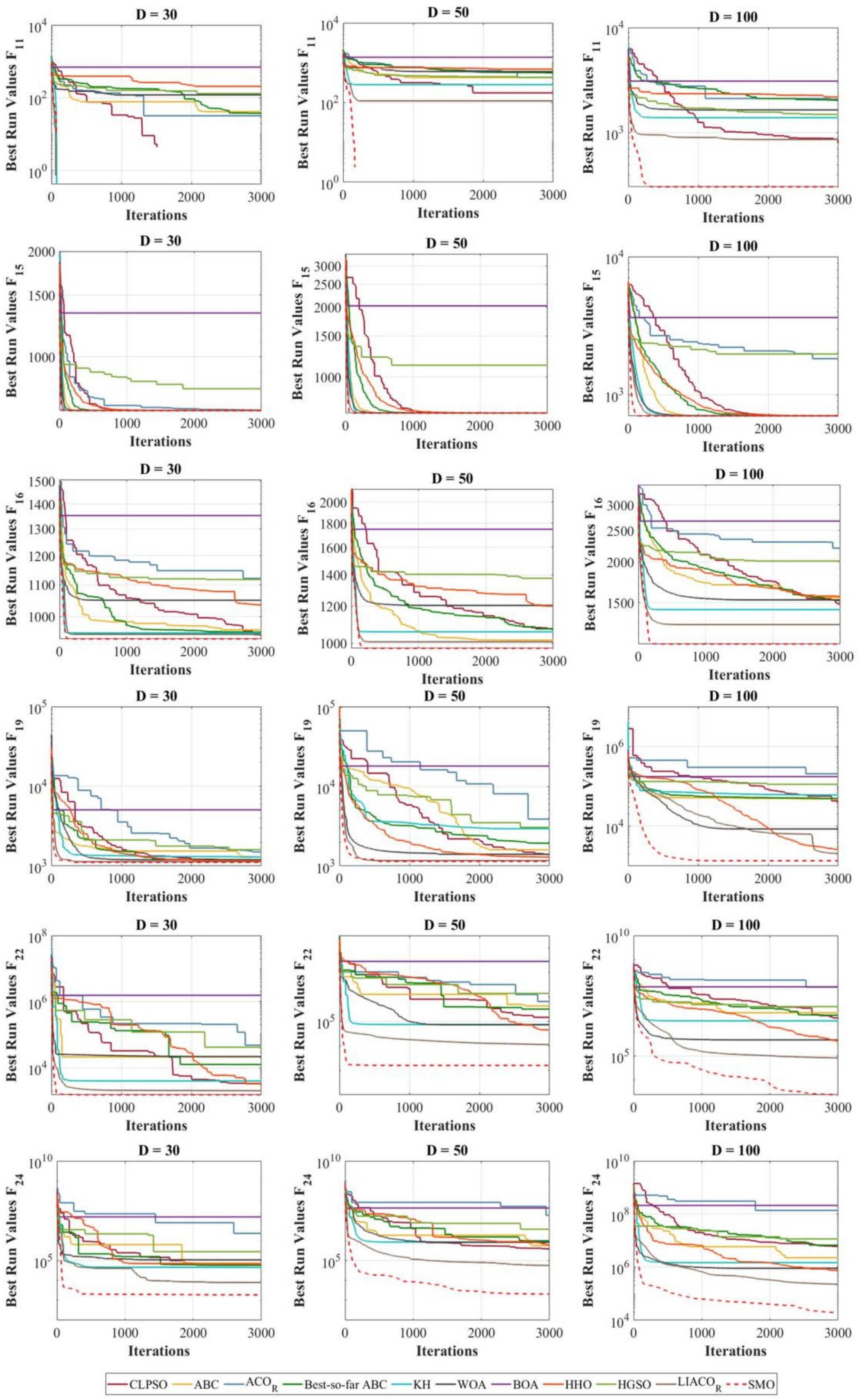

Fig. B.3. Convergence curves of SMO and competitive algorithms on the rest of test functions.

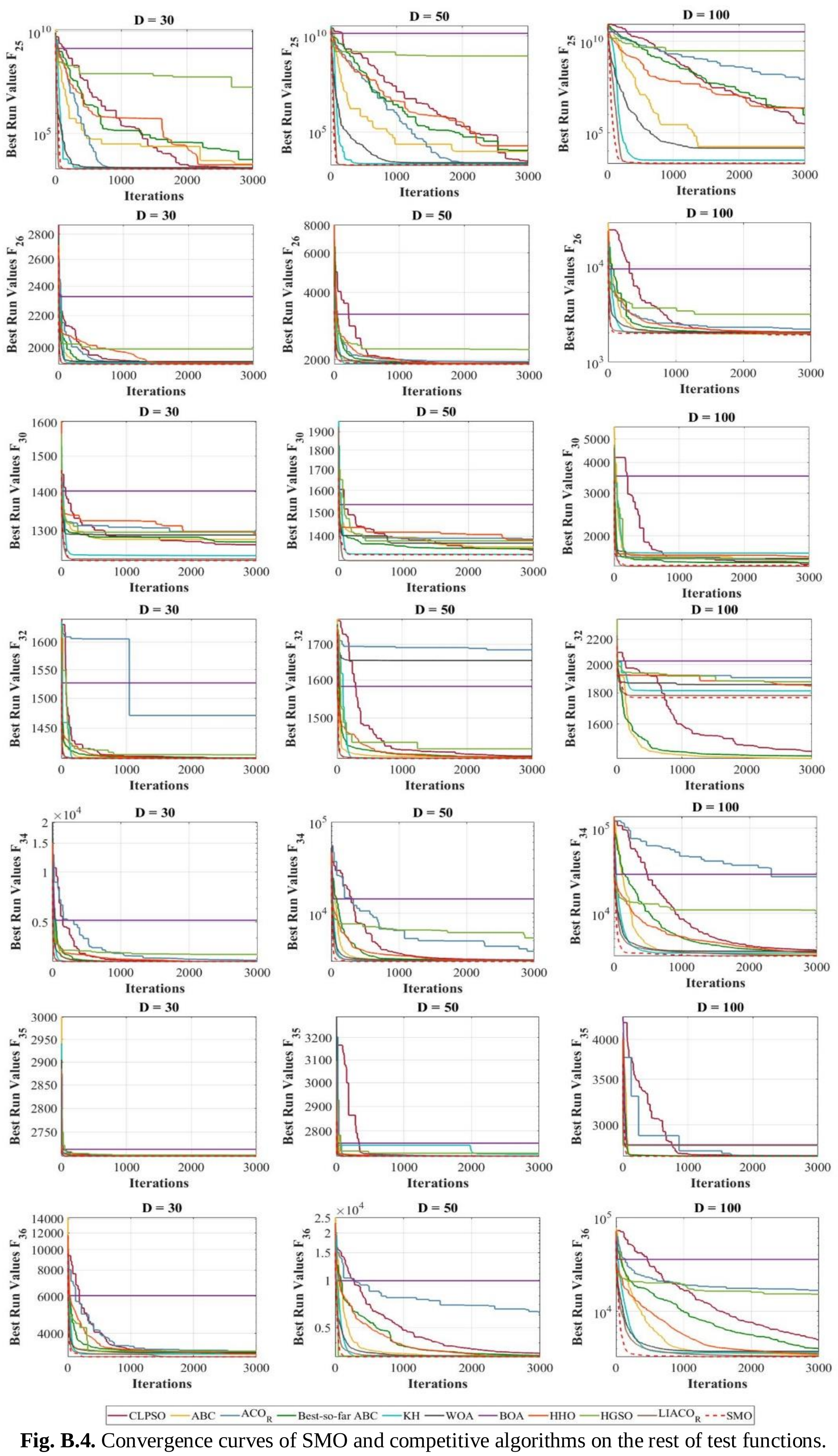

Fig. B.4. Convergence curves of SMO and competitive algorithms on the rest of test functions.

References

[1] W. Zhao, C. Du, S. Jiang, An adaptive multiscale approach for identifying multiple flaws based on XFEM and a discrete artificial fish swarm algorithm, Computer Methods in Applied Mechanics and Engineering, 339 (2018) 341-357.
[2] L. Xia, L. Zhang, Q. Xia, T. Shi, Stress-based topology optimization using bi-directional evolutionary structural optimization method, Computer Methods in Applied Mechanics and Engineering, 333 (2018) 356-370.
[3] C. Wang, J.M. Koh, T. Yu, N.G. Xie, K.H. Cheong, Material and shape optimization of bi-directional functionally graded plates by GIGA and an improved multi-objective particle swarm optimization algorithm, Computer Methods in Applied Mechanics and Engineering, 366 (2020) 113017.
[4] S. Gholizadeh, M. Danesh, C. Gheyratmand, A new Newton metaheuristic algorithm for discrete performance-based design optimization of steel moment frames, Computers & Structures, 234 (2020) 106250.
[5] M. Papadrakakis, N.D. Lagaros, Y. Tsompanakis, Structural optimization using evolution strategies and neural networks, Computer methods in applied mechanics and engineering, 156 (1998) 309-333.
[6] H.R. Sayarshad, Using bees algorithm for material handling equipment planning in manufacturing systems, The International Journal of Advanced Manufacturing Technology, 48 (2010) 1009-1018.
[7] H. Faris, I. Aljarah, M.A. Al-Betar, S. Mirjalili, Grey wolf optimizer: a review of recent variants and applications, Neural computing and applications, 30 (2018) 413-435.
[8] X.-S. Yang, Optimization and metaheuristic algorithms in engineering, Metaheuristics in water, geotechnical and transport engineering, (2013) 1-23.
[9] I. Fister Jr, X.-S. Yang, I. Fister, J. Brest, D. Fister, A brief review of nature-inspired algorithms for optimization, arXiv preprint arXiv:1307.4186, (2013).
[10] I. BoussaïD, J. Lepagnot, P. Siarry, A survey on optimization metaheuristics, Information sciences, 237 (2013) 82-117.
[11] E.-G. Talbi, Metaheuristics: from design to implementation, John Wiley & Sons, 2009.
[12] M. Dorigo, G. Di Caro, Ant colony optimization: a new meta-heuristic, in: Proceedings of the 1999 congress on evolutionary computation-CEC99 (Cat. No. 99TH8406), IEEE, 1999, pp. 1470-1477.
[13] A. Colorni, M. Dorigo, V. Maniezzo, Distributed Optimization by Ant Colonies, actes de la première conférence européenne sur la vie artificielle, in: Elsevier Publishing, 1991, pp. 134-142.
[14] D. Karaboga, B. Basturk, A powerful and efficient algorithm for numerical function optimization: artificial bee colony (ABC) algorithm, Journal of global optimization, 39 (2007) 459-471.
[15] A. Banharnsakun, T. Achalakul, B. Sirinaovakul, The best-so-far selection in artificial bee colony algorithm, Applied Soft Computing, 11 (2011) 2888-2901.
[16] S. Mirjalili, Moth-flame optimization algorithm: A novel nature-inspired heuristic paradigm, Knowledge-Based Systems, 89 (2015) 228-249.
[17] S. Saremi, S. Mirjalili, A. Lewis, Grasshopper optimisation algorithm: theory and application, Advances in Engineering Software, 105 (2017) 30-47.
[18] N.A. Kallioras, N.D. Lagaros, D.N. Avtzis, Pity beetle algorithm–A new metaheuristic inspired by the behavior of bark beetles, Advances in Engineering Software, 121 (2018) 147-166.
[19] S. Arora, S. Singh, Butterfly optimization algorithm: a novel approach for global optimization, Soft Computing, 23 (2019) 715-734.
[20] K. Zervoudakis, S. Tsafarakis, A mayfly optimization algorithm, Computers & Industrial Engineering, 145 (2020) 106559.
[21] B. Wang, X. Jin, B. Cheng, Lion pride optimizer: An optimization algorithm inspired by lion pride behavior, Science China Information Sciences, 55 (2012) 2369-2389.
[22] S. Mirjalili, S.M. Mirjalili, A. Lewis, Grey wolf optimizer, Advances in engineering software, 69 (2014) 46-61.
[23] G.-G. Wang, S. Deb, L.d.S. Coelho, Elephant herding optimization, in: 2015 3rd International Symposium on Computational and Business Intelligence (ISCBI), IEEE, 2015, pp. 1-5.
[24] G. Dhiman, V. Kumar, Spotted hyena optimizer: a novel bio-inspired based metaheuristic technique for engineering applications, Advances in Engineering Software, 114 (2017) 48-70.
[25] M. Jain, V. Singh, A. Rani, A novel nature-inspired algorithm for optimization: Squirrel search algorithm, Swarm and evolutionary computation, 44 (2019) 148-175.
[26] A. Benyamin, F. Soleimanian Gharehchopogh, M. Seyedali, Artificial Gorilla Troops Optimizer: A New Nature-Inspired Metaheuristic Algorithm for Global Optimization Problems, International Journal of Intelligent Systems (2021).
[27] D. Połap, M. Woźniak, Red fox optimization algorithm, Expert Systems with Applications, 166 (2021) 114107.
[28] R. Eberhart, J. Kennedy, A new optimizer using particle swarm theory, in: MHS'95. Proceedings of the Sixth International Symposium on Micro Machine and Human Science, Ieee, 1995, pp. 39-43.

[29] M. Mahmoodi, M. Amini, A. Behzadian, A. Karimipour, Cross Flow Plate Fin Heat Exchanger Entropy Generation Minimization Using Particle Swarm Optimization Algorithm, Journal of Current Research in Science, 1 (2013) 369.
[30] J.J. Liang, A.K. Qin, P.N. Suganthan, S. Baskar, Comprehensive learning particle swarm optimizer for global optimization of multimodal functions, IEEE transactions on evolutionary computation, 10 (2006) 281-295.
[31] X.-B. Meng, X.Z. Gao, L. Lu, Y. Liu, H. Zhang, A new bio-inspired optimisation algorithm: Bird Swarm Algorithm, Journal of Experimental & Theoretical Artificial Intelligence, 28 (2016) 673-687.
[32] A.A. Heidari, S. Mirjalili, H. Faris, I. Aljarah, M. Mafarja, H. Chen, Harris hawks optimization: Algorithm and applications, Future Generation Computer Systems, 97 (2019) 849-872.
[33] H. Zamani, M.H. Nadimi-Shahraki, A.H. Gandomi, CCSA: Conscious Neighborhood-based Crow Search Algorithm for Solving Global Optimization Problems, Applied Soft Computing, (2019) 105583.
[34] A. Mohammadi-Balani, M.D. Nayeri, A. Azar, M. Taghizadeh-Yazdi, Golden eagle optimizer: A nature-inspired metaheuristic algorithm, Computers & Industrial Engineering, 152 (2021) 107050.
[35] B. Abdollahzadeh, F. Soleimanian Gharehchopogh, S. Mirjalili, African vultures optimization algorithm: A new nature-inspired metaheuristic algorithm for global optimization problems, Computers & Industrial Engineering, 158 (2021) 107408.
[36] H. Zamani, M.H. Nadimi-Shahraki, A.H. Gandomi, QANA: Quantum-based avian navigation optimizer algorithm, Engineering Applications of Artificial Intelligence, 104 (2021).
[37] W. Zhao, L. Wang, S. Mirjalili, Artificial hummingbird algorithm: A new bio-inspired optimizer with its engineering applications, Computer Methods in Applied Mechanics and Engineering, 388 (2022) 114194.
[38] X. Li, A new intelligent optimization-artificial fish swarm algorithm, Doctor thesis, Zhejiang University of Zhejiang, China, (2003) 27.
[39] A.H. Gandomi, A.H. Alavi, Krill herd: a new bio-inspired optimization algorithm, Communications in nonlinear science and numerical simulation, 17 (2012) 4831-4845.
[40] S. Mirjalili, A. Lewis, The whale optimization algorithm, Advances in engineering software, 95 (2016) 51-67.
[41] S. Mirjalili, A.H. Gandomi, S.Z. Mirjalili, S. Saremi, H. Faris, S.M. Mirjalili, Salp Swarm Algorithm: A bio-inspired optimizer for engineering design problems, Advances in Engineering Software, 114 (2017) 163-191.
[42] D. Zaldivar, B. Morales, A. Rodríguez, A. Valdivia-G, E. Cuevas, M. Pérez-Cisneros, A novel bio-inspired optimization model based on Yellow Saddle Goatfish behavior, Biosystems, 174 (2018) 1-21.
[43] S. Shadravan, H. Naji, V.K. Bardsiri, The Sailfish Optimizer: A novel nature-inspired metaheuristic algorithm for solving constrained engineering optimization problems, Engineering Applications of Artificial Intelligence, 80 (2019) 20-34.
[44] J.-S. Chou, D.-N. Truong, A novel metaheuristic optimizer inspired by behavior of jellyfish in ocean, Applied Mathematics and Computation, 389 (2021) 125535.
[45] E. Atashpaz-Gargari, C. Lucas, Imperialist competitive algorithm: an algorithm for optimization inspired by imperialistic competition, in: 2007 IEEE congress on evolutionary computation, Ieee, 2007, pp. 4661-4667.
[46] Y. Xu, Z. Cui, J. Zeng, Social emotional optimization algorithm for nonlinear constrained optimization problems, in: International Conference on Swarm, Evolutionary, and Memetic Computing, Springer, 2010, pp. 583-590.
[47] H. Shayeghi, J. Dadashpour, Anarchic society optimization based PID control of an automatic voltage regulator (AVR) system, Electrical and Electronic Engineering, 2 (2012) 199-207.
[48] A.H. Kashan, League Championship Algorithm (LCA): An algorithm for global optimization inspired by sport championships, Applied Soft Computing, 16 (2014) 171-200.
[49] A. Sadollah, H. Sayyaadi, H.M. Lee, J.H. Kim, Mine blast harmony search: A new hybrid optimization method for improving exploration and exploitation capabilities, Applied Soft Computing, 68 (2018) 548-564.
[50] R. Moghdani, K. Salimifard, Volleyball premier league algorithm, Applied Soft Computing, 64 (2018) 161-185.
[51] Q. Askari, I. Younas, M. Saeed, Political Optimizer: A novel socio-inspired meta-heuristic for global optimization, Knowledge-Based Systems, 195 (2020) 105709.
[52] Q. Askari, M. Saeed, I. Younas, Heap-based optimizer inspired by corporate rank hierarchy for global optimization, Expert Systems with Applications, 161 (2020) 113702.
[53] H. Mohammadzadeh, F. Soleimanian Gharehchopogh, Feature Selection with Binary Symbiotic Organisms Search Algorithm for Email Spam Detection, International Journal of Information Technology & Decision Making, 20 (2021) 469-515.
[54] A. Benyamin, F. Soleimanian Gharehchopogh, B. Saeid, Discrete farmland fertility optimization algorithm with metropolis acceptance criterion for traveling salesman problems, International Journal of Intelligent Systems, 36 (2021) 1270-1303.
[55] S. Ouadfel, M. Abd Elaziz, Enhanced crow search algorithm for feature selection, Expert Systems with Applications, 159 (2020) 113572.

[56] Y. Jiang, Q. Luo, Y. Wei, L. Abualigah, Y. Zhou, An efficient binary Gradient-based optimizer for feature selection, Mathematical Biosciences and Engineering: MBE, 18 (2021) 3813-3854.
[57] H. Mohmmadzadeh, F. Soleimanian Gharehchopogh, An efficient binary chaotic symbiotic organisms search algorithm approaches for feature selection problems, The Journal of Supercomputing, (2021) 1-43.
[58] S. Taghian, M.H. Nadimi-Shahraki, H. Zamani, Comparative Analysis of Transfer Function-based Binary Metaheuristic Algorithms for Feature Selection, in: 2018 International Conference on Artificial Intelligence and Data Processing (IDAP), IEEE, 2018, pp. 1-6.
[59] M.B. Dezfouli, M.H. Nadimi-Shahraki, H. Zamani, A Novel Tour Planning Model using Big Data, in: 2018 International Conference on Artificial Intelligence and Data Processing (IDAP), IEEE, 2018, pp. 1-6.
[60] G. Zhu, S. Kwong, Gbest-guided artificial bee colony algorithm for numerical function optimization, Applied mathematics and computation, 217 (2010) 3166-3173.
[61] M.H. Nadimi-Shahraki, A. Fatahi, H. Zamani, S. Mirjalili, L. Abualigah, M. Abd Elaziz, Migration-Based Moth-Flame Optimization Algorithm, Processes, 9 (2021) 2276.
[62] B. Morales-Castañeda, D. Zaldivar, E. Cuevas, F. Fausto, A. Rodríguez, A better balance in metaheuristic algorithms: Does it exist?, Swarm and Evolutionary Computation, 54 (2020) 100671.
[63] C. Lu, L. Gao, J. Yi, Grey wolf optimizer with cellular topological structure, Expert Systems with Applications, 107 (2018) 89-114.
[64] S. Gupta, K. Deep, A memory-based grey wolf optimizer for global optimization tasks, Applied Soft Computing, 93 (2020) 106367.
[65] M.H. Nadimi-Shahraki, S. Taghian, S. Mirjalili, An improved grey wolf optimizer for solving engineering problems, Expert Systems with Applications, 166 (2021) 113917.
[66] A.H. Gandomi, K. Deb, R.C. Averill, S. Rahnamayan, M.N. Omidvar, Using semi-independent variables to enhance optimization search, Expert Systems with Applications, 120 (2019) 279-297.
[67] D.H. Wolpert, W.G. Macready, No free lunch theorems for optimization, IEEE transactions on evolutionary computation, 1 (1997) 67-82.
[68] J. Liang, B. Qu, P. Suganthan, A.G. Hernández-Díaz, Problem definitions and evaluation criteria for the CEC 2013 special session on real-parameter optimization, Computational Intelligence Laboratory, Zhengzhou University, Zhengzhou, China and Nanyang Technological University, Singapore, Technical Report, 201212 (2013) 281-295.
[69] J. Liang, B. Qu, P. Suganthan, Problem definitions and evaluation criteria for the CEC 2014 special session and competition on single objective real-parameter numerical optimization, Computational Intelligence Laboratory, Zhengzhou University, Zhengzhou China and Technical Report, Nanyang Technological University, Singapore, 635 (2013).
[70] G. Wu, R. Mallipeddi, P. Suganthan, Problem definitions and evaluation criteria for the CEC 2017 competition on constrained real-parameter optimization, National University of Defense Technology, Changsha, Hunan, PR China and Kyungpook National University, Daegu, South Korea and Nanyang Technological University, Singapore, Technical Report, (2017).
[71] A. Kumar, G. Wu, M.Z. Ali, R. Mallipeddi, P.N. Suganthan, S. Das, A test-suite of non-convex constrained optimization problems from the real-world and some baseline results, Swarm and Evolutionary Computation, 56 (2020) 100693.
[72] L. Gu, R. Yang, C.-H. Tho, M. Makowskit, O. Faruquet, Y.L. Y. Li, Optimisation and robustness for crashworthiness of side impact, International Journal of Vehicle Design, 26 (2001) 348-360.
[73] F. Wilcoxon, Individual comparisons by ranking methods, in: Breakthroughs in statistics, Springer, 1992, pp. 196-202.
[74] H. Hildenbrandt, C. Carere, C.K. Hemelrijk, Self-organized aerial displays of thousands of starlings: a model, Behavioral Ecology, 21 (2010) 1349-1359.
[75] A. Attanasi, A. Cavagna, L. Del Castello, I. Giardina, T.S. Grigera, A. Jelić, S. Melillo, L. Parisi, O. Pohl, E. Shen, Information transfer and behavioural inertia in starling flocks, Nature physics, 10 (2014) 691.
[76] Starlings over Gretna, in.
[77] F.S. Levin, An introduction to quantum theory, Cambridge University Press, 2002.
[78] D. McMahon, Quantum computing explained, John Wiley & Sons, 2007.
[79] A.J. King, D.J. Sumpter, Murmurations, Current Biology, 22 (2012) R112-R114.
[80] K. Hussain, M.N.M. Salleh, S. Cheng, Y. Shi, On the exploration and exploitation in popular swarm-based metaheuristic algorithms, Neural Computing and Applications, 31 (2019) 7665-7683.
[81] K. Socha, M. Dorigo, Ant colony optimization for continuous domains, European journal of operational research, 185 (2008) 1155-1173.
[82] F.A. Hashim, E.H. Houssein, M.S. Mabrouk, W. Al-Atabany, S. Mirjalili, Henry gas solubility optimization: A novel physics-based algorithm, Future Generation Computer Systems, 101 (2019) 646-667.
[83] M.G. Omran, S. Al-Sharhan, Improved continuous Ant Colony Optimization algorithms for real-world engineering optimization problems, Engineering Applications of Artificial Intelligence, 85 (2019) 818-829.

[84] M.H. Nadimi-Shahraki, S. Taghian, S. Mirjalili, H. Faris, MTDE: An effective multi-trial vector-based differential evolution algorithm and its applications for engineering design problems, Applied Soft Computing, 97 (2020) 106761.
[85] M. Abd Elaziz, A.H. Elsheikh, D. Oliva, L. Abualigah, S. Lu, A.A. Ewees, Advanced Metaheuristic Techniques for Mechanical Design Problems, Archives of Computational Methods in Engineering, (2021) 1-22.
[86] A.M. Altabeeb, A.M. Mohsen, L. Abualigah, A. Ghallab, Solving capacitated vehicle routing problem using cooperative firefly algorithm, Applied Soft Computing, 108 (2021) 107403.
[87] H.K. Zahrani, M.H. Nadimi-Shahraki, H.R. Sayarshad, An intelligent social-based method for rail-car fleet sizing problem, Journal of Rail Transport Planning & Management, 17 (2021) 100231.
[88] M.R. Ghasemi, H. Varaee, A fast multi-objective optimization using an efficient ideal gas molecular movement algorithm, Engineering with Computers, 33 (2017) 477-496.
[89] M. Premkumar, P. Jangir, B.S. Kumar, R. Sowmya, H.H. Alhelou, L. Abualigah, A.R. Yildiz, S. Mirjalili, A New Arithmetic Optimization Algorithm for Solving Real-World Multiobjective CEC-2021 Constrained Optimization Problems: Diversity Analysis and Validations, IEEE Access, (2021).
[90] M.R. Ghasemi, H. Varaee, Enhanced IGMM optimization algorithm based on vibration for numerical and engineering problems, Engineering with Computers, 34 (2018) 91-116.
[91] J.S. Arora, Introduction to optimum design, Elsevier, 2004.
[92] A.D. Belegundu, A study of mathematical programming methods for structural optimization. The University of Iowa, 1982.
[93] C.A.C. Coello, Use of a self-adaptive penalty approach for engineering optimization problems, Computers in Industry, 41 (2000) 113-127.
[94] B. Kannan, S.N. Kramer, An augmented Lagrange multiplier based method for mixed integer discrete continuous optimization and its applications to mechanical design, (1994).
[95] S.S. Rao, Engineering Optimization. Jon Wiley And Sons, Inc ISBN 0-471-55034-5, (1996).
[96] C.S. Beightler, D.T. Phillips, Applied geometric programming, John Wiley & Sons, 1976.
[97] B.D. Youn, K. Choi, R.-J. Yang, L. Gu, Reliability-based design optimization for crashworthiness of vehicle side impact, Structural and Multidisciplinary Optimization, 26 (2004) 272-283.
[98] B.S. Yildiz, N. Pholdee, S. Bureerat, A.R. Yildiz, S.M. Sait, Enhanced grasshopper optimization algorithm using elite opposition-based learning for solving real-world engineering problems, Engineering with Computers, (2021) 1-13.
[99] B.D. Youn, K.K. Choi, A new response surface methodology for reliability-based design optimization, Computers & structures, 82 (2004) 241-256.
[100] D.M. Himmelblau, Applied Nonlinear Programming McGraw-Hill Book Company, New York, (1972).
[101] J.N. Siddall, Optimal engineering design: principles and applications, CRC Press, 1982.
[102] M. Pant, R. Thangaraj, V. Singh, Optimization of mechanical design problems using improved differential evolution algorithm, International Journal of Recent Trends in Engineering, 1 (2009) 21.
[103] N. Andrei, N. Andrei, Nonlinear optimization applications using the GAMS technology, Springer, 2013.